10. Publikace autora

Publikace autora jsou přiloženy v tomto pořadí:

1. **Vostarek, F.,** Sankova, B. & Sedmera, D. 2014. **Studying dynamic events in the developing myocardium.** *Prog Biophys Mol Biol,* **115,** 261-9.

(IF = 3.377)

2. Sedmera, D., Kockova, R**., Vostarek, F.** & Raddatz, E. 2015. **Arrhythmias in the developing heart.** *Acta Physiol (Oxf),* **213,** 303-20.

(IF = 4.251)

3. **Vostarek, F.**, Svatunkova, J. & Sedmera, D. 2016. **Acute temperature effects on function of the chick embryonic heart.** *Acta Physiol (Oxf),* **217,** 276-86.

(IF = 4.066)

Progress in Biophysics and Molecular Biology 115 (2014) 261–269

Contents lists available at ScienceDirect

Progress in Biophysics and Molecular Biology

journal homepage: www.elsevier.com/locate/pbiomolbio

Review

Studying dynamic events in the developing myocardium

Frantisek Vostarek [a, b], Barbora Sankova [a, c], David Sedmera [a, c, *]

[a] Institute of Physiology, Academy of Sciences of the Czech Republic, Czech Republic
[b] Faculty of Science, Charles University, Prague, Czech Republic
[c] Institute of Anatomy, First Medical Faculty, Charles University, Prague, Czech Republic

ARTICLE INFO

Article history:
Available online 19 June 2014

Keywords:
Optical mapping
Calcium imaging
High-speed cameras
Embryo
Heart
Cardiac conduction system

ABSTRACT

Differentiation and conduction properties of the cardiomyocytes are critically dependent on physical conditioning both *in vitro* and *in vivo*. Historically, various techniques were introduced to study dynamic events such as electrical currents and changes in ionic concentrations in live cells, multicellular preparations, or entire hearts. Here we review this technological progress demonstrating how each improvement in spatial or temporal resolution provided answers to old and provoked new questions. We further demonstrate how high-speed optical mapping of voltage and calcium can uncover pacemaking potential within the outflow tract myocardium, providing a developmental explanation of ectopic beats originating from this region in the clinical settings.

Contents

1. Biomechanics at cell and organ level

1.1. From whole hearts down to cellular level

To study dynamic electrical and mechanical events occurring in the heart, simplification of the complex, three-dimensional *in vivo* system is often advantageous. This can go down to the single cell level, since isolated cardiomyocytes can spontaneously beat *in vitro* and cell culture setup is useful for studying subcellular and

* Corresponding author. Academy of Sciences of the Czech Republic, Institute of Physiology, Videnska 1083, 14220, Prague 4, Czech Republic.
E-mail address: dsedmera@biomed.cas.cz (D. Sedmera).

http://dx.doi.org/10.1016/j.pbiomolbio.2014.06.002
0079-6107/

molecular events or drug screening purposes. If myocytes are grown *in vitro* for a prolonged period of time, they form a sheet – a functional syncytium connected by gap junctions, simplifying thus the three-dimensional geometry of myocardium into a single plane.

Historically, cells were cultivated just on plain plastic, or surfaces coated with various extracellular matrix molecules (collagen – isotropic or aligned, fibronectin) to promote attachment and influence cellular properties (Atance et al., 2004). A strong stimulus for muscle growth is work load, or stretch; so subjecting cell cultures grown on elastic membrane to mechanical loading using a pump-powered cell stretcher (Kofidis et al., 2004; Miller et al., 2000) is a way to model differentiation normally occurring during development. The next step in bringing the cell culture more closely to *in vivo* situation is growing the cells on more sophisticated 3D scaffolding (Atance et al., 2004; Evans et al., 2003) to form tissue constructs of various complexity (Tobita et al., 2006). Each of these new technological advancements, enabled by parallel development of chemistry (new polymers), mechanical engineering (stretching apparatuses) and biology (cell isolation protocols, differentiation of cardiomyocytes from stem cells) allowed answering new sets of questions. Similar to the situation *in vivo*, cell culture conditions markedly influence the functional parameters of cells; here we will focus on their conduction properties, and extend it back to the whole organ level. This area has so far received comparatively little interest in tissue engineering aimed at construction of implantable artificial myocardium (Yildirim et al., 2007), but in addition to perfusion and mechanical properties of tissue-engineered constructs, it is of vital importance for integration with the host myocardium and electrical stability.

1.2. Tissue geometry and conduction properties

Mechanical loading has profound effects on growth, behavior, differentiation and conduction properties in isolated myocytes (cell cultures). Similarly, for *in vivo* studies, people tend to view genes at the root of everything, and sometimes forget that muscles in particular are critically dependent on mechanical stimuli, and organisms in general on epigenetic influences (Pesevski and Sedmera, 2013). What is less clear is the importance of tissue geometry, also referred to as myocardial architecture, which can be elegantly simplified *in vitro*. Patterned cardiomyocyte cultures, enabled by combination of printed circuit technology and cell culture by the Rohr lab in Bern, Switzerland (Kucera et al., 1998; Rohr et al., 1999) are just an example how availability of new technology helped to document the importance of tissue geometry for cardiac electrical conduction. Strands of myocytes, mimicking bundles of conduction fibers, carry electrical impulses at much higher speed than a large expansion of planar myocardial sheet, which acts as a sink. In such system, effects of various pharmacological agents or gap junctional uncoupling can be studied with ease. It was long believed that the role of cardiac fibroblasts is mostly structural support of the heart, and electrically they function as a mere isolator. Importance of fibroblast–myocyte interactions was revealed in well-defined co-culture experiments (Rohr, 2012) and showed that gap junctional, and possibly also electrical, communication exists between these two cell types.

1.3. Importance of physical conditioning for myocardial growth and differentiation

Effect of altered mechanical loading – an epigenetic stimulus – on developing heart and its conduction system could be studied also at the organ level, *in vivo* as well as *in vitro*. Elegant studies by Thompson and associates (Thompson et al., 2003) showed that at the early developmental stages, the fate of cardiomyocytes in the tubular heart (proliferation vs. differentiation) is plastic, and could be reversed by simply inverting the slice of the cardiac tube inside out. This gradient persists also in the trabeculated heart, and could be modeled mathematically (Damon et al., 2009). Cardiovascular development from biomechanical perspective was reviewed by Larry Taber (Taber, 2001). Growth and remodeling are two important processes occurring during both development and adaptations of the cardiovascular system to changing functional requirements. Most cardiac growth during prenatal development is based on hyperplasia (Clark et al., 1989; Sedmera and Thompson, 2011). At the tissue level, an important biomechanical parameter is the residual strain, changes in which are a sensitive indicator of active remodeling (Taber and Chabert, 2002). This regional growth can be easily measured as an opening angle obtained by cutting open a circular section of the vessel or heart. A decrease in opening angle following creation of pressure overload by conotruncal banding correlated with induced growth 12 h after the procedure. These events can be also modeled mathematically. Schroder and colleagues (Schroder et al., 2002) found that the material properties of the developing heart are regulated by mechanical loading and that microtubules play an important role in this adaptive response during cardiac morphogenesis. Specifically, there was an increased amount of both total and polymerized beta tubulin the hypoplastic left ventricle. This smaller ventricle was also stiffer (analyzed by increased hysteresis loop); both parameters were normalized by the treatment with colchicine, which induced microtubule depolymerization.

During the transition from the trabeculated to compact myocardium, spiraling of myofibers within the left ventricular compact layer is the major factor of fetal myocardial differentiation (Jouk et al., 1995; Sedmera et al., 2000). Tobita and associates analyzed the angle of myocyte inclination during normal and abnormal hemodynamic loading (Tobita et al., 2005); they found that increased pressure loading accelerated this normal morphogenetic process, while there was a delay in the settings of hemodynamically-induced left ventricular hypoplasia. Therefore, hemodynamically induced changes in myocardial architecture in these models (Sedmera et al., 1999) that are based on changes in cell proliferation (deAlmeida et al., 2007; Sedmera et al., 2002a) could be the morphological substrate of altered electrical pathways. These were investigated as well using optical mapping on isolated hearts (Hall et al., 2004; Reckova et al., 2003). We found that increased pressure loading accelerated maturation of ventricular conduction system, while there was a dysfunction of the (morphologically normal) left bundle branch in left ventricular hypoplasia. At the molecular level, these changes were paralleled by up/down regulation of conduction system differentiation marker connexin40.

The hemodynamic unloading of the developing heart could be easily taken to extreme by culturing the spontaneously beating, but not pumping heart *in vitro*. In such settings, we noticed not only an arrest of normal differentiation of the ventricular conduction system, but actually a regression towards even more immature conduction patterns (Sankova et al., 2010). To test whether these profound changes were not simply an artefact of organ culture, we performed re-loading of the ventricle by a droplet of viscous silicone oil, which stretches the ventricle and was shown previously to considerably increase myocardial oxygen and glucose consumption (Romano et al., 2001). Remarkably, this led to a complete rescue of conduction phenotype to *in vivo* values, showing that simple myocyte stretch, rather than hemodynamic shear stress transmitted through the endothelium, is the governing factor in early conduction system differentiation. It agreed well with our older data testing the importance of hemodynamically induced signaling via endothelin receptors, which was found to be important during

the later (bundle branches differentiation), but not the early stages of conduction system formation in the chick embryonic heart *in vivo* (Sedmera et al., 2008).

2. Functional imaging of the developing heart

2.1. History of electrophysiological recordings in impulse propagation studies

These functional studies, including those performed on cell cultures, would not be possible without adequate technology for recording of impulse propagation in the heart. The golden standard for action potential recordings are microelectrodes, including those arranged in arrays (sock, brush, or balloon electrodes). They work very well on large adult hearts (sheep, pig, human), but are of limited use in embryos (spatial issues, fragility). Nevertheless, a few carefully positioned electrodes poked into the isolated chick embryonic heart allowed determination of general direction of impulse propagation and enabled postulation of ventricular trabeculae as nascent network of the ventricular conduction system (Arguello et al., 1986; de Jong et al., 1992). Using just two electrodes, Chuck and colleagues (Chuck et al., 1997) discovered the transition in ventricular activation of the chick embryonic heart from primitive base-to-apex direction to mature apex-to-base pattern, and correlated this event with ventricular septation. These results were later confirmed using high-resolution optical mapping studies, discussed in more detail below. For certain question, and in particular in larger, late gestation avian hearts, microelectrodes are still useful, as was proved recently by the Leiden group (Kolditz et al., 2008, 2007). Two exploration electrodes, together with simultaneous recording of volume-conducted ECG, were enough to demonstrate the accessory atrio-ventricular pathways occurring normally during fetal avian development, and their increased frequency in a model of epicardial ablation that results in deficient formation of fibrous atrioventricular insulation.

2.2. Optical methods for visualization of electrical impulse spreading

However, alternative optical methods, recently reviewed (Boukens and Efimov, 2014), exist for studying spread of electrical activation in excitable tissue by means of supravital staining with voltage-sensitive dyes (Kamino et al., 1981). This approach depends on several technological platforms. First, of course, is the availability of suitable probes that must be stable and robust enough to give sufficient signal of either voltage or intracellular ion concentration. Then, epifluorescence microscope is commonly used for studying smaller samples (embryonic hearts, cells), but for larger hearts, incident illumination systems (typically using light emitting diodes) and barrier filter in front of a macroscope lens are widely used (Fedorov et al., 2007). Last, the amount of data recorded from numerous channels (10 × 10 in the beginning, over 100 × 100 nowadays) at high sampling rate (typically over 1 kHz at 16 bits per channel) requires an adequate computing power – typically dedicated RAM as an intermediate step, either on-board or in the computer attached to the photodiode array or high speed camera. Improvements in any of these potential bottlenecks could, and often did, result in new discoveries.

Major problems of optical probes for studying dynamic events are their instability, photobleaching with associated toxicity of breakdown products, and low response. The most popular voltage-sensitive dye, di-4-ANEPPS (Witkowski et al., 1997) is excited by a broad range of wavelengths, but the voltage-dependent response in emitted fluorescence is in the range >590 nm. Once incorporated to the membrane, it is fairly rapidly internalized, so modification of the lipophilic part by a longer aliphatic chain (di-8-ANEPPS) is advantageous in some preparations, such as isolated cells (Kucera et al., 1998). Novel, longer wavelength dyes use excitation wavelengths better penetrating to the tissues and less toxic for the cells for improved survival (Sakai et al., 1998).

The first detectors employed were light-sensitive photodiodes, which are individually tunable and have an excellent signal to noise ratio. They were arranged into a customizable photodiode array, positioned over an image projected by the imaging setup. This approach was pioneered by the Kamino group in Japan (Hirota et al., 1985; Kamino, 1991; Kamino et al., 1981). The system was used to study the earliest sites of electrical activity in the chick and rat heart, as well as the effect of atrial myocardial architecture (pectinate muscles) on impulse propagation in frog atria (Komuro et al., 1986). Photodiode arrays are today commercially available, and still in use to study events from cell level (Kucera et al., 1998) to early rabbit embryonic heart (Chuck et al., 2004).

An interesting approach used another new technological breakthrough, notably laser scanning system, to study changes in voltage (Dillon and Morad, 1981). These authors showed in the frog heart that myocardial architecture is an important determinant of preferential conduction pathway. While this system did not become widely accepted, laser scanning confocal microscope in a line scan mode, which can achieve speeds up to 2 kHz, is rather popular to study calcium transients and sparks in isolated cells (Toischer et al., 2010), and is useable also for voltage sensitive dyes in isolated hearts (Fig. 1), where it has the advantage of possibility to select precisely the depth from which the signal is acquired, and makes thus data interpretation less complex.

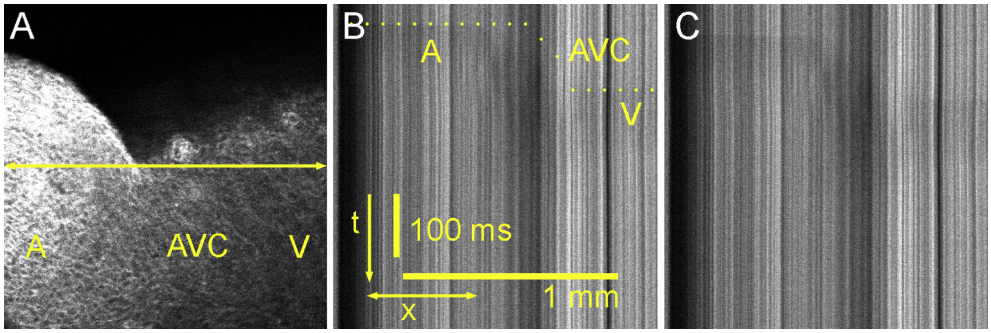

Fig. 1. Proof of principle demonstration of high speed line scan imaging of voltage in the embryonic heart. A: XY scan of a Stage 21 chick embryonic heart in a plane containing atrium (A), atrioventricular canal (AV) and ventricle (V). B: Xt recording at 1 kHz along the line indicated in A showing the slowing of the propagation velocity in the AV canal. Beginning of the action potential is indicated by the yellow dots. C: raw data from B.

2.3. High-speed cameras for optical mapping

However, significant new information about cardiac electrophysiology could be gathered from simultaneously increasing the temporal resolution to the domain of milliseconds, and spatial to micrometers. The Morley group relied on a Dalsa camera with frame rate just below 1000 fps and spatial resolution 64 × 64 pixels (Gutstein et al., 2001; Hall et al., 2000; Jalife et al., 1998, 1999; Morley and Jalife, 2000; Morley and Vaidya, 2001; Morley et al., 1999; Rentschler et al., 2001, 2002; Tamaddon et al., 2000; Vaidya et al., 2001). For dedicated systems, such resolution was deemed completely satisfactory, as any increase in spatial resolution would be tied with decreased pixel size and therefore number of photons hitting it per unit of time, and there would be a problem with data streaming (for example, one second recording of 100 × 100 pixels at 16 bits and 1 kHz takes about 25 Mb – a significant problem for the personal computers in the 1990s and even 2000s). Another plague of optical recordings of beating hearts are motion artifacts. In principle, such mechanical events could be, and were, used for analysis of the heart rhythm (Buechling et al., 2009; Raddatz, 1997), but for voltage studies they pose a considerable problem, especially for analysis of repolarization. Therefore, motion inhibitors (excitation-contraction uncoupling agents) such as BDM (Efimov et al., 1997), cytochalasin D (Biermann et al., 1998; Jalife et al., 1998), blebbistatin (Efimov et al., 1997; Fedorov et al., 2010, 2007; Jou et al., 2011; Sankova et al., 2012) were introduced. These agents enabled considerable improvement in signal quality and are considered indispensable by many investigators. However, they have caveats in their own respect due to their inherent toxicity, effects on action potential duration or pacemaking potentials. Alternative methods were therefore developed for improvement of signal to noise ration, such as signal averaging (Rentschler et al., 2001, 2002) or pixel tracking using dual wavelength imaging (Leaf et al., 2008). They seem to work well as long as the heart beat is regular and the conduction pathway does not differ from one cycle to another, which is most of the time true (Sankova et al., 2012). However, pixel tracking requires either two camera system or rapid wavelength switching, compromising somewhat the spatial and/or temporal resolution.

Unlike sock or balloon electrodes, which truly allow mapping of the heart chamber in three dimensions, the optical approach is typically restricted to a single view, reducing the three dimensional organ in a single plane. This is accentuated by some groups that further flatten the imaged surface to reduce the ambiguity of the curved surface (Larsen et al., 2012), but such artificial stretching could alter conduction properties of the myocardium due to physical uncoupling or action on stretch-sensitive ion channels. The problem of a limited area of view, particularly troublesome when studying complex arrhythmias such as ventricular fibrillation (Boukens and Efimov, 2014), could be solved by using dual/multiple camera systems (easily achieved in a hanging Langendorff preparation), flipping the heart (Ammirabile et al., 2012; Sedmera et al., 2004), or using angled mirror (Gurjarpadhye et al., 2007) for simultaneous viewing of ±75% of the heart surface. This last approach sacrifices some of the spatial resolution of the camera, but saves considerable expenses of the setup.

2.4. New developments in high-speed imaging: getting the high resolution, too

Increase in hardware performance and availability of ready-to-use systems enabled recordings of multiple parameters at once, such as simultaneous voltage and calcium imaging (Chen et al., 2010). The first such dual recording was reported by Efimov and associates (Efimov et al., 1994). The main advantage of such approach is to study electromechanical dissociation during ischemia. In such settings, long calcium transients with no ATP can occur without any voltage changes, but also alternans is possible either at the level of voltage or calcium changes (Choi and Salama, 2000). Dual simultaneous imaging can provide exact correlation, impossible with any other method.

Newer generation of cameras is marked by "competition" between two different designs – CCD vs. CMOS or sCMOS (for continuous

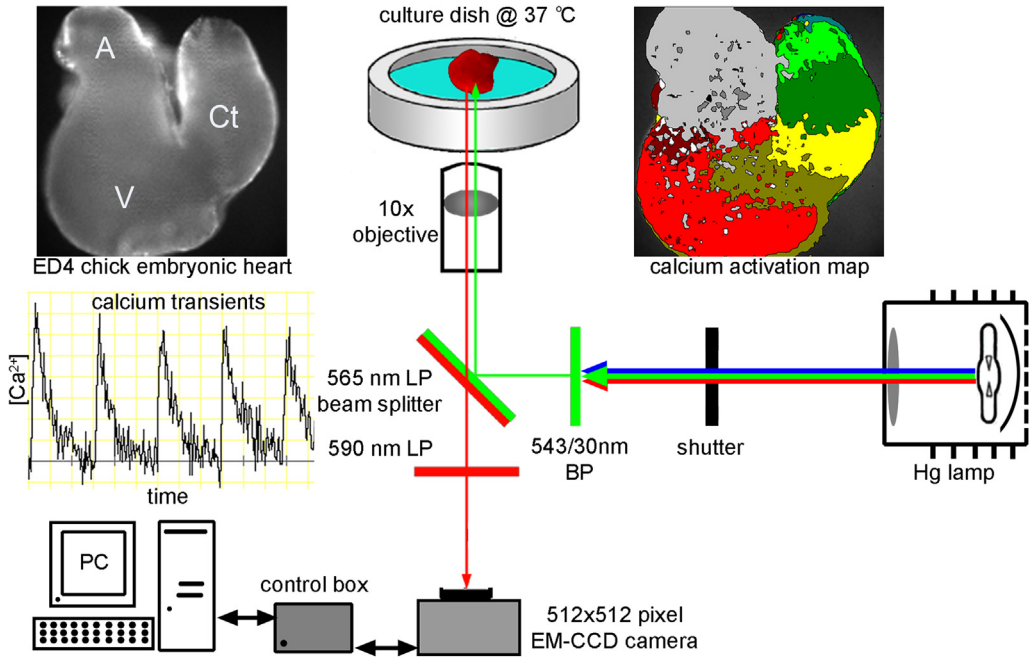

Fig. 2. Setup for voltage (di-4-ANEPPS) or calcium (rhod-2) imaging. The system is centered around an inverted microscope (Nikon Eclipse) with objectives ranging from 4× (whole heart imaging) to 63× water immersion (isolated cells). Current high-speed camera has a maximum resolution of 512 × 512 pixels and can achieve rate of 1300 fps, although not simultaneously.

updates and discussion of this topic, see http://www.microscopy-analysis.com/). While the use of add-on image intensifiers (Reckova et al., 2003; Sedmera et al., 2003) was gradually abandoned, EM-CCD cameras still present very sensitive and reproducible detectors, and due to their speed at full frame rate are useful also in other low-light application (e.g. spinning disc confocal, light sheet microscopy). Newer CMOS sensors possess excellent sensitivity and readout speeds up to 10,000 fps in dedicated systems (Ultima L) are available in practice. Recent developments widen the spectrum of cameras usable for optical mapping – the newest cameras (e.g. Andor, Hamamatsu) allow full frame (over 1 megapixel) high resolution imaging at over hundred frames per second; with sub-array and binning, rates over 1,000 fps could be easily achieved at still reasonable spatial resolution. Such versatile systems might open the door to the area of high-speed imaging even to labs that do not primarily intend to build such setups.

2.5. Calcium imaging in the developing heart

Measuring calcium concentrations in time at relatively low temporal resolution was successfully performed in the past in events such as egg fertilization or cell signaling (Brooker et al., 1990; Sun et al., 1992). High-speed imaging of calcium in embryonic mouse heart (Valderrabano et al., 2006) resulted in increased sensitivity and allowed signal detection also in the atrioventricular canal, enabling detection of various arrhythmias. As important events in the cardiac myocytes occur rather rapidly (e.g. calcium sparks) and at a small spatial scale (parts of cells), both high speed and high resolution are desirable. Thus, our experimental approach (Fig. 2) of imaging normal and stressed embryonic hearts from 100 × 100 to 512 × 512 pixel, 0.5–20 ms resolution presents a significant technological improvement that brings important new pieces of information, such as precise localization of sites of conduction block and uncovering of ectopic pacemakers (Ammirabile et al., 2012; Benes et al., 2014; Hoogaars et al., 2007; Leaf et al., 2008) in the isolated embryonic heart model.

Our current setup for high speed/high resolution calcium and voltage imaging is depicted in Fig. 2. It allows for speed from about 50 fps (full frame mode) up to 1300 fps (ROH mode – with 128 × 128 pixel subarray and 8 × 8 binning, 3/4 of the chip therefore being used for readout). Data acquisition and processing is performed as described previously (Nanka et al., 2008; Sankova et al., 2010), with the exception of different staining protocol with the rhod-2 calcium indicator. Calcium signal has the advantage over voltage in being positive (i.e., increase, rather than decrease of fluorescence), and higher signal-to-noise ratio is especially advantageous in regions with lower signal amplitude, such as the atrioventricular canal and the outflow tract (Reckova et al., 2003).

Chick embryonic hearts subjected to hypoxia fall into atrioventricular conduction block (Sedmera et al., 2002b; Tran et al., 1996). This could unmask a potential backup pacemaker. We observed occasionally temporary conduction blocks during stabilization of the preparation prior to imaging. Our analysis showed that they were of different kinds, ranging from sino-atrial, atrioventricular, to ventriculo-conotruncal, similar to *in vivo* block induced by digoxin in ED4 embryo (Paff et al., 1964). The embryonic outflow tract is myocardial at this stage, and a distinct wave on ECG for corresponds to its activation (Sabourin et al., 2011; Sarre et al., 2006). Pacemaking activity of low frequency is known to be present in the isolated outflow tract (Raddatz, 1997; Sarre et al., 2009), but the exact location of this pacemaker was not known. In the settings of conduction block, we observed activity of the conotruncal pacemaker in two of 59 hearts; the activity originated at the base of the outflow tract with a frequency of 30 bpm at 37 °C in the example depicted in Fig. 3. The atrial rate was in this case 142 bpm, typical for this stage *in vitro* (Sedmera et al., 2002b).

3. New frontiers in dynamic imaging

3.1. Ectopic or backup pacemaker in the outflow tract myocardium

We then set to investigate whether similar properties are present also in the mammalian heart. In the mouse, experimental creation of complete AV block by cutting the atrioventricular junction with fine scissors did not result in manifestation of ectopic activity (24 fresh hearts cut at ED11.5 or 12.5), analyzed by voltage sensitive dye method described in detail previously (Sankova et al., 2012). However, when ED11.5 mouse embryonic hearts were cultured (originally for different purposes – mechanical unloading and pharmacology, to build upon previous studies of Sankova et al. (2010) and Rentschler et al. (2002)) for 24 h in M16 media, we observed frequently (in 36%, 9 of 25 spontaneously beating hearts) a complete atrioventricular block with atrial rate of 88 ± 28 bpm, while the ventricles were activated retrogradely by a low-frequency (37 ± 9 bpm) ectopic backup pacemaker in the base of the outflow tract (Fig. 4). This phenomenon was also observed in hearts cultured from ED10.5 to ED11.5, although at lower frequency (2 of 9 hearts). The retrograde propagation was different from the activation of the freshly isolated chick heart in block (compare with

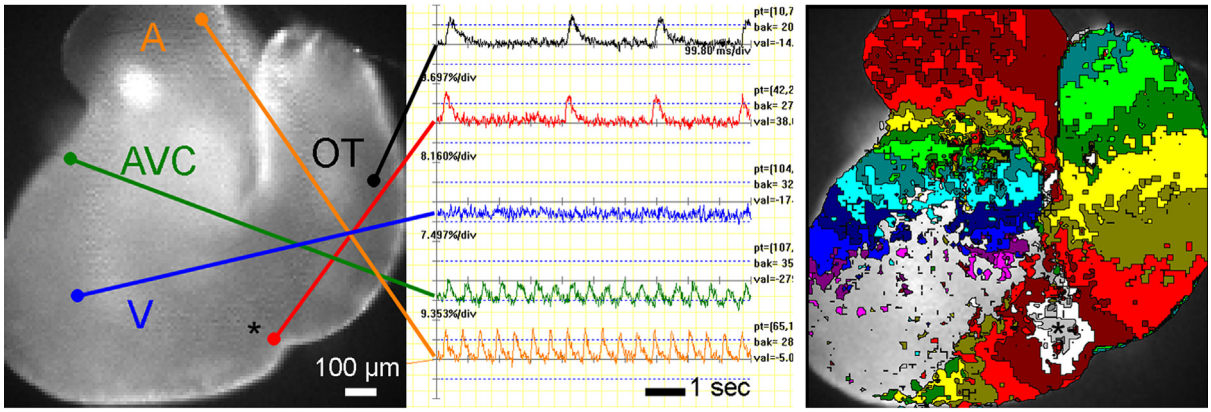

Fig. 3. Ectopic pacemaker in the outflow tract of ED4 chick embryonic heart. The heart is in complete atrioventricular block, located at the transition of the atrioventricular canal and ventricle; by co-incidence, the timing of the ectopic beat correlates with the normal cardiac cycle initiation. A, atrium; AV, atrioventricular canal; OT, outflow tract; V, ventricle. Color isochrones are in 7.68 ms intervals. Scale bar 1 mm.

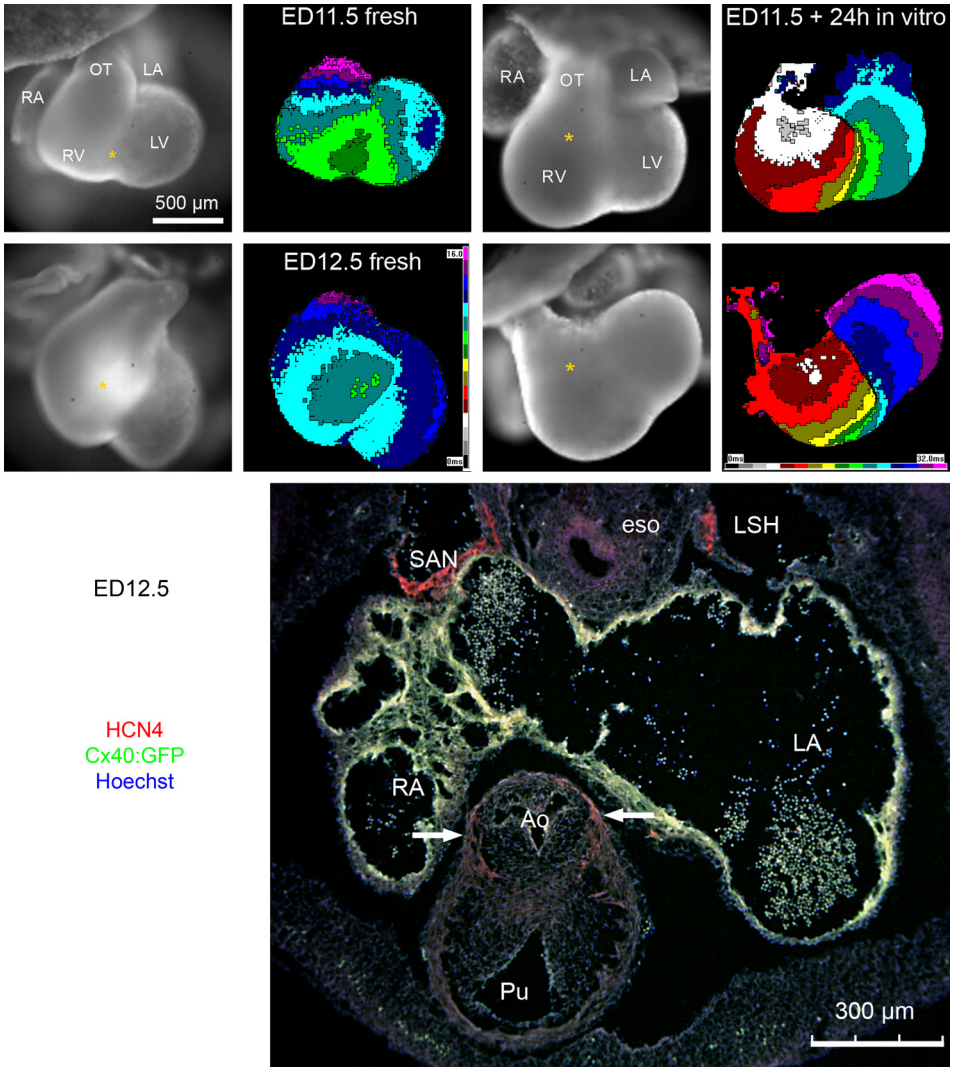

Fig. 4. Ectopic activation of cultured mouse embryonic hearts. Typical ventricular activation of freshly isolated hearts proceeds either via the primary interventricular ring (ED11.5), or from the right apical breakthrough (ED12.5). The site of first activation is marked with an asterisk. Colors represent 1 ms isochronal intervals. Two examples showing the ventricular activation from the outflow tract region illustrate the position of the ectopic pacemaker at the base of the outflow tract (OT; orange asterisks). Note that the conduction is considerably slower, color isochronal intervals being 2 ms. Transverse histological section through this region shows higher intensity of staining for HCN_4, responsible for the pacemaking activity, in this region; normally, the highest levels are found in the area of the sinoatrial node (SAN), with some remnants in the left sinus horn (LSH) myocardium. Staining performed in conjunction of study by Benes et al. (2014). Ao, aorta; eso, esophagus; LA, left atrium; LV, left ventricle; Pu, pulmonary artery; RA, right atrium; RV, right ventricle.

Fig. 3), where the wavefront did not propagate back to the ventricular myocardium.

During development, the outflow tract (as well as inflow) myocardium is added to the cardiac tube from the pharyngeal mesenchyme (van den Berg et al., 2009). This cell source is referred to as the second heart field and it is distinguished by Isl-1 expression (Kelly et al., 2001; Kelly and Buckingham, 2002). Right ventricular outflow tract is a frequent site of ectopic activity in humans (Braunwald et al., 2001); our results showing the location of the ectopic pacemaker site coinciding with stronger HCN_4 expression might be responsible to a large extent for the spontaneous depolarization (Fig. 4), and thus could provide a developmental explanation for this phenomenon. In this context, a paper by Boukens and colleagues analyzed the origin of ectopic pacemaking in the outflow tract in Brugada patients (Boukens et al., 2013). Study in a mouse model revealed expression of Tbx2 in the outflow tract myocardium, responsible for maintaining the primitive phenotype (i.e., slow conduction and automaticity potential). This features disappeared in the adulthood, but could be unmasked by either genetic of pharmacological sodium channel blockade. Persistence (Reaume et al., 1995) of very slowly conducting (our unpublished data) outflow tract myocardium was also noted in the mouse fetuses with Cx43 deletion, which have generally severe conduction problems and predisposition for ventricular arrhythmias (Vaidya et al., 2001).

3.2. *Imaging the dispensable heart: lessons from the zebrafish*

Zebrafish heart is of considerably simpler design than its mammalian counterpart, possessing only a single atrial and single ventricular chamber (Hu et al., 2001). In addition, its transparency and self-contained early development make it ideal for longitudinal imaging studies. Its small size enables use of high-power optics, allowing excellent 3D rendering and cell counting; furthermore, coupled with its low metabolic requirements due to poikilothermy, heart function is not essential for embryonic survival during the

first week of development. All these features allow functional studies of genes crucial for cardiovascular development that are not feasible in the mouse model due to early embryonic lethality. It is thus not surprising that new technical advances in developmental imaging come from this field.

Particularities of this model organism allowed calcium imaging after dye injection at a single cell stage (Milan et al., 2006). Motion control, critical for optical mapping, was elegantly achieved by using the *silent heart* mutant with normal cardiac morphology and electrical behavior but no contraction. Combination of this approach allowed imaging of previously inaccessible early stages of conduction system differentiation, and showed critical requirement of neuregulin and notch signaling for atrioventricular delay development.

Optogenetics approach was used to localize the pacemaker region at various stages of zebrafish heart development (Arrenberg et al., 2010). Stable transfection with halorhodopsin and channelrhodopsin-2 allowed precise temporal and spatial control of cardiac function. In this way, patterned light illumination enabled disabling and pacing studies that allowed mapping of pacemaker shift during heart development. Light-sheet microscopy setup also bypassed the photobleaching and phototoxicity problems, reported earlier (Sedmera et al., 2003).

Confocal and 3D particles imaging using zebrafish embryos expressing fluorescent proteins under myocardial and endocardial promoters (Hove and Craig, 2012) allowed detailed, 3D monitoring of cardiac function from the earliest time points. This setup permitted fairly precise biomechanical studies and resolution of early cardiac mechanics at much higher resolution than other imaging modalities, such as ultrasound biomicroscopy (McQuinn et al., 2007).

Advantages and drawbacks of genetically encoded vs. injected calcium indicators in zebrafish studies were reviewed recently (Kettunen, 2012). It is important to mention fruitful transfer of techniques from the mouse model, where genetically encoded calcium indicators were originally reported (Tallini et al., 2007) and used to study calcium dynamics specifically in the Purkinje fibers. Transmembrane voltage indicator acting via FRET ('mermaid') was recently transfected into zebrafish embryos (Tsutsui et al., 2010), and allows screening for potentially arrhythmogenic drugs or functional evaluation of different ion channel mutations in a whole heart model.

In conclusion, we have structured this paper around new technologies, pinpointing what unexpected piece of information they uncovered in the field. Technological progress for its own sake is of little value if it does not bring any novel findings or opens new questions. In our opinion, fruitful avenues of future research in this arena will involve three-dimensional imaging studies of cardiac excitation, enabled by simultaneous improvement in light sources, optics, and computing power. This will allow precise definition of conduction pathways, hitherto inferred only from 2D recordings. Genetically encoded fluorescent probes are also of high value, both for large-scale screening as well as for spatially precise electrophysiological studies.

Editors' note

Please see also related communications in this issue by Fedorchak et al. (2014) and Ambrosi et al. (2014).

Acknowledgments

We would like to thank Ms. Alena Kvasilova for performing the histological staining shown in Fig. 4. Supported by Ministry of Education PRVOUK P35/LF1/5, and institutional RVO: 67985823. Further support comes from the Grant Agency of the Czech Republic P302/11/1308 and 13-12412S. B.S. was supported by Charles University in Prague, First Faculty of Medicine training fellowship program. F.V. is supported by GA UK training grant no. 716214.

References

Ambrosi, C.M., Klimas, A., Yu, J., Entcheva, E., 2014. Cardiac applications of optogenetics. Prog. Biophys. Mol. Biol. 115 (2-3), 294–304. http://dx.doi.org/10.1016/j.pbiomolbio.2014.07.001.

Ammirabile, G., Tessari, A., Pignataro, V., Szumska, D., Sardo, F.S., Benes Jr., J., Balistreri, M., Bhattacharya, S., Sedmera, D., Campione, M., 2012. Pitx2 confers left morphological, molecular, and functional identity to the sinus venosus myocardium. Cardiovasc. Res. 93, 291–301.

Arguello, C., Alanis, J., Pantoja, O., Valenzuela, B., 1986. Electrophysiological and ultrastructural study of the atrioventricular canal during the development of the chick embryo. J. Mol. Cell. Cardiol. 18, 499–510.

Arrenberg, A.B., Stainier, D.Y., Baier, H., Huisken, J., 2010. Optogenetic control of cardiac function. Science 330, 971–974.

Atance, J., Yost, M.J., Carver, W., 2004. Influence of the extracellular matrix on the regulation of cardiac fibroblast behavior by mechanical stretch. J. Cell. Physiol. 200, 377–386.

Benes Jr., J., Ammirabile, G., Sankova, B., Campione, M., Krejci, E., Kvasilova, A., Sedmera, D., 2014. The role of connexin40 in developing atrial conduction. FEBS Lett. 588, 1465–1469.

Biermann, M., Rubart, M., Moreno, A., Wu, J., Josiah-Durant, A., Zipes, D.P., 1998. Differential effects of cytochalasin D and 2,3 butanedione monoxime on isometric twitch force and transmembrane action potential in isolated ventricular muscle: implications for optical measurements of cardiac repolarization. J. Cardiovasc. Electrophysiol. 9, 1348–1357.

Boukens, B.J., Efimov, I., 2014. A century of optocardiography. IEEE Rev. Biomed. Eng. 7, 115–125.

Boukens, B.J., Sylva, M., de Gier-de Vries, C., Remme, C.A., Bezzina, C.R., Christoffels, V.M., Coronel, R., 2013. Reduced sodium channel function unmasks residual embryonic slow conduction in the adult right ventricular outflow tract. Circ. Res. 113, 137–141.

Braunwald, E., Zipes, D.P., Libbt, P., 2001. Heart Disease: a Textbook of Cardiovascular Medicine. Saunders, Philadelphia, p. 2281.

Brooker, G., Seki, T., Croll, D., Wahlestedt, C., 1990. Calcium wave evoked by activation of endogenous or exogenously expressed receptors in Xenopus oocytes. Proc. Natl. Acad. Sci. U. S. A. 87, 2813–2817.

Buechling, T., Akasaka, T., Vogler, G., Ruiz-Lozano, P., Ocorr, K., Bodmer, R., 2009. Non-autonomous modulation of heart rhythm, contractility and morphology in adult fruit flies. Dev. Biol. 328, 483–492.

Chen, F., De Diego, C., Chang, M.G., McHarg, J.L., John, S., Klitzner, T.S., Weiss, J.N., 2010. Atrioventricular conduction and arrhythmias at the initiation of beating in embryonic mouse hearts. Dev. Dyn. 239, 1941–1949.

Choi, B.R., Salama, G., 2000. Simultaneous maps of optical action potentials and calcium transients in guinea-pig hearts: mechanisms underlying concordant alternans. J. Physiol. 529 (Pt 1), 171–188.

Chuck, E.T., Freeman, D.M., Watanabe, M., Rosenbaum, D.S., 1997. Changing activation sequence in the embryonic chick heart. Implications for the development of the His-Purkinje system. Circ. Res. 81, 470–476.

Chuck, E.T., Meyers, K., France, D., Creazzo, T.L., Morley, G.E., 2004. Transitions in ventricular activation revealed by two-dimensional optical mapping. Anat. Rec. 280A, 990–1000.

Clark, E.B., Hu, N., Frommelt, P., Vandekieft, G.K., Dummett, J.L., Tomanek, R.J., 1989. Effect of increased pressure on ventricular growth in stage 21 chick embryos. Am. J. Physiol. 257, H55–H61.

Damon, B.J., Remond, M.C., Bigelow, M.R., Trusk, T.C., Xie, W., Perucchio, R., Sedmera, D., Denslow, S., Thompson, R.P., 2009. Patterns of muscular strain in the embryonic heart wall. Dev. Dyn. 238, 1535–1546.

de Jong, F., Opthof, T., Wilde, A.A., Janse, M.J., Charles, R., Lamers, W.H., Moorman, A.F., 1992. Persisting zones of slow impulse conduction in developing chicken hearts. Circ. Res. 71, 240–250.

deAlmeida, A., McQuinn, T., Sedmera, D., 2007. Increased ventricular preload is compensated by myocyte proliferation in normal and hypoplastic fetal chick left ventricle. Circ. Res. 100, 1363–1370.

Dillon, S., Morad, M., 1981. A new laser scanning system for measuring action potential propagation in the heart. Science 214, 453–456.

Efimov, I., Rendt, J.M., Salama, G., 1994. Optical maps of intracellular [ca^{2+}]i transients and action potentials from surface of perfused guinea pig heart. Circulation 90, 632.

Efimov, I.R., Fahy, G.J., Cheng, Y., Van Wagoner, D.R., Tchou, P.J., Mazgalev, T.N., 1997. High-resolution fluorescent imaging does not reveal a distinct atrioventricular nodal anterior input channel (fast pathway) in the rabbit heart during sinus rhythm. J. Cardiovasc. Electrophysiol. 8, 295–306.

Evans, H.J., Sweet, J.K., Price, R.L., Yost, M., Goodwin, R.L., 2003. Novel 3D culture system for study of cardiac myocyte development. Am. J. Physiol. Heart Circ. Physiol. 285, H570–H578.

Fedorchak, G.R., Kaminski, A., Lammerding, J., 2014. Cellular mechanosensing: Getting to the nucleus of it all. Prog. Biophys. Mol. Biol. 115 (2-3), 76–92. http://dx.doi.org/10.1016/j.pbiomolbio.2014.06.009.

Fedorov, V.V., Glukhov, A.V., Chang, R., Kostecki, G., Aferol, H., Hucker, W.J., Wuskell, J.P., Loew, L.M., Schuessler, R.B., Moazami, N., Efimov, I.R., 2010. Optical

mapping of the isolated coronary-perfused human sinus node. J. Am. Coll. Cardiol. 56, 1386–1394.
Fedorov, V.V., Lozinsky, I.T., Sosunov, E.A., Anyukhovsky, E.P., Rosen, M.R., Balke, C.W., Efimov, I.R., 2007. Application of blebbistatin as an excitation-contraction uncoupler for electrophysiologic study of rat and rabbit hearts. Heart Rhythm 4, 619–626.
Gurjarpadhye, A., Hewett, K.W., Justus, C., Wen, X., Stadt, H., Kirby, M.L., Sedmera, D., Gourdie, R.G., 2007. Cardiac neural crest ablation inhibits compaction and electrical function of conduction system bundles. Am. J. Physiol. Heart Circ. Physiol. 292, H1291–H1300.
Gutstein, D.E., Morley, G.E., Tamaddon, H., Vaidya, D., Schneider, M.D., Chen, J., Chien, K.R., Stuhlmann, H., Fishman, G.I., 2001. Conduction slowing and sudden arrhythmic death in mice with cardiac- restricted inactivation of connexin43. Circ. Res. 88, 333–339.
Hall, C.E., Hurtado, R., Hewett, K.W., Shulimovich, M., Poma, C.P., Reckova, M., Justus, C., Pennisi, D.J., Tobita, K., Sedmera, D., Gourdie, R.G., Mikawa, T., 2004. Hemodynamic-dependent patterning of endothelin converting enzyme 1 expression and differentiation of impulse-conducting Purkinje fibers in the embryonic heart. Development 131, 581–592.
Hall, D.G., Morley, G.E., Vaidya, D., Ard, M., Kimball, T.R., Witt, S.A., Colbert, M.C., 2000. Early onset heart failure in transgenic mice with dilated cardiomyopathy. Pediatr. Res. 48, 36–42.
Hirota, A., Kamino, K., Komuro, H., Sakai, T., Yada, T., 1985. Early events in development of electrical activity and contraction in embryonic rat heart assessed by optical recording. J. Physiol. 369, 209–227.
Hoogaars, W.M., Engel, A., Brons, J.F., Verkerk, A.O., de Lange, F.J., Wong, L.Y., Bakker, M.L., Clout, D.E., Wakker, V., Barnett, P., Ravesloot, J.H., Moorman, A.F., Verheijck, E.E., Christoffels, V.M., 2007. Tbx3 controls the sinoatrial node gene program and imposes pacemaker function on the atria. Genes Dev. 21, 1098–1112.
Hove, J.R., Craig, M.P., 2012. High-speed confocal imaging of zebrafish heart development. Methods Mol. Biol. 843, 309–328.
Hu, N., Yost, H.J., Clark, E.B., 2001. Cardiac morphology and blood pressure in the adult zebrafish. Anat. Rec. 264, 1–12.
Jalife, J., Morley, G.E., Tallini, N.Y., Vaidya, D., 1998. A fungal metabolite that eliminates motion artifacts. J. Cardiovasc. Electrophysiol. 9, 1358–1362.
Jalife, J., Morley, G.E., Vaidya, D., 1999. Connexins and impulse propagation in the mouse heart. J. Cardiovasc. Electrophysiol. 10, 1649–1663.
Jou, C.J., Spitzer, K.W., Tristani-Firouzi, M., 2011. Blebbistatin effectively uncouples the excitation-contraction process in zebrafish embryonic heart. Cell. Physiol. Biochem. 25, 419–424.
Jouk, P.S., Usson, Y., Michalowicz, G., Parazza, F., 1995. Mapping of the orientation of myocardial cells by means of polarized light and confocal scanning laser microscopy. Microsc. Res. Technol. 30, 480–490.
Kamino, K., 1991. Optical approaches to ontogeny of electrical activity and related functional organization during early heart development. Physiol. Rev. 71, 53–91.
Kamino, K., Hirota, A., Fujii, S., 1981. Localization of pacemaking activity in early embryonic heart monitored using voltage-sensitive dye. Nature 290, 595–597.
Kelly, R.G., Brown, N.A., Buckingham, M.E., 2001. The arterial pole of the mouse heart forms from Fgf10-expressing cells in pharyngeal mesoderm. Dev. Cell. 1, 435–440.
Kelly, R.G., Buckingham, M.E., 2002. The anterior heart-forming field: voyage to the arterial pole of the heart. Trends Genet. 18, 210–216.
Kettunen, P., 2012. Calcium imaging in the zebrafish. Adv. Exp. Med. Biol. 740, 1039–1071.
Kofidis, T., Balsam, L., de Bruin, J., Robbins, R.C., 2004. Distinct cell-to-fiber junctions are critical for the establishment of cardiotypical phenotype in a 3D bioartificial environment. Med. Eng. Phys. 26, 157–163.
Kolditz, D.P., Wijffels, M.C., Blom, N.A., van der Laarse, A., Hahurij, N.D., Lie-Venema, H., Markwald, R.R., Poelmann, R.E., Schalij, M.J., Gittenberger-de Groot, A.C., 2008. Epicardium-derived cells in development of annulus fibrosis and persistence of accessory pathways. Circulation 117, 1508–1517.
Kolditz, D.P., Wijffels, M.C., Blom, N.A., van der Laarse, A., Markwald, R.R., Schalij, M.J., Gittenberger-de Groot, A.C., 2007. Persistence of functional atrioventricular accessory pathways in postseptated embryonic avian hearts: implications for morphogenesis and functional maturation of the cardiac conduction system. Circulation 115, 17–26.
Komuro, H., Sakai, T., Hirota, A., Kamino, K., 1986. Conduction pattern of excitation in the amphibian atrium assessed by multiple-site optical recording of action potentials. Jpn. J. Physiol. 36, 123–137.
Kucera, J.P., Kleber, A.G., Rohr, S., 1998. Slow conduction in cardiac tissue, II: effects of branching tissue geometry. Circ. Res. 83, 795–805.
Larsen, A.P., Sciuto, K.J., Moreno, A.P., Poelzing, S., 2012. The voltage-sensitive dye di-4-ANEPPS slows conduction velocity in isolated guinea pig hearts. Heart Rhythm 9, 1493–1500.
Leaf, D.E., Feig, J.E., Vasquez, C., Riva, P.L., Yu, C., Lader, J.M., Kontogeorgis, A., Baron, E.L., Peters, N.S., Fisher, E.A., Gutstein, D.E., Morley, G.E., 2008. Connexin40 imparts conduction heterogeneity to atrial tissue. Circ. Res. 103, 1001–1008.
McQuinn, T.C., Bratoeva, M., Dealmeida, A., Remond, M., Thompson, R.P., Sedmera, D., 2007. High-frequency ultrasonographic imaging of avian cardiovascular development. Dev. Dyn. 236, 3503–3513.
Milan, D.J., Giokas, A.C., Serluca, F.C., Peterson, R.T., Macrae, C.A., 2006. Notch1b and neuregulin are required for specification of central cardiac conduction tissue. Development 133, 1125–1132.
Miller, C.E., Donlon, K.J., Toia, L., Wong, C.L., Chess, P.R., 2000. Cyclic strain induces proliferation of cultured embryonic heart cells. In Vitro Cell. Dev. Biol. Anim. 36, 633–639.
Morley, G.E., Jalife, J., 2000. Cardiac gap junction remodeling by stretch: is it a good thing? Circ. Res. 87, 272–274.
Morley, G.E., Vaidya, D., 2001. Understanding conduction of electrical impulses in the mouse heart using high-resolution video imaging technology. Microsc. Res. Tech. 52, 241–250.
Morley, G.E., Vaidya, D., Samie, F.H., Lo, C., Delmar, M., Jalife, J., 1999. Characterization of conduction in the ventricles of normal and heterozygous Cx43 knockout mice using optical mapping. J. Cardiovasc. Electrophysiol. 10, 1361–1375.
Nanka, O., Krizova, P., Fikrle, M., Tuma, M., Blaha, M., Grim, M., Sedmera, D., 2008. Abnormal myocardial and coronary vasculature development in experimental hypoxia. Anat. Rec. (Hoboken) 291, 1187–1199.
Paff, G.H., Boucek, R.J., Klopfenstein, H.S., 1964. Experimental heart block in the chick embryo. Anat. Rec. 149, 217–224.
Pesevski, Z., Sedmera, D., 2013. Prenatal adaptations to overload. In: Ostadal, B., Dhalla, N.S. (Eds.), Cardiac Adaptations. Springer Science+Business Media, New York, pp. 41–57.
Raddatz, E., 1997. Response of the embryonic heart to hypoxia and reoxygenation: an in vitro model. Exp. Clin. Cardiol. 2, 128–134.
Reaume, A.G., de Sousa, P.A., Kulkarni, S., Langille, B.L., Zhu, D., Davies, T.C., Juneja, S.C., Kidder, G.M., Rossant, J., 1995. Cardiac malformation in neonatal mice lacking connexin43. Science 267, 1831–1834.
Reckova, M., Rosengarten, C., deAlmeida, A., Stanley, C.P., Wessels, A., Gourdie, R.G., Thompson, R.P., Sedmera, D., 2003. Hemodynamics is a key epigenetic factor in development of the cardiac conduction system. Circ. Res. 93, 77–85.
Rentschler, S., Vaidya, D.M., Tamaddon, H., Degenhardt, K., Sassoon, D., Morley, G.E., Jalife, J., Fishman, G.I., 2001. Visualization and functional characterization of the developing murine cardiac conduction system. Development 128, 1785–1792.
Rentschler, S., Zander, J., Meyers, K., France, D., Levine, R., Porter, G., Rivkees, S.A., Morley, G.E., Fishman, G.I., 2002. Neuregulin-1 promotes formation of the murine cardiac conduction system. Proc. Natl. Acad. Sci. U. S. A. 99, 10464–10469.
Rohr, S., 2012. Arrhythmogenic implications of fibroblast-myocyte interactions. Circ. Arrhythm. Electrophysiol. 5, 442–452.
Rohr, S., Kleber, A.G., Kucera, J.P., 1999. Optical recording of impulse propagation in designer cultures. Cardiac tissue architectures inducing ultra-slow conduction. Trends Cardiovasc. Med. 9, 173–179.
Romano, R., Rochat, A.C., Kucera, P., De Ribaupierre, Y., Raddatz, E., 2001. Oxidative and glycogenolytic capacities within the developing chick heart. Pediatr. Res. 49, 363–372.
Sabourin, J., Robin, E., Raddatz, E., 2011. A key role of TRPC channels in the regulation of electromechanical activity of the developing heart. Cardiovasc. Res. 92, 226–236.
Sakai, T., Yada, T., Hirota, A., Komuro, H., Kamino, K., 1998. A regional gradient of cardiac intrinsic rhythmicity depicted in embryonic cultured multiple hearts. Pflugers Arch. 437, 61–69.
Sankova, B., Benes Jr., J., Krejci, E., Dupays, L., Theveniau-Ruissy, M., Miquerol, L., Sedmera, D., 2012. The effect of connexin40 deficiency on ventricular conduction system function during development. Cardiovasc. Res. 25, 469–479.
Sankova, B., Machalek, J., Sedmera, D., 2010. Effects of mechanical loading on early conduction system differentiation in the chick. Am. J. Physiol. Heart Circ. Physiol. 298, H1571–H1576.
Sarre, A., Maury, P., Kucera, P., Kappenberger, L., Raddatz, E., 2006. Arrhythmogenesis in the developing heart during anoxia-reoxygenation and hypothermia-rewarming: an in vitro model. J. Cardiovasc. Electrophysiol. 17, 1350–1359.
Sarre, A., Pedretti, S., Gardier, S., Raddatz, E., 2009. Specific inhibition of HCN channels slows rhythm differently in atria, ventricle and outflow tract and stabilizes conduction in the anoxic-reoxygenated embryonic heart model. Pharmacol. Res. 61, 85–91.
Schroder, E.A., Tobita, K., Tinney, J.P., Foldes, J.K., Keller, B.B., 2002. Microtubule involvement in the adaptation to altered mechanical load in developing chick myocardium. Circ. Res. 91, 353–359.
Sedmera, D., Harris, B.S., Grant, E., Zhang, N., Jourdan, J., Kurkova, D., Gourdie, R.G., 2008. Cardiac expression patterns of endothelin-converting enzyme (ECE): implications for conduction system development. Dev. Dyn. 237, 1746–1753.
Sedmera, D., Hu, N., Weiss, K.M., Keller, B.B., Denslow, S., Thompson, R.P., 2002a. Cellular changes in experimental left heart hypoplasia. Anat. Rec. 267, 137–145.
Sedmera, D., Kucera, P., Raddatz, E., 2002b. Developmental changes in cardiac recovery from anoxia-reoxygenation. Am. J. Physiol. Regul. Integr. Comp. Physiol. 283, R379–R388.
Sedmera, D., Pexieder, T., Rychterova, V., Hu, N., Clark, E.B., 1999. Remodeling of chick embryonic ventricular myoarchitecture under experimentally changed loading conditions. Anat. Rec. 254, 238–252.
Sedmera, D., Pexieder, T., Vuillemin, M., Thompson, R.P., Anderson, R.H., 2000. Developmental patterning of the myocardium. Anat. Rec. 258, 319–337.
Sedmera, D., Reckova, M., Bigelow, M.R., DeAlmeida, A., Stanley, C.P., Mikawa, T., Gourdie, R.G., Thompson, R.P., 2004. Developmental transitions in electrical activation patterns in chick embryonic heart. Anat. Rec. 280A, 1001–1009.
Sedmera, D., Reckova, M., DeAlmeida, A., Sedmerova, M., Biermann, M., Volejnik, J., Sarre, A., Raddatz, E., McCarthy, R.A., Gourdie, R.G., Thompson, R.P., 2003. Functional and morphological evidence for a ventricular conduction system in the zebrafish and Xenopus heart. Am. J. Physiol. Heart Circ. Physiol. 284, H1152–H1160.

Sedmera, D., Thompson, R.P., 2011. Myocyte proliferation in the developing heart. Dev. Dyn. 240, 1322–1334.
Sun, F.Z., Hoyland, J., Huang, X., Mason, W., Moor, R.M., 1992. A comparison of intracellular changes in porcine eggs after fertilization and electroactivation. Development 115, 947–956.
Taber, L.A., 2001. Biomechanics of cardiovascular development. Annu. Rev. Biomed. Eng. 3, 1–25.
Taber, L.A., Chabert, S., 2002. Theoretical and experimental study of growth and remodeling in the developing heart. Biomech. Model Mechanobiol. 1, 29–43.
Tallini, Y.N., Brekke, J.F., Shui, B., Doran, R., Hwang, S.M., Nakai, J., Salama, G., Segal, S.S., Kotlikoff, M.I., 2007. Propagated endothelial Ca2+ waves and arteriolar dilation in vivo: measurements in Cx40BAC GCaMP2 transgenic mice. Circ. Res. 101, 1300–1309.
Tamaddon, H.S., Vaidya, D., Simon, A.M., Paul, D.L., Jalife, J., Morley, G.E., 2000. High-resolution optical mapping of the right bundle branch in connexin40 knockout mice reveals slow conduction in the specialized conduction system. Circ. Res. 87, 929–936.
Thompson, R.P., Reckova, M., DeAlmeida, A., Bigelow, M., Stanley, C.P., Spruill, J.B., Trusk, T., Sedmera, D., 2003. The oldest, toughest cells in the heart. In: Chadwick, D.J., Goode, J. (Eds.), Development of the Cardiac Conduction System, vol. 250. Wiley, Chichester, pp. 157–176.
Tobita, K., Garrison, J.B., Li, J.J., Tinney, J.P., Keller, B.B., 2005. Three-dimensional myofiber architecture of the embryonic left ventricle during normal development and altered mechanical loads. Anat. Rec. A Discov. Mol. Cell. Evol. Biol. 283, 193–201.
Tobita, K., Liu, L.J., Janczewski, A.M., Tinney, J.P., Nonemaker, J.M., Augustine, S., Stolz, D.B., Shroff, S.G., Keller, B.B., 2006. Engineered early embryonic cardiac tissue retains proliferative and contractile properties of developing embryonic myocardium. Am. J. Physiol. Heart Circ. Physiol. 291, H1829–H1837.
Toischer, K., Rokita, A.G., Unsold, B., Zhu, W., Kararigas, G., Sossalla, S., Reuter, S.P., Becker, A., Teucher, N., Seidler, T., Grebe, C., Preuss, L., Gupta, S.N., Schmidt, K., Lehnart, S.E., Kruger, M., Linke, W.A., Backs, J., Regitz-Zagrosek, V., Schafer, K., Field, L.J., Maier, L.S., Hasenfuss, G., 2010. Differential cardiac remodeling in preload versus afterload. Circulation 122, 993–1003.
Tran, L., Kucera, P., de Ribaupierre, Y., Rochat, A.C., Raddatz, E., 1996. Glucose is arrhythmogenic in the anoxic-reoxygenated embryonic chick heart. Pediatr. Res. 39, 766–773.
Tsutsui, H., Higashijima, S., Miyawaki, A., Okamura, Y., 2010. Visualizing voltage dynamics in zebrafish heart. J. Physiol. 588, 2017–2021.
Vaidya, D., Tamaddon, H.S., Lo, C.W., Taffet, S.M., Delmar, M., Morley, G.E., Jalife, J., 2001. Null mutation of connexin43 causes slow propagation of ventricular activation in the late stages of mouse embryonic development. Circ. Res. 88, 1196–1202.
Valderrabano, M., Chen, F., Dave, A.S., Lamp, S.T., Klitzner, T.S., Weiss, J.N., 2006. Atrioventricular ring reentry in embryonic mouse hearts. Circulation 114, 543–549.
van den Berg, G., Abu-Issa, R., de Boer, B.A., Hutson, M.R., de Boer, P.A., Soufan, A.T., Ruijter, J.M., Kirby, M.L., van den Hoff, M.J., Moorman, A.F., 2009. A caudal proliferating growth center contributes to both poles of the forming heart tube. Circ. Res. 104, 179–188.
Witkowski, F.X., Clark, R.B., Larsen, T.S., Melnikov, A., Giles, W.R., 1997. Voltage-sensitive dye recordings of electrophysiological activation in a Langendorff-perfused mouse heart. Can. J. Cardiol. 13, 1077–1082.
Yildirim, Y., Naito, H., Didie, M., Karikkineth, B.C., Biermann, D., Eschenhagen, T., Zimmermann, W.H., 2007. Development of a biological ventricular assist device: preliminary data from a small animal model. Circulation 116, I16–I23.

ACTA PHYSIOLOGICA

Acta Physiol 2015, **213**, 303–320

REVIEW

Arrhythmias in the developing heart

D. Sedmera,[1,2] R. Kockova,[2,3] F. Vostarek[2] and E. Raddatz[4]

1 Institute of Anatomy, First Faculty of Medicine, Charles University, Prague, Czech Republic

2 Institute of Physiology, Academy of Sciences of the Czech Republic, Prague, Czech Republic

3 Department of Cardiology, Institute of Clinical and Experimental Medicine, Prague, Czech Republic

4 Department of Physiology, Faculty of Biology and Medicine, University of Lausanne, Lausanne, Switzerland

Received 13 August 2014,
revision requested 8 September 2014,
revision received 1 October 2014,
accepted 23 October 2014
Correspondence: D. Sedmera, Academy of Sciences of the Czech Republic, Institute of Physiology, Videnska 1083, 14220 Prague 4, Czech Republic.
E-mail: dsedmera@biomed.cas.cz

Abstract

Prevalence of cardiac arrhythmias increases gradually with age; however, specific rhythm disturbances can appear even prior to birth and markedly affect foetal development. Relatively little is known about these disorders, chiefly because of their relative rarity and difficulty in diagnosis. In this review, we cover the most common forms found in human pathology, specifically congenital heart block, pre-excitation, extrasystoles and long QT syndrome. In addition, we cover pertinent literature data from prenatal animal models, providing a glimpse into pathogenesis of arrhythmias and possible strategies for treatment.

Keywords anti-arrhythmic drugs, cardiac development, chick embryo, conduction system, hypoxia, mouse.

Disturbances of cardiac rhythm in the human foetus

During routine obstetric examination, foetal rhythm disturbances may be detected in at least 2% of pregnancies (Copel *et al.* 2000, Jaeggi & Nii 2005). Foetal arrhythmias account for about 10–20% of referrals for foetal cardiology assessment (Srinivasan & Strasburger 2008). Due to a number of limitations, a foetal electrocardiogram (cardiotocogram) is not the ideal method for assessment of arrhythmias. A relatively novel and efficient method for foetal heart electrical activity recording is foetal magnetocardiography (Strasburger *et al.* 2008, Strasburger & Wakai 2010). However, this method is not widely available and is preferred only after the 20th week of gestation because it is less reliable in the earlier stages of pregnancy. Thus, echocardiography remains the principal method in evaluation of heart rhythm disturbance in the foetus. In addition to heart rhythm analysis, echocardiography may reveal other signs associated with prolonged or persistent foetal rhythm disturbances, such as hydrops (pleural or pericardial effusion, ascites) in its early as well as more advanced stages. The severity of foetal heart failure can be then monitored using the 'heart failure score' presented by Huhta (2005).

Using all three standard echocardiographic modalities (B-mode, M-mode and Doppler), we can assess atrial and ventricular contraction frequencies and their time relations. An equivalent for P wave on electrocardiogram is the A wave detected by pulse wave Doppler in mitral inflow or atrial wall motion detected by M-mode. Similarly, the beginning of retrograde flow in the superior vena cava indicates the beginning of atrial systole. Atrioventricular (AV) valve closure, semilunar valve opening and positive Doppler flow in the aorta are equivalents of the beginning of QRS complex. Simultaneous Doppler recording in the superior vena cava and the aorta shows the time correlation between the atrial and ventricular systole – times corresponding to the P wave and QRS complex on the ECG. These parameters allow us to calculate the heart rate, AV delay and diagnose different types of arrhythmias by measuring the mechanical response of the heart chambers to the electrical stimulus.

The relationship between foetal arrhythmia and structural heart disease is not clearly established. Stewart and Copel found no clear relationship between foetal arrhythmia and structural heart disease

(Stewart *et al.* 1983, Copel *et al.* 2000). In the observational study published by Stewart and associates, only two foetuses from 17 with documented ectopic beats had structural heart disease. No structural heart disease was found in five foetuses with tachycardia (heart rate over 180 bpm), but four of eight foetuses with documented bradycardia had severe structural heart disease. Copel and colleagues reported only two of 10 foetuses diagnosed with significant arrhythmia – one with supraventricular tachycardia and one with a second-degree AV block – associated with structural heart disease of all 614 foetuses with irregular heart rhythm. On the other hand, there is evidence that foetal arrhythmia may be associated with structural heart disease. Schmidt *et al.* (1991) reported that 53% of foetuses (of a total of 55) with complete AV block had concomitant structural heart disease (left atrial isomerism, discordant AV connection). Vergani *et al.* (2005) reported structural heart anomalies in five of six foetuses with bradycardia from a total cohort of 114 infants with foetal arrhythmias. Only two of four foetuses with AV block survived. Eronen reported 12 foetuses (three supraventricular and three ventricular ectopic activities, four AV blocks and two sinus bradycardias) with significant arrhythmia associated with structural heart disease from a total of 125 foetuses with significant arrhythmia (Eronen 1997). She also found 95% survival in foetuses with sole significant arrhythmia compared to a 75% mortality in those with arrhythmia associated with structural heart disease. Interestingly, the total mortality in the group of foetuses with structural heart disease was only 67%. Based on these two observational studies, it could be speculated that bradyarrhythmias are more frequently associated with structural heart disease and have a worse outcome than tachyarrhythmias or irregular heart rhythm, which are frequently curable or might resolve spontaneously during development.

For simplicity, we may divide foetal arrhythmias into the three groups (Fig. 1): ectopic beats, mostly originating in atrial ectopic foci; tachyarrhythmias, which are defined as heart rates over 180 bpm; and bradyarrhythmias, defined as heart rates below 110 bpm (Jaeggi & Nii 2005).

Of these three types, extrasystoles typically have the best outcomes (Reed 1989). Vergani *et al.* (2005) reported that 38% of cases with extrasystoles (in 87 foetuses) resolved *in utero* and 49% at birth. Only one neonate required postnatal therapy, and in nine neonates, the arrhythmia was still present at 1-year follow-up without need for therapy. Two foetuses with extrasystoles converted to supraventricular tachycardia *in utero* and were successfully treated pharmacologically with no impact on their further development.

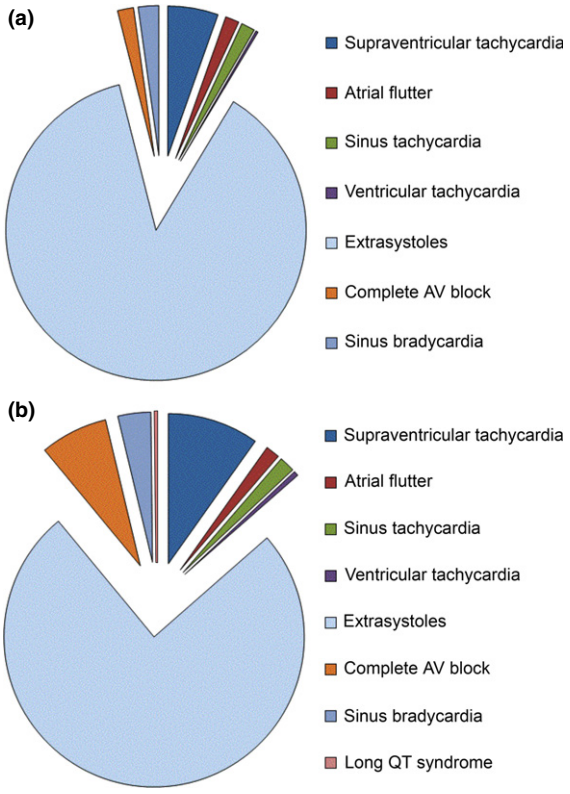

Figure 1 Epidemiology of foetal arrhythmias in humans. (a) Incidence of various types of arrhythmias in non-selected population ($N = 406$, collated from references (Copel *et al.* 2000), (Vergani *et al.* 2005)). (b) Incidence in highly selected population ($N = 591$, collated from references (Stewart *et al.* 1983), (Reed *et al.* 1990), (Eronen 1997), (Vergani *et al.* 2005), (Zhao *et al.* 2006)).

None of these were associated with structural heart disease.

Prolonged foetal tachycardia is usually a serious condition often leading to foetal hydrops or even death. Simpson & Sharland (1998) reported hydrops occurrence in 41% of 127 foetuses diagnosed with tachycardia. Seventy-five non-hydropic foetuses from this cohort responded well to transplacental treatment (mostly with digoxin) with an excellent survival to birth (96%). Conversely, only two-thirds of hydropic foetuses with tachycardia responded to transplacental treatment, and of these, only 73% survived till birth. Thus, foetal hydrops is a negative prognostic sign suggesting severe hemodynamic consequences from the underlying causes – for example, arrhythmia and/or structural heart disease.

Sustained or prolonged bradycardia (heart rates <100 bpm) or tachycardia (heart rates over 180 bpm) are of clinical significance and might have a significant impact on further foetal development *in utero*; even later postnatal development might be affected. Jaeggi

and Nii reported foetal tachycardia as the most frequent arrhythmia in the foetus and was present in 57% of 66 foetuses examined with proven serious arrhythmia (Jaeggi & Nii 2005). Supraventricular tachycardia was present in 40% of cases, atrial flutter accounted for 11%, and sinus tachycardia was present in 6%.

Diagnosis, classification and management of foetal arrhythmias

The 12-lead ECG that is so useful in newborn or adult cardiology suffers from major limitations in the foetus. Echocardiography is typically the only way to diagnose tachyarrhythmia in the foetus, and it is not easy to differentiate between different types of tachyarrhythmias. Supraventricular tachycardia with mostly 1 : 1 AV conduction can be distinguished from atrial flutter, with mostly 2 : 1 AV conduction block, due to excessive atrial frequency in flutter (about 440–480 bpm) translating into a 220–240 bpm ventricular rate. In AV re-entry, the time interval between the ventricular and atrial activity would be short, while in atrial tachycardia originating from ectopic foci, this time interval is usually prolonged. Ventricular tachycardia with typical dissociation of ventricular and atrial rhythm or conducted 1 : 1 from ventricles to atria is extremely rare in the foetus as most tachyarrhythmias originate in the atria. In such cases, it is clear that only an experienced physician trained in echocardiography can make the correct diagnosis.

The most frequent foetal tachyarrhythmia is supraventricular tachycardia represented by three different types: AV re-entrant tachycardia, permanent junctional reciprocating tachycardia and atrial ectopic tachycardia. The second most frequent foetal tachyarrhythmia is atrial flutter caused by a macro-re-entry circuit located in the atria. The final differentiation is often made only after birth when the arrhythmia persists or reoccurs, or a delta wave typical for the accessory pathway is present on the 12-lead ECG. The treatment strategy for most types of tachyarrhythmias is based on transplacental digoxin administration in non-hydropic foetuses. Sotalol, flecainide or amiodarone is mostly reserved for hydropic foetuses or more resistant tachyarrhythmias. Treatment is required for pure sinus tachycardia with typical heart rates of 180–200 bpm usually caused by foetal distress, foetal thyrotoxicosis, anaemia etc.

Sustained or prolonged bradycardia is present in 43% of significant foetal arrhythmia cases, as presented by Jaeggi & Nii (2005). Complete AV block accounts for 38%, and only 5% manifest as sinus bradycardia cases. The treatment of foetal bradycardia is limited. For significant number of foetuses with complete heart block caused by maternal autoantibodies, transplacental treatment with beta-receptor-stimulating agents, corticosteroids or immunosuppressives is recommended. In principle, foetal pacemaker implantation (Liddicoat *et al.* 1997) should be considered using minimally invasive techniques (Sydorak *et al.* 2001, Eghtesady *et al.* 2011, Nicholson *et al.* 2012).

During sinus bradycardia, there is 1 : 1 AV coupling with a slow frequency of atrial contractions (<100 bpm). Simple sinus bradycardia may be caused by foetal distress with episodes of hypoxia and blood flow redistribution, while brain and heart are supplied preferentially. Sinus bradycardia can be a manifestation of foetal long QT syndrome, and all newborns with a history of foetal heart rate below the 3rd percentile should be assessed for this entity early after birth (Mitchell *et al.* 2012). Sinus bradycardia may be a rare manifestation of sinus node dysfunction. Supraventricular bigeminy or trigeminy with AV block must always be excluded when assessing the foetus for bradycardia. The telltale sign would be an atrial frequency above that of the ventricle and an irregular heart rhythm. The outcome is usually benign and this arrhythmia mostly does not require treatment.

Foetal AV block

The most frequent cause of bradycardia is congenital AV block. First-degree AV block is characterized by prolonged AV conduction with 1 : 1 AV coupling. It is necessary to realize that AV conduction time increases during gestation and the exact numbers also differ for various ECHO modalities. Normal values for 30–34 weeks of gestational stage are 122.7 ± 11.1 ms by left ventricle inflow/outflow Doppler method, 116.5 ± 8.8 ms by Doppler method in the superior vena cava/aorta, 142.4 ± 14.2 by atrial contraction/ventricular systole as measured via Tissue Doppler Imaging (TDI) of the basal right ventricular free wall (Nii *et al.* 2006).

We distinguish two types of second-degree AV block. Wenckebach type (Mobitz I) second-degree AV block is characterized by the gradual lengthening of AV conduction time terminated by a dropped ventricular contraction. Mobitz type (Mobitz II) of second-degree AV block is typified by sudden loss of ventricular contraction, while AV conduction time remains unchanged. A specific type of Mobitz II AV block is 2 : 1 conduction when every second atrial beat is not conducted to the ventricles.

The third-degree AV block (complete heart block) has the most serious impact on further foetal development leading frequently to foetal demise. Atrial and

ventricular electrical and mechanical activities are completely independent in this type of AV block. This always leads to significant and prolonged bradycardia. The only physiological pathway to compensate the decrease in cardiac output caused by bradycardia is the Frank-Starling mechanism which might be limited at early stages according to data from animal experiments (Kockova *et al.* 2013). When increased stroke volume fails to compensate severe foetal bradycardia, heart failure occurs leading to foetal hydrops.

Foetal complete heart block occurs more frequently in conjunction with various congenital structural heart diseases (Stewart *et al.* 1983, Jaeggi & Nii 2005, Vergani *et al.* 2005). Schmidt reported that 53% of foetuses diagnosed with complete heart block had associated complex congenital heart disease (Schmidt *et al.* 1991). Another major reason for congenital complete heart block is maternal autoimmune disease such as lupus erythematosus, Sjögren syndrome, rheumatoid arthritis or unclassified systemic rheumatoid disease. Elevated titres of anti – Ro/SSA and anti – La/SSB antibodies are typically found in mothers affected by the above-mentioned autoimmune diseases. The risk of developing foetal complete heart block in pregnant women with positive anti-Ro/SSA antibodies is about 2% (Brucato *et al.* 2001). These antibodies cause myocardial inflammation specifically affecting the AV node leading to various degrees of AV conduction impairment, which usually occurs around 20–24 gestational weeks. This might also present as endomyocardial fibrosis in the foetus or newborn. Because complete heart block has been shown to be associated with very high mortality rates ranging between 18% and 43% (Jaeggi & Nii 2005), there has been a major effort to prevent this autoimmune disease. Corticosteroids were administrated to pregnant women with positive titres of autoantibodies intravenously or orally (Reinisch *et al.* 1978, Friedman *et al.* 2009), but major side effects were noticed afterwards including oligohydramnion, foetal adrenal suppression, intrauterine grow retardation and so on. Corticosteroid treatment is recommended only for advanced heart block with significant and prolonged bradycardia with a high risk of hydrops development. Isolated prolongation of AV conduction only rarely leads to progressive AV block, as shown by Jaeggi *et al.* (2011) in anti-Ro and anti-La positive mothers, and corticosteroid treatment is therefore not recommended. Recently, current recommendations of the American Heart Association regarding diagnosis and management of foetal heart disease, including prenatal arrhythmias, were summarized in a form of Scientific Statement (Donofrio *et al.* 2014).

Importance of the cardiac conduction system for the origin of arrhythmias

It is widely recognized in clinical practice that the cardiac conduction system (CCS) can be a focal point of arrhythmogenesis (Braunwald *et al.* 2001). This propensity was extensively analysed from developmental perspective by Jongbloed and associates (Jongbloed *et al.* 2004) using CCS-LacZ transgenic mouse model. Detailed analysis of the developing CCS was performed on hearts at embryonic day (ED) 9.5–15.5 stained for beta-galactosidase activity and co-stained with the myocardial marker HHF35 followed by three-dimensional reconstruction. CCS-lacZ expression detected by X-gal staining was observed in the sinoatrial node, left and right venous valves, septum spurium, right and left AV ring, His bundle, bundle branches, moderator band, Bachmann's bundle, left atrial posterior wall surrounding the pulmonary venous orifice and later on in the pulmonary vein wall. These data supported the idea that areas derived from the developing CCS may form the arrhythmogenic substrate in adult hearts.

A comparative study between patients with left atrial tachycardia originating from the junction of mitral annulus and aortic ring and mouse embryos demonstrated the presence of the developing specialized conduction system in this region starting at embryonic age 11.5 (Gonzalez *et al.* 2004).

Particular attention was focused on the developmental origin of pulmonary vein myocardium (Mommersteeg *et al.* 2007a), which is derived from the second heart field. The area around the pulmonary veins entrance is in humans a frequent site of origin of atrial fibrillation, so its electrical insulation by catheter intervention is a frequent procedure during clinical intervention for ablation of this increasingly prevalent human arrhythmia. A recent study based on HCN4-Cre mouse line with LacZ or eGFP reporter (Liang *et al.* 2013) precisely delineated relative contributions of first and second heart lineages to the CCS and provided a time line of developmental expression of this CCS marker in concert with other markers during its formation.

Genetic and epigenetic determination of the CCS

To better appreciate the developmental potential of CCS to generate arrhythmias, one needs to consider the mechanisms governing its induction and patterning (reviewed in (Gourdie *et al.* 2003), (Christoffels *et al.* 2010). Lineage tracing experiments performed by the Mikawa lab have shown that cardiac pacemaker cells

  doi: 10.1111/apha.12418

are physically segregated and molecularly programmed in a tertiary heart field prior to the onset of cardiac morphogenesis, and this process depends on Wnt signalling (Bressan *et al.* 2013). Recently, the genetic cascade governing specification of cardiac pacemaking tissues was elucidated by the Amsterdam group (Mommersteeg *et al.* 2007b). Restricted expression pattern of the homeodomain transcription factor Shox2 in the sinus venosus myocardium, including the sinoatrial nodal region and the venous valves, was found to be important for the recruitment of these cells to the pacemaking fate (Blaschke *et al.* 2007). The authors furthermore demonstrated aberrant expression of gap junction proteins connexin 40 and 43 as well as the transcription factor Nkx2.5 specifically within the sinoatrial nodal region, leading to embryonic lethality between ED11.5 and ED13.5 in $Shox2^{-/-}$ mice. Finally, they showed that Shox2 deficiency interferes with pacemaking function in embryonic zebrafish *in vivo*. Particular attention was also devoted to specification of pulmonary venous myocardium (Mommersteeg *et al.* 2007a), which is a significant source of atrial fibrillation. Genetic labelling reveals that atrial cells do not contribute to this specific population, characterized by Nkx2.5 expression distinguishing it from the systemic venous return. Maintenance of this phenotype is dependent on Pitx2c, which prevents it from adopting the Cx40-negative, Hcn4-positive pacemaking phenotype of the right-sided sinoatrial node.

Embryonic pacemaking differs in details from the mechanisms operating in the adult sinoatrial node. The early stages are crucially dependent on the calcium clock, as demonstrated by Wakimoto *et al.* (2000) who studied the functional importance of sodium-calcium exchanger (NCX) for heartbeat initiation and maintenance. To address this question, they generated Ncx1-deficient mice by gene targeting to determine the *in vivo* function of the exchanger. The hearts of $Ncx^{-/-}$ embryonic deficiency in Ncx, embryos did not beat, and cardiomyocytes frequently underwent apoptosis leading to embryonic lethality between ED9 and ED10.

To study cardiac physiology near the onset of the heartbeat in embryonic mouse hearts, Chen and associates performed dual optical mapping of membrane voltage and intracellular calcium (Chen *et al.* 2010). Action potentials and calcium transients were detected in approx. 50% of mouse embryo hearts at ED8.5 and 100% at E9.0, indicating that the heartbeat starts between ED8 and ED9. Cardiac activity was abolished by calcium channel blocker nifedipine and the I (f) blocker ZD7288, suggesting that both HCN4 and voltage-dependent calcium channels are important for embryonic pacemaking. The role of sodium channels and intracellular calcium cycling is of lesser importance at this early stage.

From the functional side, endothelin signalling was shown to be necessary not for specification like in birds (Gourdie *et al.* 1998), but normal function of the embryonic pacemaker in mammals (Karppinen *et al.* 2013). Stimulation with endothelin-1 increased beating frequency of ED9–ED11 cardiomyocytes. Inhibition by receptor antagonist tezosentan led to dose-dependent bradycardia *in vitro* as well as *in utero*, but only during the early (ED12.5) and not late (ED18.5) embryonic stages. Irregular rhythm was also observed, and use of specific antagonists indicated that the effects are mediated via endothelin receptor B.

Location of the first activation site in the rat embryonic heart was investigated by the Kamino group (Hirota *et al.* 1985). At the time of heartbeat initiation, the first pacemaking activity was located in the left side of the sinus venosus, but within a few hours migrated to the right side, where the definitive pacemaker is located. A similar situation was reported also in avian embryos; remnants of this initial left-sided activity were reported in a small proportion of normal avian hearts at later stages of development (Sedmera *et al.* 2006); under normal conditions, no such left-sided activity was reported in a large series of embryonic mice (Leaf *et al.* 2008, Ammirabile *et al.* 2012, Benes *et al.* 2014).

Considerably less is known about the mechanisms regulating specification of the remaining components of the CCS. Neuregulin was proposed as a factor influencing differentiation of the ventricular myocytes towards the conduction phenotype (Rentschler *et al.* 2002), but this secreted molecule has many important functions in the embryonic cardiomyocytes, such as their survival (Liu *et al.* 2010). The neuregulin/Erb signalling cascade could function in concert with endothelin signalling, which was shown to be important in Purkinje fibre differentiation in the chick (Gourdie *et al.* 1998, 2003, Takebayashi-Suzuki *et al.* 2000, Sedmera *et al.* 2008). Other important factors participating in formation of the His bundle and its branches include Nkx2.5 (Jay *et al.* 2004), Irx3 (Zhang *et al.* 2011) and T-box transcription factors (Jerome & Papaioannou 2001, Moskowitz *et al.* 2004, Hoogaars *et al.* 2007, Aanhaanen *et al.* 2009, Frank *et al.* 2012).

Differentiation of embryonic myocytes into the conducting phenotype is governed also by the epigenetic factors, of which mechanical loading is of the most critical importance. *In vitro* unloading of chick embryonic hearts (Sankova *et al.* 2010) led to de-differentiation of the ventricular conduction system that could be rescued by ventricular stretching using a droplet of silicone oil. These experiments resolved the issue

arising from previous *in vivo* studies using altered haemodynamics models (Reckova *et al.* 2003, Hall *et al.* 2004) that showed that increased hemodynamic loading accelerated, while reduced ventricular preload inhibited ventricular CCS differentiation by attributing the stimulus to myocyte stretching, rather than to shear stress-induced signalling from the endocardium.

Studies on chick embryos *in vivo* showed that hypoxia can accelerate maturation of the AV junction and lead to earlier appearance of mature (apex-to-base) ventricular activation patterns (Nanka *et al.* 2008), possibly through increased apoptosis of the AV myocardium. Another player in developing proper fibrous insulation of the AV junction is the developing epicardium (Kolditz *et al.* 2007, 2008), and perturbations of this process may lead to ventricular pre-excitation. Electrical insulation of the His bundle is also dependent on immigrating cardiac neural crest cells (Gurjarpadhye *et al.* 2007).

Spontaneously occurring arrhythmias in embryos

This area of embryonic arrhythmias is not well investigated for numerous reasons. First, there are the methodological difficulties inherent to all observational studies of mammalian embryos that are shielded *in utero* by maternal tissues. The most significant breakthrough in this respect was availability of high-resolution ultrasound (Phoon *et al.* 2002, Phoon 2006, Nomura-Kitabayashi *et al.* 2009, Lo *et al.* 2010), paralleling the advances in human embryonic echocardiography (Maeno *et al.* 1999, Pedra *et al.* 2002). The second obstacle is the relative rarity of such events (compare with the situation in clinical settings, discussed above) necessitating the examination of large numbers of embryos. Therefore, most arrhythmias detected in the embryonic hearts could be at least in part be due to 'gentle' alterations of physiological conditions, as it is close to impossible to monitor the embryonic mammalian heart in a completely non-invasive manner.

Various arrhythmias in the isolated mouse embryonic heart were revealed using simultaneous voltage and calcium optical mapping (Valderrabano *et al.* 2006). The focus of this study was on AV conduction during transition from immature base-to-apex to mature apex-to-base ventricular activation pattern. The authors hypothesized that after this transition, the remnants of the myocardial AV ring remain transiently able to conduct, providing a possible substrate for arrhythmias. They noted that arrhythmias were rare under normal conditions, with only occasional AV blocks (4%) and junctional rhythms in four of 309 embryonic hearts analysed. The frequency notably increased after isoproterenol stimulation with 6% incidence of ventricular ectopic rhythms. Addition of carbachol after isoproterenol caused dissociated antegrade and retrograde AV ring conduction in almost 10% of ED10.5–ED11.5 hearts. Re-entry persisting for multiple beats was also observed, but none occurred at ED9.5. Rare cases of irregular rhythm (sinoatrial and AV block, alternating patterns of ventricular activation) were also observed in our large mouse series (Sankova *et al.* 2012), while ectopics originating from the outflow tract myocardium were seen exclusively in ED10.5–ED11.5 hearts cultured for 24 h (Vostarek *et al.* 2014). AV re-entry was observed as a rarity in one ED4 chick heart (Fig. 2).

Genetic mouse models of arrhythmias

As noted above, spontaneous arrhythmias are very rare in normal embryonic hearts, thus facilitating analysis of results in experimental perturbation models. The importance of catecholaminergic signalling in development and function of the CCS was recently reported by Steve Ebert's group (Baker *et al.* 2012). These results are in good agreement with previous studies showing lethality of mouse embryos deficient in a component of adrenergic signalling, beta-adrenergic receptor kinase (Jaber *et al.* 1996).

Studies by Collin Phoon validated ultrasound biomicroscopy as a prime tool for *in vivo* identification of abnormal mouse embryonic heart function, including arrhythmias. Using this technique, they studied longitudinally embryonic ED10.5–ED14.5 NFATc1$^{-/-}$ embryos and control littermates (Phoon *et al.* 2004). The null embryos, lacking the outflow valves, die prior to completion of ventricular septation from presumed heart failure. The authors showed that abnormal blood flow was present at E12.5 when outflow valves normally first develop. Reduced cardiac output and diastolic dysfunction contributed to heart failure, but contractile function remained unexpectedly normal. The only arrhythmia detected prior to embryonic demise was progressive bradycardia, indicating that embryonic heart failure occurs rapidly in this mouse model.

Mutations in TBX3 cause congenital anomalies in patients with ulnar-mammary syndrome (Frank *et al.* 2012). Data from both mice and humans suggest multiple roles of this transcription factor in morphogenesis and function of the CCS. Disruption of Tbx3 function in different regions of the developing heart caused discrete phenotypes and lethal arrhythmias. Sinus pauses (normally present at low frequency in adult mice) and bradycardia indicated sinoatrial node dysfunction; pre-excitation and AV block revealed problems in the AV junction. These arrhythmias were accompanied by perturbed expression of several ion

  doi: 10.1111/apha.12418

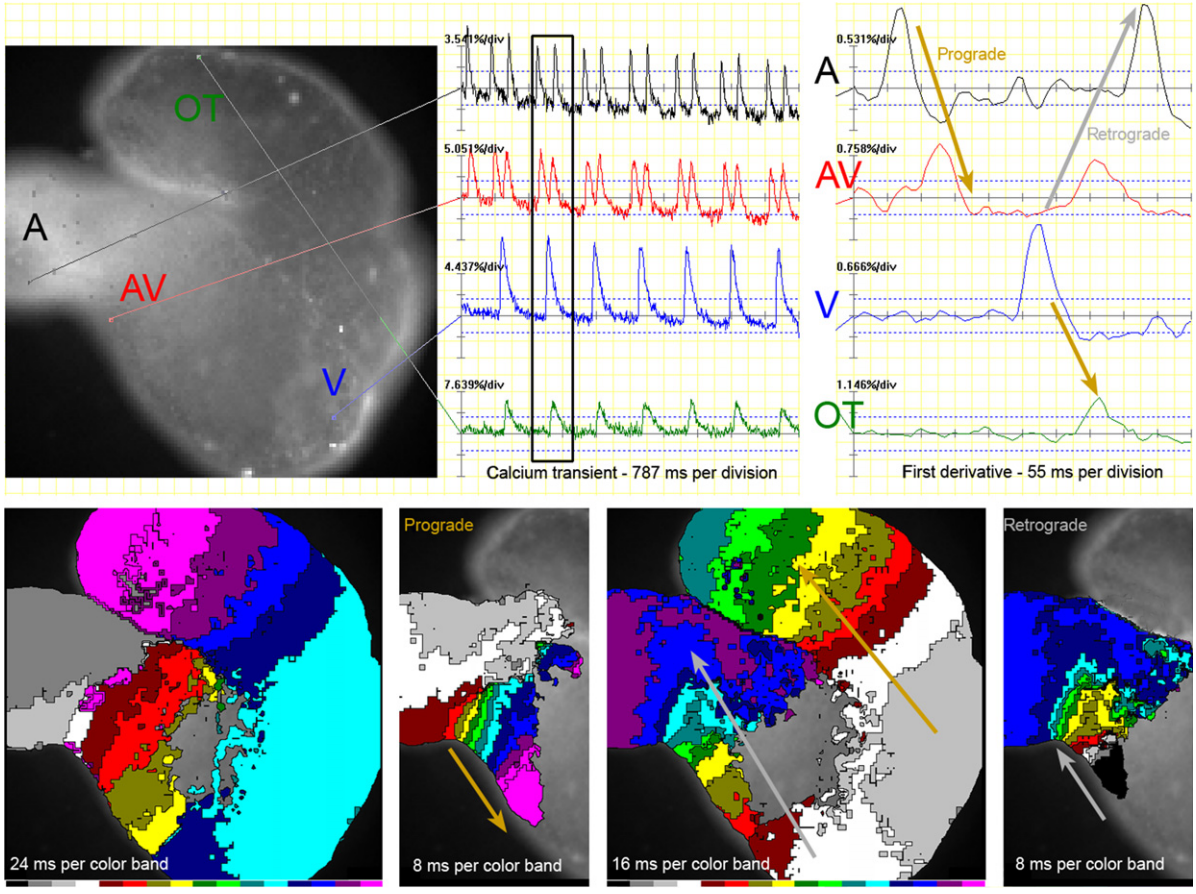

Figure 2 Atrioventricular re-entry in ED4 chick embryonic heart. Top panels show the embryonic heart from the back and time course of calcium transients. The first derivative panel shows both prograde activation (from the atrium to the ventricle to the outflow tract, orange arrow) and retrograde activation from the ventricle back to the AV canal and atrium (grey arrow). Activation maps in the bottom depict this phenomenon at different temporal scales. Note that the activation pattern of the atrium differs between prograde and retrograde activation. A, atrium; AV, atrioventricular canal; V, ventricle; OT, outflow tract. For better visualization of the activation sequence, see the Movie S1.

channel components (e.g. upregulation of Kcne3, Chac1, Kcnj4 and downregulation of Scn7a), despite normal expression of previously identified CCS markers, raising the possibility of functional disturbances in apparently morphologically normal CCS.

The Notch signalling cascade was found to be important in regulation of AV conduction in the mouse (Rentschler *et al.* 2011), and activation of Notch signalling during development consistently led to accessory AV pathways and pre-excitation. On the other hand, inhibition of this cascade led to AV node hypoplasia and loss of expression of slowly conducting connexin 30.2 gap junction channels, resulting in shortened AV delay.

Drug-induced arrhythmias in mammalian models

A significant worry of every clinician taking care of women of childbearing age is the teratogenic potential of prescribed medicines. This does not only impact overt morphological anomalies, but also more subtle functional alterations, such as mild neurological defects, or indeed, embryonic arrhythmias that in extreme cases can lead to embryonic or foetal death.

As mentioned above, propensity to arrhythmia depends considerably on developmental stage. At the earliest stages, where the heart is small and conduction generally slow, the only 'allowed' arrhythmias are alterations of heart rate of which bradycardia is the most dangerous as it can lead to reduced cardiac output and embryonic death. Once the cardiac chambers are formed (Moorman *et al.* 2010), alternating regions of fast and slow conduction develop, creating a heterogeneity in conduction that can lead to unidirectional or bidirectional blocks, re-entry and more complex arrhythmias (Valderrabano *et al.* 2006). With further development, the heart becomes more complex with the establishment of the coronary vascular network and autonomic innervation (Hildreth

et al. 2009). In humans, sensitivity to bradycardia in premature infants suggests that the heart rate response to cholinergic stimulation may change during development (Maurer 1979). This hypothesis was tested on isolated intact foetal mouse hearts (ED13–ED22). Acetylcholine led to a marked (−50%) heart rate decrease in the micromolar range in ED13–ED14 hearts, but the decrease was progressively blunted with increasing age with a mere 3% drop at ED21–ED22 with the same dose. Physostigmine significantly enhanced the cholinergic response in older hearts, suggesting that the effect is at least in part due to increasing intrinsic cholinesterase activity with gestational age.

Unlike the adult heart, whose energy needs are mostly met by fatty acid oxidation, the developing myocardium relies mostly on glycolysis. Chen *et al.* (2007) investigated how inhibition of glycolysis affects membrane voltage and calcium transients in embryonic mouse hearts. Glycolysis inhibition by 10 mM 2-deoxyglucose or 0.1 mM iodoacetate decreased significantly heart rate and induced (unspecified) arrhythmias in over 50% of the treated hearts. Similar effects were noted when oxidative phosphorylation was blocked by 500 nM p-(trifluoromethoxy)phenylhydrazone. During experiments aimed at elucidation of pacemaking mechanisms in early mouse heart (Chen *et al.* 2010), the investigators observed various arrhythmias, including AV re-entry induced by adenosine (ADO). This occurred at stages that had already differentiated fast-conducting atrial and ventricular chamber myocardium and slowly conducting AV canal.

Anti-epileptic drugs frequently act on ion channels regulating membrane potential in excitable tissues; some of these channels are present also in the developing heart. This could be one explanation for the known teratogenic potential of these substances. Danielsson *et al.* (1997) investigated the capacity of phenytoin, a hERG channel blocker inhibiting the IKr that is critical for embryonic heart function, to induce embryonic hypoxia via adverse effects on the embryonic heart using a whole embryo culture model. In these mouse embryo studies, phenytoin caused a concentration-dependent decrease in embryonic heart rate, with temporary or permanent cardiac arrest at the highest dosage. The exact concentration, as well as incidence of other arrhythmias, was strain-dependent. Similar results were obtained in rat embryos.

Arrhythmogenic properties of phenytoin were examined in mouse (Azarbayjani & Danielsson 2002). Between ED9 and ED13, a dose-dependent bradycardia and other unspecified arrhythmias such as AV block were observed at maternal plasma concentrations in the micromolar range. Patch-clamp recording on HERG-transfected cells demonstrated that phenytoin inhibits the inward rectifier potassium current. The authors attributed these effects to reactive oxygen species (ROS) generated at reoxygenation after resumption of normal rhythm, as an antioxidant agent alpha-phenyl-*N*-tert-butyl-nitrone showed protective effects. A similar mechanism was proposed for another teratogenic anti-epileptic drug, trimethadione and its pharmacologically active metabolite dimethadione. The same group of investigators then followed up by showing that these effects were exacerbated in combination with several anti-epileptics (phenytoin, phenobarbital, dimethadione and carbamazepine), supporting the idea that the increased risk for malformations following polytherapy is linked to an increased risk for cardiac rhythm disturbance (Danielsson *et al.* 2007).

Almokalant, a class III anti-arrhythmic drug, caused embryotoxicity in the mouse (Skold & Danielsson 2000), most likely secondary to its adverse effects on the embryonic heart, as dose-dependent bradycardia and periods of cardiac arrest were observed in whole embryo culture at ED10. Thus, all drugs capable of causing embryonic bradycardia should be regarded as potentially embryotoxic and used during pregnancy with extreme caution.

Chick embryonic model

The cardiac electrical activity in the chick embryo has been investigated in pioneering works, *in vivo* (Van Mierop 1967, Rajala *et al.* 1984, Tazawa *et al.* 1989, Sugiyama *et al.* 1996), in the intact embryo (Hoff & Kramer 1939, Paff *et al.* 1964), the dissected heart (Paff *et al.* 1968, Paff & Boucek 1975, Kasuya *et al.* 1977, Hirota *et al.* 1987), isolated cardiac chambers (Boucek *et al.* 1959, Arguello *et al.* 1986) and in cultured cardiomyocytes (Shrier & Clay 1982). In particular, ECG of the whole heart displays characteristic P, QRS and T components which allows assessment of the beating rate from PP or RR interval, AV conduction from PR interval, duration of the ventricular activation from QT interval and intraventricular conduction from of the QRS complex width. The spatio-temporal interpretation of the ECG is facilitated by the fact that ventricular activation occurs in a 'base-to-apex' fashion, and there is no differentiated conduction system at early developmental stages (Chuck *et al.* 1997, Reckova *et al.* 2003).

The principal types of arrhythmias observed in the validated 4-day-old embryonic chick heart model under various stresses (e.g. anoxia–reoxygenation) or exposed to pharmacological agents are transient atrial tachycardia (range 180–300 bpm) and bradycardia (range 110–140 bpm), atrial ectopy, first-degree atrioventricular blocks (AVB), second-degree AVB (2 : 1 to

  doi: 10.1111/apha.12418

8 : 1), Wenckebach phenomenon (Mobitz type I), third-degree AVB (ventricular escape beats) and bursts of irregular activity followed by intermittent atrial arrest (cardioplegia) as previously documented (Sarre *et al.* 2006) and presented in Figure 3. Some of these arrhythmias resemble those observed in the human foetus (Strasburger & Wakai 2010).

Effects of drugs inducing arrhythmias can be conveniently studied in the chick embryo *in vivo*. Paff and collaborators described heart blocks after digoxin treatment (Paff *et al.* 1964), defining the stage of chamber formation as critical for induction of conal (40 h of incubation) and AV block (42 h). Before these stages, the only reaction of the embryonic heart to drug treatment was complete cardiac arrest. The authors noted similarity between this AV block and the situation in humans, including the Wenckebach phenomenon. The Rochester group studied effects of

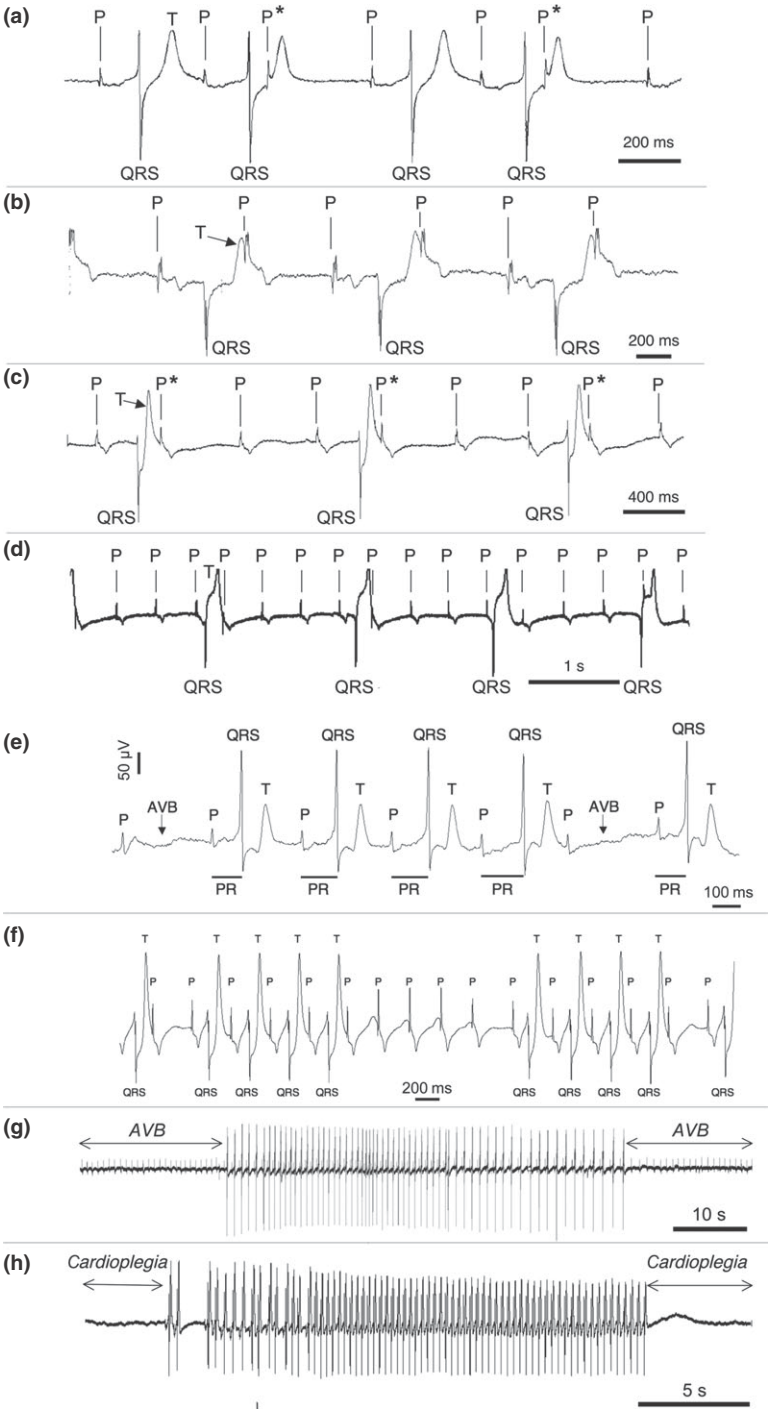

Figure 3 Examples of major types of arrhythmias observed in the 4-day-old embryonic chick heart. ECG of the isolated heart displays characteristic P wave, QRS complex and T wave components. (a) Atrial ectopy, (b) 2 : 1 AVB, (c) atrial ectopy + 3 : 1 AVB, (d) ventricular escape beats (third-degree AVB), (e) Wenckebach phenomenon (Mobitz type I), (f) episode of heart block + Wenckebach, (g) third-degree AVB + bursting activity and (h) intermittent sinoatrial arrest (cardioplegia) + bursting activity. AVB, atrioventricular block. Asterisk indicates atrial premature beat.

various cardiac drugs on the developing cardiovascular system. Isoproterenol at a teratogenic dose induced increased vascular resistance and reduced cardiac output (Clark *et al.* 1985), suggesting the presence of a functional adrenergic signalling system in the 4-day-old embryonic heart. On the other hand, chronic verapamil (calcium antagonist) infusion decreased both cardiac and embryonic growth through decreased cardiac performance (Clark *et al.* 1991, Sedmera *et al.* 1998) and led to delayed ventricular morphogenesis (increased trabeculation, decreased compact layer thickness). Recently, Kockova and colleagues studied the effects of beta blockers and ivabradine on cardiac function and embryonic survival (Kockova *et al.* 2013). High doses led to mortality through decreased cardiac output, based upon bradycardia and insufficient Frank-Starling compensation. Partial AV blocks were also observed in both early (day 4) and later (day 8) embryos.

Arrhythmias during anoxia–reoxygenation

In the 4-day-old embryonic chick heart model (Raddatz *et al.* 1997, Sarre *et al.* 2006), the chrono-, dromo- and inotropic disturbances and the ultrastructural modifications (e.g. mitochondrial and nuclear swelling) induced by 30-min anoxia followed by 60-min reoxygenation are reversible within a period of time depending on the developmental stage; the older the embryo, the lower the reversibility (Sedmera *et al.* 2002). Anoxia induces bradycardia, atrial ectopy, first-, second-, and third-degree AVB and transient cardioplegia. Reoxygenation provokes also the Wenckebach phenomenon and ventricular escape beats. At the onset of reoxygenation, PR, QT and ventricular electromechanical delay (reflecting excitation-contraction (EC) coupling) significantly increase, whereas atrial EC coupling remains unchanged. Ventricular contractility at the apex and intraventricular conduction are also significantly reduced by anoxia–reoxygenation (Fig. 4), but no fibrillations, no re-entry and no ventricular ectopic beats are observed. At reoxygenation, arrhythmias and conduction disturbances are associated with a burst of ROS production (Sarre *et al.* 2005, Raddatz *et al.* 2011) and reduced by the antioxidant ascorbic acid (Fig. 5). Although the presence of glucose at the physiological concentration of 8 mM prolongs cardiac activity during anoxia, it enhances the reoxygenation-induced ROS production and arrhythmias relative to glucose-free conditions (Tran *et al.* 1996, Raddatz *et al.* 2011). This observation underscores the role that alterations of glycolytic activity may play in arrhythmogenesis associated with ROS. Nitric oxide (NO) at supraphysiological concentration delays post-anoxic recovery of AV propagation, and sinoatrial pacemaker cells are less responsive to NO (Terrand *et al.* 2003). An NO synthase inhibitor (L-NAME) prolongs the ventricular electromechanical delay during anoxia and delays its recovery during reoxygenation, while an NO donor (DETA-NONOate) has opposite effects (Maury *et al.* 2004). Thus, a NO-dependent pathway appears to contribute to regulation of ventricular excitation–contraction coupling in the anoxic–reoxygenated embryonic heart.

It should also be mentioned that a cycle of cooling (4 °C, 30 min)/rewarming (37 °C, 60 min) under normoxia is less arrhythmogenic than anoxia (30 min) followed by reoxygenation (60 min). However, between 15 and 20 min of rewarming, when temperature rises from 27 to 31 °C, the beating rate

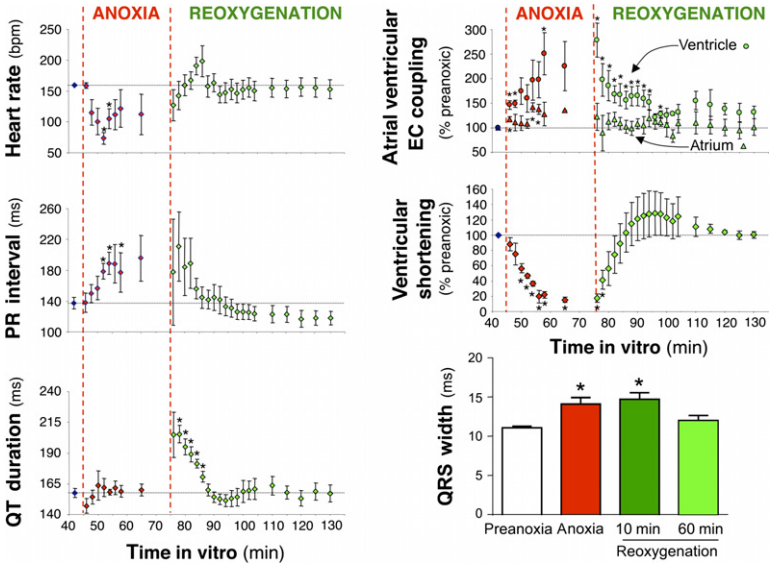

Figure 4 In a 4-day-old chick embryonic heart, heart rate, atrioventricular (AV) propagation (PR interval), QT duration, atrial and ventricular excitation-contraction (EC) coupling, contractility (apical ventricular shortening) and intraventricular conduction (QRS width) are markedly altered during anoxia and reoxygenation, but fully recover after 30–40 min. Mean ± SEM; $n = 4$; $n = 20$ for QRS determination; bpm, beats per minute. $^*P < 0.05$ vs. preanoxic values.

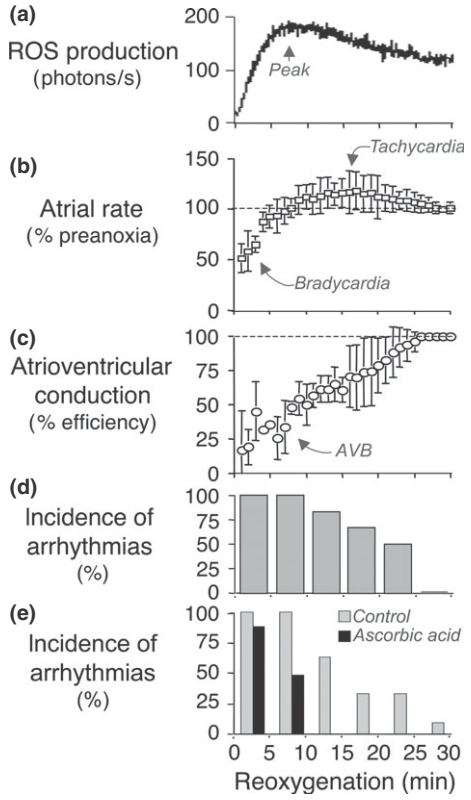

Figure 5 Functional recovery of the 4-day-old embryonic chick heart during the first 30 min of reoxygenation after preceding 30 min of anoxia. (a) typical reactive oxygen species (ROS) production determined by lucigenin-induced chemiluminescence peaking after about 8 min (arrow). (b) atrial rate reported as percentage of the pre-anoxic value. (c) efficiency of the atrioventricular (AV) propagation calculated as the ratio of the ventricular to the atrial electrical activity duration and expressed as a percentage, 100% representing one-to-one AV conduction. (d) highest incidence of arrhythmias is associated with the burst of ROS. (e) antioxidant ascorbic acid (Vit C, 10 mM) reduces incidence of arrhythmias. Mean ± SD; horizontal dashed lines represent basal pre-anoxic levels; b and c: $n = 3$; d and e: $n = 6$.

transiently accelerates, the PR interval is prolonged, and the rate of recovery of QT decreased, clearly indicating that this range of temperature is critical for the return to normal rhythmicity (Sarre *et al.* 2006).

Acidosis (transition from pH 7.4 to 6.5), which can occur under prolonged anoxia, has negative chrono-, dromo- and inotropic effects, essentially characterized by intermittent atrial and ventricular activity (bursts). At pH 6.5, heart rate and AV conduction velocity remain significantly decreased, whereas ventricular shortening and contractility recover after 5 min. Under acidotic anoxia and during reoxygenation, inactivation of HCO_3-dependent mechanisms increases the incidence of arrhythmias. This indicates that in the anoxic–reoxygenated embryonic heart pH regulation appears to depend predominantly on HCO_3 availability and transport. The Na^+/H^+ exchange (NHE) appears to be protective only under anoxia (Meiltz *et al.* 1998).

Under normoxia, H_2O_2 differentially modulates ERK, p38 and JNK pathways in atria, ventricle and outflow tract (Gardier *et al.* 2010). Only exposure to a rather high concentration of H_2O_2 (>500 μM) leads to cardioplegia and markedly increased phosphorylation of ERK2 and p38 specifically in atria and outflow tract, without modifying the level of JNK phosphorylation. Moreover, during the post-anoxic reoxygenation, the phosphorylation level of ERK2 and p38 is altered specifically in the ventricle. During the early phase of post-anoxic reoxygenation, the Janus Kinase 2/Signal Transducer and Activator of Transcription 3 (JAK2/STAT3) pathway is activated by ROS, interacts with Reperfusion Injury Salvage Kinase (RISK) proteins [(PI3K, Akt, Glycogen Synthase Kinase 3beta (GSK3beta)), Extracellular signal-Regulated Kinase 2 (ERK2)] and reduces arrhythmias (Pedretti & Raddatz 2011).

The hyperpolarization-activated cyclic nucleotide-gated (HCN) channels are expressed very early during cardiogenesis and play an important role in the control of the rate of diastolic depolarization in pacemaker cells of atria, ventricle and outflow tract (Sarre *et al.* 2010). Inhibition of the HCN channels by ivabradine has a negative chronotropic effect in all these cardiac regions (characterized by a decreasing AV-conotruncal gradient of intrinsic beating rate) and stabilizes the PR interval under normoxia but does not alter the types and duration of arrhythmias during anoxia–reoxygenation.

Pharmacological opening of the mitochondrial KATP channel by diazoxide selectively improves recovery of the PR interval and ventricular E-C coupling during reoxygenation, via NO-, ROS- and PKC-dependent pathways (Sarre *et al.* 2005) and reduces reoxygenation-induced JNK activity in the ventricle (Sarre *et al.* 2008). Furthermore, the open-state of the sarcolemmal L-Type Ca^{2+} channel, mitochondrial Ca^{2+} uniporter and mitochondrial KATP channel can be a major determinant of JNK activity and anoxia–reoxygenation-induced arrhythmias.

The TRPC1, 3, 4, 5, 6 and 7 isoforms of the voltage-insensitive cationic transient receptor potential canonical (TRPC) channels are expressed in the heart of 4-day-old chick embryos and can form a macromolecular complex with the alpha1C subunit of the L-type voltage-gated calcium channel (Cav1.2). Under normoxia, inhibition of TRPCs by SKF96365 leads to negative chrono-, dromo- and inotropic effects, prolongs QT interval and triggers Wenckebach phenomenon, clearly indicating that inactivation of these

channels is implicated in arrhythmias. Blockade of the TRPC3 isoform by Pyr3 affects AV conduction specifically, whereas inhibition of all TRPCs by SKF combined with that of Cav1.2 by nifedipine results in severe arrhythmias and finally in cardioplegia (Sabourin *et al.* 2011).

Proarrhythmic Ca^{2+} overload can result from Ca^{2+} entry through sarcolemmal voltage-dependent L-type and T-type Ca^{2+} channels (Cav1.2 and Cav3.1, respectively) and voltage-independent cation channels (TRPC), as well as Ca^{2+} release from the sarcoplasmic reticulum after anomalous activation of ryanodine receptor (RyR2) channels by ryanodine (Tenthorey *et al.* 1998) and/or inhibition of sarco/endoplasmic reticulum Ca2+-ATPase (SERCA) by thapsigargin (Sabourin *et al.* 2012). The L-type Ca^{2+} channel agonist Bay-K-8644 induces atrial tachycardia and tends to prolong arrhythmias during reoxygenation (Bruchez *et al.* 2008). ROS and reactive nitrogen species (RNS) are known to alter the redox state and increase activity of RyR2 leading to a potentially proarrhythmic Ca^{2+} release. Pharmacological opening of RyR channels with ryanodine (10 nM) triggers severe arrhythmias (mainly bursting activity) under normoxia and during anoxia and reoxygenation, whereas verapamil (10 nM), an antagonist of L-type Ca^{2+} channel at this concentration, affords protection against reoxygenation-induced arrhythmias (Tenthorey *et al.* 1998). Furthermore, relative to the Cav3.1 channel (T-type), the Cav1.2 channel (L-type) plays a major role in spontaneous electrical activity of the embryonic chick heart. Indeed, inhibition of Cav1.2 with nifedipine induces a progressive and significant shortening of QT and prolongs the ventricular electromechanical delay, whereas specific inhibition of Cav3.1 with mibefradil has only a slight effect (Sabourin *et al.* 2011).

Adenosine is a crucial regulator of the developing cardiovascular system, derives from intra- and extracellular ATP degradation and accumulates in the myocardial interstitial fluid under hypoxia or ischaemia. In the embryonic heart, developing normally in an environment poor in oxygen, the physiological concentration of ADO is much higher than in the adult normoxic heart and ADO metabolism relies on ecto-nucleoside triphosphate diphosphohydrolase (CD39), ecto-5′-nucleotidase (CD73), adenosine kinase (AdK) and ADO deaminase (ADA). CD39 and CD73 sequentially convert ATP to ADO and ADA convert ADO into inosine (INO). ADO is transported by equilibrative (ENT1,3,4) or concentrative (CNT3) transporters and interacts with the four subtypes of ADO receptors (AR), A_1AR, $A_{2A}AR$, $A_{2B}AR$ and A_3AR (Robin *et al.* 2011, 2013). ADO or A_1AR activation transiently provokes bradycardia, second-degree AVB and Mobitz type I second-degree AVB (Wenckebach phenomenon). These transient pacemaking and AV conduction disturbances are induced by A_1AR activation through concomitant stimulation of NADPH oxidase and phospholipase C (PLC), followed by downstream ROS-dependent activation of ERK2 and ROS-independent activation of PKC with Cav1.2 channel as a possible target (Robin *et al.* 2011). Furthermore, A_1AR activation mediates also a proarrhythmic Ca^{2+} entry through the TRPC3 channel functioning as a receptor-operated channel, via the stimulation of the PLC/DAG/PKC cascade in atrial and ventricular cardiomyocytes (Sabourin *et al.* 2012). Inactivation of ENTs (i) increases myocardial ADO level, (ii) provokes atrial ectopy and AVB, (iii) prolongs P wave and QT interval and (iv) increases ERK2 phosphorylation. Inhibition of CD73, MEK/ERK pathway or A_1AR prevents these arrhythmias. Exposure to INO also causes arrhythmias associated with AVB and ERK2 phosphorylation, which are prevented by A_1AR or $A_{2A}AR$ antagonists exclusively or by MEK/ERK inhibitor. Thus, disturbances of nucleoside metabolism and transport can lead to interstitial accumulation of ADO and INO and provoke arrhythmias in an autocrine/paracrine manner through A_1AR and $A_{2A}AR$ stimulation and ERK2 activation (Robin *et al.* 2013).

Pathogenesis of autoimmunity-caused congenital heart block

It is well recognized that maternal antibodies causing lupus pass the placenta and can induce prenatal or congenital heart block (CHB, reviewed in (Buyon & Clancy 2003)). Current understanding of its pathogenesis was obtained from animal models that were instrumental in revealing its mechanisms. It is believed that the foetal cardiomyocytes undergoing apoptosis such as those in the AV canal (Cheng *et al.* 2002) expose the originally intracellular Ro and La antigens to their surface, where they can be bound by circulating maternal autoantibodies (anti-SSA/Ro-SSB/La). The macrophages then phagocytose these 'opsonized' cells, leading to the secretion of pro-inflammatory and pro-fibrotic cytokines, leading to fibrosis (which does not normally occur during prenatal tissue healing), differentiation of myofibroblasts and scarring. This overshoots the normal process of reduction of the originally broad myocardial connection between the atria and ventricles to His bundle and leads in extreme cases to a complete ventricular block. More recent studies (Kamel *et al.* 2007) linked the AV bundle and sinoatrial node dysplasia in autoimmune lupus to antiserotonin (5-HT4) receptor antibodies in mice.

One of the problems with analysing this human disease is its incomplete penetrance and far from 100%

  doi: 10.1111/apha.12418

recurrence rate in the same mother. Some of these features also complicate the murine models of lupus erythematosus, where the frequency of CHB is low as well (Suzuki *et al.* 2005). The authors' assessment of heart block incidence in murine maternal lupus models by measuring AV conduction in neonatal offspring is potentially confounded by loss by death *in utero* of the most severely affected foetuses. However, prenatal embryonic Doppler echocardiography employed in mice immunized with 60 kDa Ro, 48 kDa La or recombinant calreticulin autoantigens revealed a significant decrease in foetal heart rate and 18% incidence of lower degrees of AV block in all groups relative to controls from ED13. However, the number of pups born with an overt block was lower. This shows that a lot of potentially significant events that may even lead to foetal demise, such as foetal bradycardia and temporary conduction deficits, could be missed if one concentrates only on postnatal stages.

Qu *et al.* (2001) identified L-type calcium channel as a potential target for maternal antibodies inducing CHB in the foetus. *In vitro* studies showed the binding of these antibodies to the sarcolemma and *in vivo* demonstrated lower channel density in myocytes isolated from neonatal mice born to immunized dams. Deletion of the neuroendocrine alpha1D Ca channel in mice resulted in significant sinus bradycardia and AV block, a phenotype reminiscent to that seen in CHB. Another study by this group (Qu *et al.* 2005) confirmed expression of the alpha1D Ca channel in human foetal heart, showed the inhibitory effect of anti-Ro/La antibodies on this channel and direct cross-reactivity with this protein. This inhibition was rescued by a Ca channel activator, Bay K8644, opening a potential therapeutic avenue in this disease.

Conclusions

Despite recent advances in developmental cardiology, foetal medicine and genomics, little is known regarding the dysfunction of the developing human heart. This review shows the importance of the correct detection, characterization and diagnosis of cardiac rhythm disturbances as early as possible during *in utero* life. Experimental and transgenic animal models (e.g. sheep, mouse, chick and zebrafish) can help to decipher the cellular and molecular mechanisms underlying embryonic and foetal arrhythmias and assist in the identification of novel therapeutic targets. Such approaches also allow the investigation of the potentially deleterious short- and long-term effects of early intra-uterine stress-, drug- and mutation-induced cardiac dysrhythmias. Research in this field provides complementary scientific data to make possible the treatment of the « foetal patient » before their birth, limiting possible detrimental consequences in adulthood.

Conflict of interests

None.

We would like to thank the reviewers for their helpful comments on this manuscript and Prof. Robert G. Gourdie for final language editing. This work was supported by Ministry of Education PRVOUK P35/LF1/5, institutional RVO: 67985823 (DS), Grant Agency of the Czech Republic P302/11/1308 and 13-12412S to DS, and Swiss National Science Foundation Grants 3100A0-105901 and 310030-127633 to ER.

References

Aanhaanen, W.T., Brons, J.F., Dominguez, J.N., Rana, M.S., Norden, J., Airik, R., Wakker, V., de Gier-de Vries, C., Brown, N.A., Kispert, A., Moorman, A.F. & Christoffels, V.M. 2009. The Tbx2+ primary myocardium of the atrioventricular canal forms the atrioventricular node and the base of the left ventricle. *Circ Res* **104**, 1267–1274.

Ammirabile, G., Tessari, A., Pignataro, V., Szumska, D., Sardo, F.S., Benes, J. Jr, Balistreri, M., Bhattacharya, S., Sedmera, D. & Campione, M. 2012. Pitx2 confers left morphological, molecular, and functional identity to the sinus venosus myocardium. *Cardiovasc Res* **93**, 291–301.

Arguello, C., Alanis, J., Pantoja, O. & Valenzuela, B. 1986. Electrophysiological and ultrastructural study of the atrioventricular canal during the development of the chick embryo. *J Mol Cell Cardiol* **18**, 499–510.

Azarbayjani, F. & Danielsson, B.R. 2002. Embryonic arrhythmia by inhibition of HERG channels: a common hypoxia-related teratogenic mechanism for antiepileptic drugs? *Epilepsia* **43**, 457–468.

Baker, C., Taylor, D.G., Osuala, K., Natarajan, A., Molnar, P.J., Hickman, J., Alam, S., Moscato, B., Weinshenker, D. & Ebert, S.N. 2012. Adrenergic deficiency leads to impaired electrical conduction and increased arrhythmic potential in the embryonic mouse heart. *Biochem Biophys Res Commun* **423**, 536–541.

Benes, J. Jr, Ammirabile, G., Sankova, B., Campione, M., Krejci, E., Kvasilova, A. & Sedmera, D. 2014. The role of connexin40 in developing atrial conduction. *FEBS Lett* **588**, 1465–1469.

Blaschke, R.J., Hahurij, N.D., Kuijper, S., Just, S., Wisse, L.J., Deissler, K., Maxelon, T., Anastassiadis, K., Spitzer, J., Hardt, S.E. *et al.* 2007. Targeted mutation reveals essential functions of the homeodomain transcription factor Shox2 in sinoatrial and pacemaking development. *Circulation* **115**, 1830–1838.

Boucek, R.J., Murphy, W.P. Jr & Paff, G.H. 1959. Electrical and mechanical properties of chick embryo heart chambers. *Circ Res* **7**, 787–793.

Braunwald, E., Zipes, D.P. & Libbt, P. 2001. *Heart Disease: A Textbook of Cardiovascular Medicine*, p. 2281. Saunders, Philadelphia.

Bressan, M., Liu, G. & Mikawa, T. 2013. Early mesodermal cues assign avian cardiac pacemaker fate potential in a tertiary heart field. *Science* **340**, 744–748.

Brucato, A., Frassi, M., Franceschini, F., Cimaz, R., Faden, D., Pisoni, M.P., Muscara, M., Vignati, G., Stramba-Badiale, M., Catelli, L. *et al.* 2001. Risk of congenital complete heart block in newborns of mothers with anti-Ro/SSA antibodies detected by counterimmunoelectrophoresis: a prospective study of 100 women. *Arthritis Rheum* **44**, 1832–1835.

Bruchez, P., Sarre, A., Kappenberger, L. & Raddatz, E. 2008. The L-Type Ca+ and KATP channels may contribute to pacing-induced protection against anoxia-reoxygenation in the embryonic heart model. *J Cardiovasc Electrophysiol* **19**, 1196–1202.

Buyon, J.P. & Clancy, R.M. 2003. Neonatal lupus: review of proposed pathogenesis and clinical data from the US-based Research Registry for Neonatal Lupus. *Autoimmunity* **36**, 41–50.

Chen, F., De Diego, C., Xie, L.H., Yang, J.H., Klitzner, T.S. & Weiss, J.N. 2007. Effects of metabolic inhibition on conduction, Ca transients, and arrhythmia vulnerability in embryonic mouse hearts. *Am J Physiol Heart Circ Physiol* **293**, H2472–H2478.

Chen, F., De Diego, C., Chang, M.G., McHarg, J.L., John, S., Klitzner, T.S. & Weiss, J.N. 2010. Atrioventricular conduction and arrhythmias at the initiation of beating in embryonic mouse hearts. *Dev Dyn* **239**, 1941–1949.

Cheng, G., Wessels, A., Gourdie, R.G. & Thompson, R.P. 2002. Spatiotemporal distribution of apoptosis in embryonic chicken heart. *Dev Dyn* **223**, 119–133.

Christoffels, V.M., Hoogaars, W.M. & Moorman, A.F. 2010. Patterning and development of the conduction system of the heart: origins of the conduction system in development. In: N. Rosenthal & R.P. Harvey (eds) *Heart Development and Regeneration*, pp. 171–194. Elsevier, London.

Chuck, E.T., Freeman, D.M., Watanabe, M. & Rosenbaum, D.S. 1997. Changing activation sequence in the embryonic chick heart. Implications for the development of the His-Purkinje system. *Circ Res* **81**, 470–476.

Clark, E.B., Hu, N. & Dooley, J.B. 1985. The effect of isoproterenol on cardiovascular function in the stage 24 chick embryo. *Teratology* **31**, 41–47.

Clark, E.B., Hu, N., Turner, D.R., Litter, J.E. & Hansen, J. 1991. Effect of chronic verapamil treatment on ventricular function and growth in chick embryos. *Am J Physiol* **261**, H166–H171.

Copel, J.A., Liang, R.I., Demasio, K., Ozeren, S. & Kleinman, C.S. 2000. The clinical significance of the irregular fetal heart rhythm. *Am J Obstet Gynecol* **182**, 813–817; discussion 17–9.

Danielsson, B.R., Azarbayjani, F., Skold, A.C. & Webster, W.S. 1997. Initiation of phenytoin teratogenesis: pharmacologically induced embryonic bradycardia and arrhythmia resulting in hypoxia and possible free radical damage at reoxygenation. *Teratology* **56**, 271–281.

Danielsson, C., Azarbayjani, F., Skold, A.C., Sjogren, N. & Danielsson, B.R. 2007. Polytherapy with hERG-blocking antiepileptic drugs: increased risk for embryonic cardiac arrhythmia and teratogenicity. *Birth Defects Res A Clin Mol Teratol* **79**, 595–603.

Donofrio, M.T., Moon-Grady, A.J., Hornberger, L.K., Copel, J.A., Sklansky, M.S., Abuhamad, A., Cuneo, B.F., Huhta, J.C., Jonas, R.A., Krishnan, A. *et al.* 2014. Diagnosis and treatment of fetal cardiac disease: a scientific statement from the American Heart Association. *Circulation* **129**, 2183–2242.

Eghtesady, P., Michelfelder, E.C., Knilans, T.K., Witte, D.P., Manning, P.B. & Crombleholme, T.M. 2011. Fetal surgical management of congenital heart block in a hydropic fetus: lessons learned from a clinical experience. *J Thorac Cardiovasc Surg* **141**, 835–837.

Eronen, M. 1997. Outcome of fetuses with heart disease diagnosed *in utero*. *Arch Dis Child Fetal Neonatal Ed* **77**, F41–F46.

Frank, D.U., Carter, K.L., Thomas, K.R., Burr, R.M., Bakker, M.L., Coetzee, W.A., Tristani-Firouzi, M., Bamshad, M.J., Christoffels, V.M. & Moon, A.M. 2012. Lethal arrhythmias in Tbx3-deficient mice reveal extreme dosage sensitivity of cardiac conduction system function and homeostasis. *Proc Natl Acad Sci USA* **109**, E154–E163.

Friedman, D.M., Kim, M.Y., Copel, J.A., Llanos, C., Davis, C. & Buyon, J.P. 2009. Prospective evaluation of fetuses with autoimmune-associated congenital heart block followed in the PR Interval and Dexamethasone Evaluation (PRIDE) Study. *Am J Cardiol* **103**, 1102–1106.

Gardier, S., Pedretti, S., Sarre, A. & Raddatz, E. 2010. Transient anoxia and oxyradicals induce a region-specific activation of MAPKs in the embryonic heart. *Mol Cell Biochem* **340**, 239–247.

Gonzalez, M.D., Contreras, L.J., Jongbloed, M.R., Rivera, J., Donahue, T.P., Curtis, A.B., Bailey, M.S., Conti, J.B., Fishman, G.I., Schalij, M.J. & Gittenberger-de Groot, A.C. 2004. Left atrial tachycardia originating from the mitral annulus-aorta junction. *Circulation* **110**, 3187–3192.

Gourdie, R.G., Wei, Y., Kim, D., Klatt, S.C. & Mikawa, T. 1998. Endothelin-induced conversion of embryonic heart muscle cells into impulse-conducting Purkinje fibers. *Proc Natl Acad Sci USA* **95**, 6815–6818.

Gourdie, R.G., Harris, B.S., Bond, J., Justus, C., Hewett, K.W., O'Brien, T.X., Thompson, R.P. & Sedmera, D. 2003. Development of the cardiac pacemaking and conduction system. *Birth Defects Res C Embryo Today* **69C**, 46–57.

Gurjarpadhye, A., Hewett, K.W., Justus, C., Wen, X., Stadt, H., Kirby, M.L., Sedmera, D. & Gourdie, R.G. 2007. Cardiac neural crest ablation inhibits compaction and electrical function of conduction system bundles. *Am J Physiol Heart Circ Physiol* **292**, H1291–H1300.

Hall, C.E., Hurtado, R., Hewett, K.W., Shulimovich, M., Poma, C.P., Reckova, M., Justus, C., Pennisi, D.J., Tobita, K., Sedmera, D., Gourdie, R.G. & Mikawa, T. 2004. Hemodynamic-dependent patterning of endothelin converting enzyme 1 expression and differentiation of impulse-conducting Purkinje fibers in the embryonic heart. *Development* **131**, 581–592.

Hildreth, V., Anderson, R.H. & Henderson, D.J. 2009. Autonomic innervation of the developing heart: origins and function. *Clin Anat* **22**, 36–46.

Hirota, A., Kamino, K., Komuro, H., Sakai, T. & Yada, T. 1985. Early events in development of electrical activity and contraction in embryonic rat heart assessed by optical recording. *J Physiol* **369**, 209–227.

Hirota, A., Kamino, K., Komuro, H. & Sakai, T. 1987. Mapping of early development of electrical activity in the embryonic chick heart using multiple-site optical recording. *J Physiol* **383**, 711–728.

Hoff, E.C. & Kramer, T.C. 1939. The development of the electrocardiogram of the embryonic heart. *Am Heart J* **17**, 471–488.

Hoogaars, W.M., Engel, A., Brons, J.F., Verkerk, A.O., de Lange, F.J., Wong, L.Y., Bakker, M.L., Clout, D.E., Wakker, V., Barnett, P., Ravesloot, J.H., Moorman, A.F., Verheijck, E.E. & Christoffels, V.M. 2007. Tbx3 controls the sinoatrial node gene program and imposes pacemaker function on the atria. *Genes Dev* **21**, 1098–1112.

Huhta, J.C. 2005. Fetal congestive heart failure. *Semin Fetal Neonatal Med* **10**, 542–552.

Jaber, M., Koch, W.J., Rockman, H., Smith, B., Bond, R.A., Sulik, K.K., Ross, J. Jr, Lefkowitz, R.J., Caron, M.G. & Giros, B. 1996. Essential role of beta-adrenergic receptor kinase 1 in cardiac development and function. *Proc Natl Acad Sci USA* **93**, 12974–12979.

Jaeggi, E.T. & Nii, M. 2005. Fetal brady- and tachyarrhythmias: new and accepted diagnostic and treatment methods. *Semin Fetal Neonatal Med* **10**, 504–514.

Jaeggi, E.T., Silverman, E.D., Laskin, C., Kingdom, J., Golding, F. & Weber, R. 2011. Prolongation of the atrioventricular conduction in fetuses exposed to maternal anti-Ro/SSA and anti-La/SSB antibodies did not predict progressive heart block. A prospective observational study on the effects of maternal antibodies on 165 fetuses. *J Am Coll Cardiol* **57**, 1487–1492.

Jay, P.Y., Harris, B.S., Maguire, C.T., Buerger, A., Wakimoto, H., Tanaka, M., Kupershmidt, S., Roden, D.M., Schultheiss, T.M., O'Brien, T.X., Gourdie, R.G., Berul, C.I. & Izumo, S. 2004. Nk2–5 mutation causes anatomic hypoplasia of the cardiac conduction system. *J Clin Invest* **113**, 1130–1137.

Jerome, L.A. & Papaioannou, V.E. 2001. DiGeorge syndrome phenotype in mice mutant for the T-box gene, Tbx1. *Nat Genet* **27**, 286–291.

Jongbloed, M.R., Schalij, M.J., Poelmann, R.E., Blom, N.A., Fekkes, M.L., Wang, Z., Fishman, G.I. & Gittenberger-De Groot, A.C. 2004. Embryonic conduction tissue: a spatial correlation with adult arrhythmogenic areas. *J Cardiovasc Electrophysiol* **15**, 349–355.

Kamel, R., Garcia, S., Lezoualc'h, F., Fischmeister, R., Muller, S., Hoebek, J. & Eftekhari, P. 2007. Immunomodulation by maternal autoantibodies of the fetal serotoninergic 5-HT4 receptor and its consequences in early BALB/c mouse embryonic development. *BMC Dev Biol* **7**, 34.

Karppinen, S., Rapila, R., Makikallio, K., Hanninen, S.L., Rysa, J., Vuolteenaho, O. & Tavi, P. 2013. Endothelin-1 signalling controls early embryonic heart rate *in vitro* and *in vivo*. *Acta Physiol (Oxf)* **210**, 369–380.

Kasuya, Y., Matsuki, N. & Shigenobu, K. 1977. Changes in sensitivity to anoxia of the cardiac action potential plateau during chick embryonic development. *Dev Biol* **58**, 124–133.

Kockova, R., Svatunkova, J., Novotny, J., Hejnova, L., Ostadal, B. & Sedmera, D. 2013. Heart rate changes mediate the embryotoxic effect of antiarrhythmic drugs in the chick embryo. *Am J Physiol Heart Circ Physiol* **304**, H895–H902.

Kolditz, D.P., Wijffels, M.C., Blom, N.A., van der Laarse, A., Markwald, R.R., Schalij, M.J. & Gittenberger-de Groot, A.C. 2007. Persistence of functional atrioventricular accessory pathways in postseptated embryonic avian hearts: implications for morphogenesis and functional maturation of the cardiac conduction system. *Circulation* **115**, 17–26.

Kolditz, D.P., Wijffels, M.C., Blom, N.A., van der Laarse, A., Hahurij, N.D., Lie-Venema, H., Markwald, R.R., Poelmann, R.E., Schalij, M.J. & Gittenberger-de Groot, A.C. 2008. Epicardium-derived cells in development of annulus fibrosis and persistence of accessory pathways. *Circulation* **117**, 1508–1517.

Leaf, D.E., Feig, J.E., Vasquez, C., Riva, P.L., Yu, C., Lader, J.M., Kontogeorgis, A., Baron, E.L., Peters, N.S., Fisher, E.A., Gutstein, D.E. & Morley, G.E. 2008. Connexin40 imparts conduction heterogeneity to atrial tissue. *Circ Res* **103**, 1001–1008.

Liang, X., Wang, G., Lin, L., Lowe, J., Zhang, Q., Bu, L., Chen, Y., Chen, J., Sun, Y. & Evans, S.M. 2013. HCN4 dynamically marks the first heart field and conduction system precursors. *Circ Res* **113**, 399–407.

Liddicoat, J.R., Klein, J.R., Reddy, V.M., Klautz, R.J., Teitel, D.F. & Hanley, F.L. 1997. Hemodynamic effects of chronic prenatal ventricular pacing for the treatment of complete atrioventricular block. *Circulation* **96**, 1025–1030.

Liu, J., Bressan, M., Hassel, D., Huisken, J., Staudt, D., Kikuchi, K., Poss, K.D., Mikawa, T. & Stainier, D.Y. 2010. A dual role for ErbB2 signaling in cardiac trabeculation. *Development* **137**, 3867–3875.

Lo, C.W., Yu, Q., Shen, Y., Leatherbury, l., Francis, R., Xiao-Quing, Z., Zhang, Z., Wessels, A., Huang, G. & Chatterjee, B. 2010. Exploring the genetic basis for congenital heart disease with mouse ENU mutagenesis. In: N. Rosenthal & R.P. Harvey (ed.) *Heart Development and Regeneration*, pp. 753–778. Elsevier, London.

Maeno, Y.V., Boutin, C., Hornberger, L.K., McCrindle, B.W., Cavalle-Garrido, T., Gladman, G. & Smallhorn, J.F. 1999. Prenatal diagnosis of right ventricular outflow tract obstruction with intact ventricular septum, and detection of ventriculocoronary connections. *Heart* **81**, 661–668.

Maurer, M. Jr 1979. Developmental factors contributing to the susceptibility to bradycardia in isolated, cultured fetal mouse hearts. *Pediatr Res* **13**, 1052–1057.

Maury, P., Sarre, A., Terrand, J., Rosa, A., Kucera, P., Kappenberger, L. & Raddatz, E. 2004. Ventricular but not atrial electro-mechanical delay of the embryonic heart is altered by anoxia-reoxygenation and improved by nitric oxide. *Mol Cell Biochem* **265**, 141–149.

Meiltz, A., Kucera, P., de Ribaupierre, Y. & Raddatz, E. 1998. Inhibition of bicarbonate transport protects embryonic heart

against reoxygenation-induced dysfunction. *J Mol Cell Cardiol* **30**, 327–335.

Mitchell, J.L., Cuneo, B.F., Etheridge, S.P., Horigome, H., Weng, H.Y. & Benson, D.W. 2012. Fetal heart rate predictors of long QT syndrome. *Circulation* **126**, 2688–2695.

Mommersteeg, M.T., Brown, N.A., Prall, O.W., de Gier-de Vries, C., Harvey, R.P., Moorman, A.F. & Christoffels, V.M. 2007a. Pitx2c and Nk2–5 Are Required for the Formation and Identity of the Pulmonary Myocardium. *Circ Res* **101**, 902–909.

Mommersteeg, M.T., Hoogaars, W.M., Prall, O.W., de Gier-de Vries, C., Wiese, C., Clout, D.E., Papaioannou, V.E., Brown, N.A., Harvey, R.P., Moorman, A.F. & Christoffels, V.M. 2007b. Molecular pathway for the localized formation of the sinoatrial node. *Circ Res* **100**, 354–362.

Moorman, A.F., van den Berg, G., Anderson, R.H. & Christoffels, V.M. 2010. Early cardiac growth and the ballooning model of cardiac chamber formation. In: N. Rosenthal & R.P. Harvey (eds) *Heart Development and Regeneration*, pp. 219–236. Elsevier, London.

Moskowitz, I.P., Pizard, A., Patel, V.V., Bruneau, B.G., Kim, J.B., Kupershmidt, S., Roden, D., Berul, C.I., Seidman, C.E. & Seidman, J.G. 2004. The T-Box transcription factor Tbx5 is required for the patterning and maturation of the murine cardiac conduction system. *Development* **131**, 4107–4116.

Nanka, O., Krizova, P., Fikrle, M., Tuma, M., Blaha, M., Grim, M. & Sedmera, D. 2008. Abnormal myocardial and coronary vasculature development in experimental hypoxia. *Anat Rec (Hoboken)* **291**, 1187–1199.

Nicholson, A., Chmait, R., Bar-Cohen, Y., Zheng, K. & Loeb, G.E. 2012. Percutaneously injectable fetal pacemaker: electronics, pacing thresholds, and power budget. *Conf Proc IEEE Eng Med Biol Soc* **2012**, 5730–5733.

Nii, M., Hamilton, R.M., Fenwick, L., Kingdom, J.C., Roman, K.S. & Jaeggi, E.T. 2006. Assessment of fetal atrioventricular time intervals by tissue Doppler and pulse Doppler echocardiography: normal values and correlation with fetal electrocardiography. *Heart* **92**, 1831–1837.

Nomura-Kitabayashi, A., Phoon, C.K.L., Kishigami, S., Rosenthal, J., Yamauchi, Ÿ., Abe, K., Yamamura, K., Samtani, R., Lo, C.W. & Mishina, Y. 2009. Outflow tract cushions perform a critical valve-like function in the early embryonic heart requiring BMPRIA-mediated signaling in cardiac neural crest. *Am J Physiol Heart Circ Physiol* **297**, H1617–H1628.

Paff, G.H. & Boucek, R.J. 1975. Conal contribution to the electrocardiogram of chick embryo hearts. *Anat Rec* **182**, 169–173.

Paff, G.H., Boucek, R.J. & Klopfenstein, H.S. 1964. Experimental heart block in the chick embryo. *Anat Rec* **149**, 217–224.

Paff, G.H., Boucek, R.J. & Harrell, T.C. 1968. Observations on the development of the electrocardiogram. *Anat Rec* **160**, 575–582.

Pedra, S.R., Smallhorn, J.F., Ryan, G., Chitayat, D., Taylor, G.P., Khan, R., Abdolell, M. & Hornberger, L.K. 2002. Fetal cardiomyopathies: pathogenic mechanisms, hemodynamic findings, and clinical outcome. *Circulation* **106**, 585–591.

Pedretti, S. & Raddatz, E. 2011. STAT3alpha interacts with nuclear GSK3beta and cytoplasmic RISK pathway and stabilizes rhythm in the anoxic-reoxygenated embryonic heart. *Basic Res Cardiol* **106**, 355–369.

Phoon, C.K. 2006. Imaging tools for the developmental biologist: ultrasound biomicroscopy of mouse embryonic development. *Pediatr Res* **60**, 14–21.

Phoon, C.K., Aristizabal, O. & Turnbull, D.H. 2002. Spatial velocity profile in mouse embryonic aorta and Doppler-derived volumetric flow: a preliminary model. *Am J Physiol Heart Circ Physiol* **283**, H908–H916.

Phoon, C.K., Ji, R.P., Aristizabal, O., Worrad, D.M., Zhou, B., Baldwin, H.S. & Turnbull, D.H. 2004. Embryonic heart failure in NFATc1-/- mice: novel mechanistic insights from *in utero* ultrasound biomicroscopy. *Circ Res* **95**, 92–99.

Qu, Y., Xiao, G.Q., Chen, L. & Boutjdir, M. 2001. Autoantibodies from mothers of children with congenital heart block downregulate cardiac L-type Ca channels. *J Mol Cell Cardiol* **33**, 1153–1163.

Qu, Y., Baroudi, G., Yue, Y. & Boutjdir, M. 2005. Novel molecular mechanism involving alpha1D (Cav1.3) L-type calcium channel in autoimmune-associated sinus bradycardia. *Circulation* **111**, 3034–3041.

Raddatz, E., Kucera, P. & De Ribaupierre, Y. 1997. Response of the embryonic heart to hypoxia and reoxygenation: an *in vitro* model. *Exp Clin Cardiol* **2**, 128–134.

Raddatz, E., Thomas, A.C., Sarre, A. & Benathan, M. 2011. Differential contribution of mitochondria, NADPH oxidases, and glycolysis to region-specific oxidant stress in the anoxic-reoxygenated embryonic heart. *Am J Physiol Heart Circ Physiol* **300**, H820–H835.

Rajala, G.M., Kuhlmann, R.S. & Kolesari, G.L. 1984. The role of dysrhythmic heart function during cardiovascular teratogenesis in epinephrine-treated chick embryos. *Teratology* **30**, 385–392.

Reckova, M., Rosengarten, C., deAlmeida, A., Stanley, C.P., Wessels, A., Gourdie, R.G., Thompson, R.P. & Sedmera, D. 2003. Hemodynamics is a key epigenetic factor in development of the cardiac conduction system. *Circ Res* **93**, 77–85.

Reed, K.L. 1989. Fetal arrhythmias: etiology, diagnosis, pathophysiology, and treatment. *Semin Perinatol* **13**, 294–304.

Reed, K.L., Appleton, C.P., Anderson, C.F., Shenker, L. & Sahn, D.J. 1990. Doppler studies of vena cava flows in human fetuses. Insights into normal and abnormal cardiac physiology. *Circulation* **81**, 498–505.

Reinisch, J.M., Simon, N.G., Karow, W.G. & Gandelman, R. 1978. Prenatal exposure to prednisone in humans and animals retards intrauterine growth. *Science* **202**, 436–438.

Rentschler, S., Zander, J., Meyers, K., France, D., Levine, R., Porter, G., Rivkees, S.A., Morley, G.E. & Fishman, G.I. 2002. Neuregulin-1 promotes formation of the murine cardiac conduction system. *Proc Natl Acad Sci USA* **99**, 10464–10469.

Rentschler, S., Harris, B.S., Kuznekoff, L., Jain, R., Manderfield, L., Lu, M.M., Morley, G.E., Patel, V.V. & Epstein, J.A. 2011. Notch signaling regulates murine atrioventricu-

lar conduction and the formation of accessory pathways. *J Clin Invest* **121**, 525–533.

Robin, E., Sabourin, J., Benoit, R., Pedretti, S. & Raddatz, E. 2011. Adenosine A1 receptor activation is arrhythmogenic in the developing heart through NADPH oxidase/ERK- and PLC/PKC-dependent mechanisms. *J Mol Cell Cardiol* **51**, 945–954.

Robin, E., Sabourin, J., Marcillac, F. & Raddatz, E. 2013. Involvement of CD73, equilibrative nucleoside transporters and inosine in rhythm and conduction disturbances mediated by adenosine A1 and A2A receptors in the developing heart. *J Mol Cell Cardiol* **63**, 14–25.

Sabourin, J., Robin, E. & Raddatz, E. 2011. A key role of TRPC channels in the regulation of electromechanical activity of the developing heart. *Cardiovasc Res* **92**, 226–236.

Sabourin, J., Antigny, F., Robin, E., Frieden, M. & Raddatz, E. 2012. Activation of transient receptor potential canonical 3 (TRPC3)-mediated Ca2+ entry by A1 adenosine receptor in cardiomyocytes disturbs atrioventricular conduction. *J Biol Chem* **287**, 26688–26701.

Sankova, B., Machalek, J. & Sedmera, D. 2010. Effects of mechanical loading on early conduction system differentiation in the chick. *Am J Physiol Heart Circ Physiol* **298**, H1571–H1576.

Sankova, B., Benes, J. Jr, Krejci, E., Dupays, L., Theveniau-Ruissy, M., Miquerol, L. & Sedmera, D. 2012. The effect of connexin40 deficiency on ventricular conduction system function during development. *Cardiovasc Res* **95**, 469–479.

Sarre, A., Lange, N., Kucera, P. & Raddatz, E. 2005. mitoKATP channel activation in the postanoxic developing heart protects E-C coupling via NO-, ROS-, and PKC-dependent pathways. *Am J Physiol Heart Circ Physiol* **288**, H1611–H1619.

Sarre, A., Maury, P., Kucera, P., Kappenberger, L. & Raddatz, E. 2006. Arrhythmogenesis in the developing heart during anoxia-reoxygenation and hypothermia-rewarming: an *in vitro* model. *J Cardiovasc Electrophysiol* **17**, 1350–1359.

Sarre, A., Gardier, S., Maurer, F., Bonny, C. & Raddatz, E. 2008. Modulation of the c-Jun N-terminal kinase activity in the embryonic heart in response to anoxia-reoxygenation: involvement of the Ca2+ and mitoKATP channels. *Mol Cell Biochem* **313**, 133–138.

Sarre, A., Pedretti, S., Gardier, S. & Raddatz, E. 2010. Specific inhibition of HCN channels slows rhythm differently in atria, ventricle and outflow tract and stabilizes conduction in the anoxic-reoxygenated embryonic heart model. *Pharmacol Res* **61**, 85–91.

Schmidt, K.G., Ulmer, H.E., Silverman, N.H., Kleinman, C.S. & Copel, J.A. 1991. Perinatal outcome of fetal complete atrioventricular block: a multicenter experience. *J Am Coll Cardiol* **17**, 1360–1366.

Sedmera, D., Pexieder, T., Hu, N. & Clark, E.B. 1998. A quantitative study of the ventricular myoarchitecture in the stage 21-29 chick embryo following decreased loading. *Eur J Morphol* **36**, 105–119.

Sedmera, D., Kucera, P. & Raddatz, E. 2002. Developmental changes in cardiac recovery from anoxia-reoxygenation. *Am J Physiol Regul Integr Comp Physiol* **283**, R379–R388.

Sedmera, D., Wessels, A., Trusk, T.C., Thompson, R.P., Hewett, K.W. & Gourdie, R.G. 2006. Changes in activation sequence of embryonic chick atria correlate with developing myocardial architecture. *Am J Physiol Heart Circ Physiol* **291**, H1646–H1652.

Sedmera, D., Harris, B.S., Grant, E., Zhang, N., Jourdan, J., Kurkova, D. & Gourdie, R.G. 2008. Cardiac expression patterns of endothelin-converting enzyme (ECE): implications for conduction system development. *Dev Dyn* **237**, 1746–1753.

Shrier, A. & Clay, J.R. 1982. Comparison of the pacemaker properties of chick embryonic atrial and ventricular heart cells. *J Membr Biol* **69**, 49–56.

Simpson, J.M. & Sharland, G.K. 1998. Fetal tachycardias: management and outcome of 127 consecutive cases. *Heart* **79**, 576–581.

Skold, A.C. & Danielsson, B.R. 2000. Developmental toxicity of the class III antiarrhythmic agent almokalant in mice. Adverse effects mediated via induction of embryonic heart rhythm abnormalities. *Arzneimittelforschung* **50**, 520–525.

Srinivasan, S. & Strasburger, J. 2008. Overview of fetal arrhythmias. *Curr Opin Pediatr* **20**, 522–531.

Stewart, P.A., Tonge, H.M. & Wladimiroff, J.W. 1983. Arrhythmia and structural abnormalities of the fetal heart. *Br Heart J* **50**, 550–554.

Strasburger, J.F. & Wakai, R.T. 2010. Fetal cardiac arrhythmia detection and *in utero* therapy. *Nat Rev Cardiol* **7**, 277–290.

Strasburger, J.F., Cheulkar, B. & Wakai, R.T. 2008. Magnetocardiography for fetal arrhythmias. *Heart Rhythm* **5**, 1073–1076.

Sugiyama, T., Miyazaki, H., Saito, K., Shimada, H. & Miyamoto, K. 1996. Chick embryos as an alternative experimental animal for cardiovascular investigations: stable recording of electrocardiogram of chick embryos in vivo on the 16th day of incubation. *Toxicol Appl Pharmacol* **138**, 262–267.

Suzuki, H., Silverman, E.D., Wu, X., Borges, C., Zhao, S., Isacovics, B. & Hamilton, R.M. 2005. Effect of maternal autoantibodies on fetal cardiac conduction: an experimental murine model. *Pediatr Res* **57**, 557–562.

Sydorak, R.M., Nijagal, A. & Albanese, C.T. 2001. Endoscopic techniques in fetal surgery. *Yonsei Med J* **42**, 695–710.

Takebayashi-Suzuki, K., Yanagisawa, M., Gourdie, R.G., Kanzawa, N. & Mikawa, T. 2000. *In vivo* induction of cardiac Purkinje fiber differentiation by coexpression of preproendothelin-1 and endothelin converting enzyme-1. *Development* **127**, 3523–3532.

Tazawa, H., Suzuki, Y. & Musashi, H. 1989. Simultaneous acquisition of ECG, BCG, and blood pressure from chick embryos in the egg. *J Appl Physiol (1985)* **67**, 478–483.

Tenthorey, D., de Ribaupierre, Y., Kucera, P. & Raddatz, E. 1998. Effects of verapamil and ryanodine on activity of the embryonic chick heart during anoxia and reoxygenation. *J Cardiovasc Pharmacol* **31**, 195–202.

Terrand, J., Felley-Bosco, E., Courjault-Gautier, F., Rochat, A.C., Kucera, P. & Raddatz, E. 2003. Postanoxic func-

tional recovery of the developing heart is slightly altered by endogenous or exogenous nitric oxide. *Mol Cell Biochem* **252**, 53–63.

Tran, L., Kucera, P., de Ribaupierre, Y., Rochat, A.C. & Raddatz, E. 1996. Glucose is arrhythmogenic in the anoxic-reoxygenated embryonic chick heart. *Pediatr Res* **39**, 766–773.

Valderrabano, M., Chen, F., Dave, A.S., Lamp, S.T., Klitzner, T.S. & Weiss, J.N. 2006. Atrioventricular ring reentry in embryonic mouse hearts. *Circulation* **114**, 543–549.

Van Mierop, L.H. 1967. Location of pacemaker in chick embryo heart at the time of initiation of heartbeat. *Am J Physiol* **212**, 407–415.

Vergani, P., Mariani, E., Ciriello, E., Locatelli, A., Strobelt, N., Galli, M. & Ghidini, A. 2005. Fetal arrhythmias: natural history and management. *Ultrasound Med Biol* **31**, 1–6.

Vostarek, F., Sankova, B. & Sedmera, D. 2014. Studying dynamic events in the developing myocardium. *Prog Biophys Mol Biol*, **115**, 261–269.

Wakimoto, K., Kobayashi, K., Kuro, O.M., Yao, A., Iwamoto, T., Yanaka, N., Kita, S., Nishida, A., Azuma, S., Toyoda, Y. *et al.* 2000. Targeted disruption of Na+/Ca^{2+} exchanger gene leads to cardiomyocyte apoptosis and defects in heartbeat. *J Biol Chem* **275**, 36991–36998.

Zhang, S.S., Kim, K.H., Rosen, A., Smyth, J.W., Sakuma, R., Delgado-Olguin, P., Davis, M., Chi, N.C., Puviindran, V., Gaborit, N. *et al.* 2011. Iroquois homeobox gene 3 establishes fast conduction in the cardiac His-Purkinje network. *Proc Natl Acad Sci USA* **108**, 13576–13581.

Zhao, H., Strasburger, J.F., Cuneo, B.F. & Wakai, R.T. 2006. Fetal cardiac repolarization abnormalities. *Am J Cardiol* **98**, 491–496.

Supporting Information

Additional Supporting Information may be found in the online version of this article:

Movie S1. Example of atrioventricular re-entry in ED4 isolated chick embryonic heart visualized by optical mapping of calcium transients.

  doi: 10.1111/apha.12418

ACTA PHYSIOLOGICA

Acta Physiol 2016

Acute temperature effects on function of the chick embryonic heart

F. Vostarek,[1,2] J. Svatunkova[1] and D. Sedmera[1,3]

1 Czech Academy of Sciences, Institute of Physiology, Prague, Czech Republic

2 Faculty of Science, Charles University, Prague, Czech Republic

3 First Faculty of Medicine, Institute of Anatomy, Charles University, Prague, Czech Republic

Received 22 December 2015, revision requested 22 January 2016, revision received 11 April 2016, accepted 12 April 2016
Correspondence: D. Sedmera, Czech Academy of Sciences, Institute of Physiology, Videnska 1083, 14220 Prague 4, Czech Republic.
E-mail: dsedmera@biomed.cas.cz

Abstract

Aim: We analysed the effects of acute temperature change on the beating rate, conduction properties and calcium transients in the chick embryonic heart *in vitro* and *in ovo*.

Methods: The effects of temperature change (34, 37 and 40 °C) on calcium dynamics in isolated ED4 chick hearts *in vitro* were investigated by high-speed calcium optical imaging. For comparison and validation of *in vitro* measurements, experiments were also performed *in ovo* using videomicroscopy. Artificial stimulation experiments were performed *in vitro* and *in ovo* to uncover conduction limits of heart segments.

Results: Decrease in temperature from 37 to 34 °C *in vitro* led to a 22% drop in heart rate and unchanged amplitude of Ca^{2+} transients, compared to a 25% heart rate decrease *in ovo*. Increase in temperature from 37 to 40 °C *in vitro* and *in ovo* led to 20 and 23% increases in heart rate, respectively, and a significant decrease in amplitude of Ca^{2+} transients (atrium −35%, ventricle −38%). We observed a wide spectrum of arrhythmias *in vitro*, of which the most common was atrioventricular (AV) block (57%). There was variability of AV block locations. Pacing experiments *in vitro* and *in ovo* suggested that the AV blocks were likely caused by relative tissue hypoxia and not by the tachycardia itself.

Conclusion: The pacemaker and AV canal are the most temperature-sensitive segments of the embryonic heart. We suggest that the critical point for conduction is the connection of the ventricular trabecular network to the AV canal.

Keywords arrhythmias, calcium imaging, chick embryo, conduction block, heart development, optical mapping.

The function of the embryonic heart is strongly affected by temperature. The temperature changes affect the kinetics of ion channels, pumps and the Na^+/Ca^{2+} exchanger. Changes in the kinetics of these channels are crucial for the generation and propagation of electrical activation through the embryonic heart (Sperelakis & Lehmkuhl 1967, Chen & DeHaan 1993).

Despite homoeothermy, the avian embryo retains some flexibility from its poikilothermic ancestors and tolerates (within limits) variations in incubation temperature. The effects of temperature on developing chick embryonic heart have been extensively studied. One of the most striking findings is the effect of long-lasting hypothermia (32–36 °C), which causes cardiac hypertrophy (Warbanow 1970). These changes are accompanied by increased contractility of embryonic hearts (Warbanow 1971). Another study focused on hypothermia tests haemodynamic effects of environmental hypothermia in the stage 21

 doi: 10.1111/apha.12691

(Hamburger & Hamilton 1951) embryo. Cooling from 34.7 to 31.1 °C causes a significant decrease in heart rate by about 25%, increased vascular resistance and decrease in blood pressure and blood flow. This bradycardic response is independent of functional autonomic innervation (Nakazawa *et al.* 1985). A recent study at stage 17 shows that hypothermia is associated with bradycardia and a decrease in the peak velocity of blood during systole (Lee *et al.* 2011). The effects of environmental hyperthermia (37–40 °C) cause an increase in the heart rate by about 22% at stage 21, without changes in stroke volume (flow/rate). This study also shows a significant increase in the basal heart rate during development from stage 18 to stage 24 (Nakazawa *et al.* 1986). The long-term consequences of periods of hypothermia (31–36 °C) and hyperthermia (38–42 °C) show teratogenic and lethal effects on the chick embryo (Peterka *et al.* 1996).

An *in vitro* hypothermia-rewarming study by Sarre and colleagues shows dramatic changes in heart rate during cooling from 37 to 0 °C and subsequent rewarming to 37 °C in isolated chick embryonic hearts at stage 24. The hearts stopped beating in deep hypothermia at the critical temperature of 18 °C, and they resumed beating at the same temperature during rewarming. Changes in heart rate remained linear in the range between 34 and 37 °C (Sarre *et al.* 2006). The most recent study shows acute temperature effects on *ex vivo* zebrafish hearts studied by optical mapping, in the range from 18 to 28 °C. Cooling to 18 °C decreases heart rate by about 40% and increases atrial and ventricular APD_{50} by factors 3 and 2 respectively. It shows that the atrial APD is the most severely affected AP parameter by an acute temperature change (Lin *et al.* 2014) and that this property is conserved among vertebrates. The action potentials of atrium, atrioventricular (AV) canal, ventricle and outflow tract differ in duration – APD_{90}. The longest APD_{90} occurs in the AV canal. Arguello *et al.* (1986) suggested that prolonged APD_{90} in AV canal region was caused by longer predominance of Ca^{2+} and slow Na^+ current dependence during development, as compared to atrial or ventricular cells.

Early cardiac rhythmicity is critically dependent on intracellular dynamics of calcium ions. Calcium handling is regulated by calcium ion channels, receptors, ATPases and the Na^+/Ca^{2+} exchanger (NCX; Bers 1991), and its kinetics is strongly influenced by temperature. Embryonic cardiac rhythmicity is maintained by pacemaker cells from the developing sinoatrial node located at the inflow portion of the heart (Kamino *et al.* 1981). The pacemaker potential is generated by a specific set of ion channels. Spontaneous depolarization is initiated mainly by the funny current (I_f) or 'pacemaker' current, via the HCN channels (Na^+, K^+ currents) (DiFrancesco 1993, Moroni *et al.* 2001). A significant role during early depolarization is played also by influx of positive charges, known as the I_{NCX} during forward mode ($3Na^+$ in, $1Ca^{2+}$ out) of sodium–calcium exchanger – NCX (Haddock *et al.* 1997).

We analysed the acute effects of temperature change on electrical activity of the chick embryonic heart using *in vitro* high-speed calcium imaging. We hypothesized that temperature-dependent arrhythmias, in particular AV blocks, are due to a particular sensitivity of the AV canal to relative hypoxia. The main goal of this study was to observe changes in calcium transient dynamics as a basis for contractility and also to analyse defects in conduction through activation maps with high spatio-temporal resolution. We also performed videomicroscopy *in ovo* to compare *in vitro* temperature effects on the pacemaker *per se* with the effects on the whole embryo, in which the working heart is coupled to the vascular system.

Materials and methods

Experimental model

White Leghorn chicken eggs (Institute of Molecular Genetics, Kolec, Czech Republic) were stored at 16 °C prior to incubation. The eggs were incubated at 37.5 ± 0.5 °C in a humidified incubator until ED4 (HH stage 21–23, Hamburger & Hamilton 1951). Chick embryos were removed from the eggs and placed into Tyrode's solution (composition: NaCl 145 mmol L^{-1}, KCl 5.9 mmol L^{-1}, $CaCl_2$ 1.1 mmol L^{-1}, $MgCl_2$ 1.2 mmol L^{-1}, glucose 11 mmol L^{-1}, HEPES 5 mmol L^{-1}; pH = 7.4). Hearts were isolated from the embryos and stained in 2.5 mL Rhod-2 (1.78 mM; Invitrogen, Carlsbad, CA, USA) in Tyrode's solution for 1 h in the dark at room temperature. The hearts were then incubated in 2.5 mL Tyrode's solution for 1 h in the dark at 38 °C to de-esterify the dye loaded to the myocytes, according to manufacturer's instructions.

Optical mapping

The two-dimensional optical mapping system for embryonic hearts has been described in detail previously (Tamaddon *et al.* 2000, Rentschler *et al.* 2001). Optical calcium imaging of chick embryonic hearts was based on an established set-up (Valderrabano *et al.* 2006). We used the calcium-sensitive dye Rhod-2 with a modified set-up (Vostarek *et al.* 2014). Stained hearts were placed into a tissue bath containing 2 mL of Tyrode's solution with 0.15 μM

blebbistatin to reduce movement (Fedorov *et al.* 2007). Temperature in the glass-bottomed Petri dish (Wilco Wells, Amsterdam, the Netherlands) was maintained by a temperature-controlled stage (Linkam DC-60, Tadworth, UK). An inverted epifluorescence microscope (Nikon Eclipse TE 2000-S, Tokyo, Japan) fitted with a high-speed EM-CCD camera (Andor iXon3; Andor, Belfast, UK) was used to monitor changes in intracellular calcium concentration – visualized as changes of fluorescence over time under hypothermia (34 °C), normothermia (controls, 37 °C) and hyperthermia (40 °C). Two measurements were performed on each heart after 5 min of stabilization at different temperatures (37 and 34 °C – cooling, 34 and 37 °C – warming, 37 and 40 °C – warming). This temperature range represents the physiological range, compatible with long-term embryonic survival.

Data analysis

The obtained data were analysed by NIS Elements software (Nikon, Tokyo, Japan) and BV_Ana Analysis software (SciMedia Ltd, Costa Mesa, CA, USA). Heart rate was established from counts of calcium transients in the atrium during the 6-s interval (NIS Elements). Amplitudes of calcium transients in atrium and ventricle were analysed using NIS Elements tools. The start of the calcium transient was established as a point of beginning of the upstroke from baseline. Amplitudes were measured as the height from baseline to the peak. APD_{90} values were obtained from calcium transient recordings from atrium, AV canal and ventricle of normothermic hearts ($n = 10$), with recordings free from motion artefacts or arrhythmias. Spatiotemporal activation maps were constructed from raw data from NIS Elements using BV_Ana Analysis software. Data were filtered by high pass/low pass and median filters. The first derivative was calculated as described previously (Nanka *et al.* 2008, Sankova *et al.* 2010). Its peak was used to mark the time of activation of each pixel.

Videomicroscopy

ED4 chick embryos incubated *in ovo* were studied by videomicroscopy to measure changes in heart rate under different temperature conditions. The first measurement was performed at 34 °C, the second at 37 °C and the third at 40 °C. The embryos *in ovo* were maintained at set temperature using a custom-made styrofoam-insulated metal container filled with preheated Bath Armor pellets placed on a Torrey Pines Scientific chilling/heating plate. Ten-second movies were recorded for each temperature with a Nikon D7000 camera (640 × 480 px, 30 fps) mounted on a Leica 125 dissecting microscope; Leica Microsystems, Wetzlar, Germany with a 150 W halogen light source fitted with a green interference filter to enhance contrast of blood. Data analysis was performed using ImageJ software; National Institutes of Health, Bethesda, MD, USA. Two regions of interest were selected on atrium and ventricle, respectively, and heart rate values were obtained by the measurement of changes in grey-scale levels in time during blood flow (Sedmera *et al.* 1999, Kockova *et al.* 2013).

Electrical stimulation in ovo

Atrial and ventricular pacing was performed in ED4 chick embryonic hearts after spontaneous rhythm recordings were obtained. A platinum bipolar electrode was positioned over the atrium using a Narishige micromanipulator; Narishige International USA, Inc., Amityville, NY, USA. The heart was stimulated in overdrive mode at a gradually increasing/decreasing rate (from 120 to 600 beats min^{-1}), with 2-ms pulses twice the diastolic threshold, which was between 1.5 and 2.5 mA (Sedmera *et al.* 2003). The pacing frequency at which conduction disturbances appeared was considered the limit of sustainable conduction rate. Video recordings were obtained and analysed as described above.

Electrical stimulation in vitro *(voltage recordings)*

Chick ED4 embryonic hearts were isolated with a piece of adjacent body wall to allow for fixation to the dish bottom. Hearts were stained in 500 μL of voltage-sensitive dye di-4-ANEPPS (2.5 mM; Invitrogen) for 5 min. They were then briefly rinsed and pinned face-up in a custom-made oxygenated tissue bath containing 20 mL of Tyrode's solution with added 0.1 μM blebbistatin to reduce movement. Atrial and ventricular pacing was performed by a platinum bipolar electrode, which was positioned over the atrium or ventricle using a Narishige micromanipulator. The hearts were stimulated in overdrive mode at varying rates (atrium from 200 up to 400 beats min^{-1} and ventricle from 300 up to 600 beats min^{-1}) to uncover capture and conduction limits. Data acquisition and analysis were performed using the Ultima L high-speed camera; SciMedia Ltd, Costa Mesa, CA, USA and bundled software as described recently (Sankova *et al.* 2010).

Statistical analysis

The data from optical mapping were divided into two groups according to the temperature: hypothermia group (37 and 34 °C) and hyperthermia group (37 and 40 °C). Each group included at least 45 hearts,

and significance of difference was tested by two-tailed Student's paired *t*-test. The occurrence of third-degree AV block in the three groups, hypothermia, normothermia and hyperthermia hearts, was tested by Pearson's chi-square test. The number of hearts analysed *in ovo* was 19, and each heart was tested at all three temperatures. In all cases, values are presented as mean ± SD, and $P < 0.05$ was considered statistically significant.

Results

Experiments in vitro

Changes in calcium transients dynamics. Electrical activity of the chick embryonic hearts (monitored by calcium optical imaging) was strongly affected by acute temperature changes. The most striking was modulation of sinus rhythm frequency. We tested the acute effects in three temperatures. We set 37 °C as a default (baseline *in vitro*) temperature – normothermia, hypothermia at 34 °C and hyperthermia at 40 °C. We observed a nearly linear dependence of the sinus rhythm on temperature under these conditions. The rhythm changed by approx. 20% in hypothermia ($P < 0.001$) and hyperthermia ($P < 0.001$), in comparison with normothermia (Fig. 1).

We then focused on changes in amplitude of the calcium transients. The acceleration of heart rate during hyperthermia caused a significant decrease in calcium transient amplitude in both the atrium and ventricle (Fig. 1d), while no significant changes were observed during hypothermia (Fig. 1b).

We also observed a wide spectrum of rhythm disturbances (for examples, see Supplemental Video S1). These arrhythmias were divided into two main groups.

Defects in rhythm generation – direct influence on the pacemaker. Defects in generation of electrical impulse represented 28% of all arrhythmias. Most common were atrial extrasystoles and sinus pauses (missed beats), which together represented 22% of all observed arrhythmias (Table 1). Atrial extrasystoles and sinus pauses were two times more frequent during hyperthermia than in the normothermia group, while almost none were found in hypothermia. Complete cardiac arrest developed only in three of the 99 hearts analysed. We also uncovered junction rhythm activity in the AV canal in two cases during hyperthermia, at considerably high firing rates (160 and 180 beats min^{-1}).

Defects in impulse propagation. This phenomenon was observed most frequently during hyperthermia, less commonly during normothermia, and was observed only as a few conduction blocks during hypothermia. Defects in impulse propagation

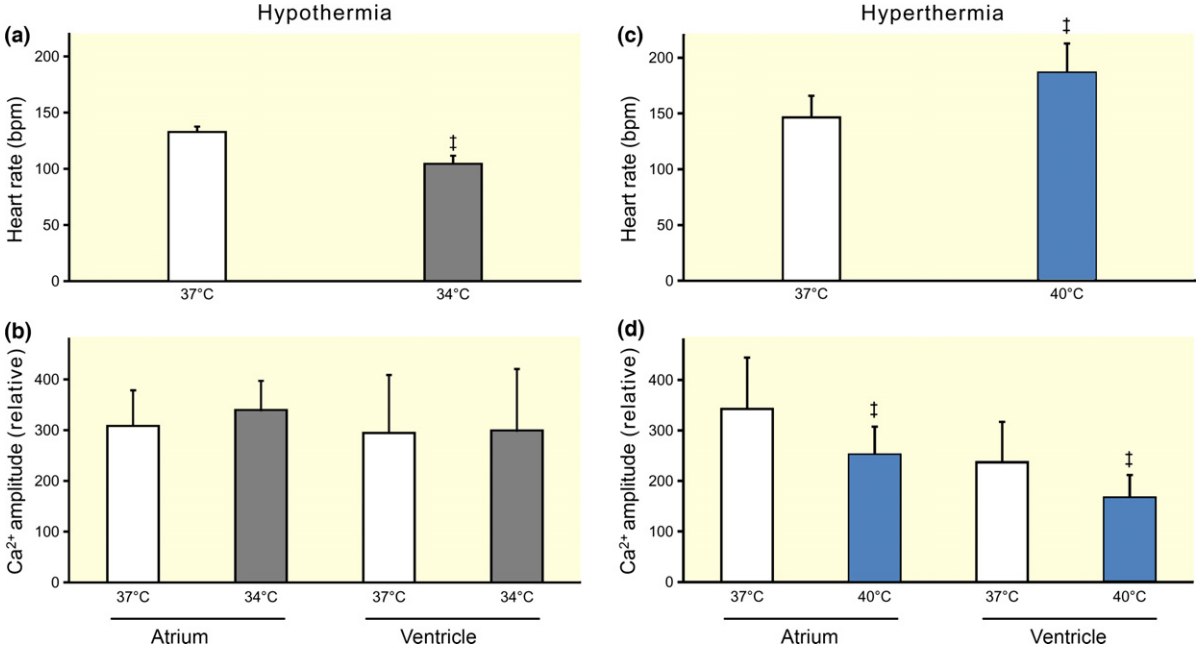

Figure 1 Effects of acute temperature changes on heart rate and amplitudes of Ca^{2+} transients in ED4 chick embryonic heart *in vitro*. (a) Decrease in temperature from 37 to 34 °C led *in vitro* to a 22% drop of intrinsic heart rate ($n = 45$). (b) Hypothermia caused no significant changes in amplitude of Ca^{2+} transients ($n = 45$). (c) Increase in temperature from 37 to 40 °C lead *in vitro* to a 20% acceleration of intrinsic heart rate ($n = 54$). (d) Hyperthermia caused a significant decrease in the amplitude of Ca^{2+} transients ($n = 54$, atrium −35%, ventricle −38%, mean ± SD, ‡$P < 0.001$).

  doi: 10.1111/apha.12691

Table 1 Arrhythmias observed in ED4 chick embryonic hearts *in vitro*. Complete spectrum of observed arrhythmias in hypothermia, normothermia and hyperthermia (total number of observed arrhythmias = 106)

Type of arrhythmia	Occurrence (%)
Complete cardiac arrest	3
Atrial extrasystoles	10
Sinus pauses	12
Junction rhythm	2
Atrial block	3
Second-degree AV block	22
Third-degree AV block	35
Mid-ventricular block	2
Ventriculo-conotruncal block	8
AV re-entry	3
Total	100

AV, atrioventricular.

represented 72% of all observed arrhythmias ($n = 106$, Table 1). In three cases, conduction blocks were observed in conduction through the atrium (atrial block), in two cases in the middle of the ventricle (mid-ventricular block) and in 8% of cases ($n = 106$ observed arrhythmias) at the boundary between the ventricle and outflow tract (ventriculo-conotruncal block). Our attention was especially focused on conduction in the AV canal. Development of conduction blocks in the AV canal (second- or third-degree AV block) presented 57% of all observed arrhythmias. The most common defect was a complete AV block, which developed in one case during hypothermia ($n = 45$ hearts, Pearson's chi-square test $P < 0.03$), in 15% of cases in normothermia (stabilization, $n = 99$ hearts) and 39% in hyperthermia ($n = 54$ hearts, Pearson's chi-square test $P < 0.001$). Third-degree AV block represented 35% of all observed arrhythmias ($n = 106$). The second most common defect was second-degree AV block (22% of all arrhythmias), which developed in 11% of cases during hypothermia ($n = 45$), in 10% of cases in normothermia (stabilization, $n = 99$) and 14% in hyperthermia ($n = 54$). The most common was an intermittent second-degree AV block in 65% of second-degree AV blocks, Wenckebach phenomenon represented 30% of second-degree AV blocks, and Mobitz II was observed only in one case. Occasionally, we noted rare arrhythmias such as AV re-entry, but only in three cases of the 106 arrhythmias observed (Table 1).

Locations of AV blocks – optical activation maps. Optical mapping allowed us to focus specifically on the localization of third-degree AV blocks. Activation maps were created from calcium data in BV_Ana Analysis software. Comparison of standard conduction in normothermia and various types of the third-degree AV block is shown in Figure 2. The locations of block were variable within the AV canal. In 59% of cases, the conduction stopped uniformly across the AV canal. In the remaining 41% of cases, we observed a different AV block pattern, wherein conduction stopped either at the inner curvature or at the AV canal–ventricular boundary, along the outer curvature (Fig. 2f). The most critical part of the AV canal was the distal region at the boundary of the ventricle. The distal region of AV canal developed 53% of AV blocks. By contrast, the proximal AV region developed 37% of blocks and conduction stopped in the middle part of the AV canal in the remaining 10% of blocks.

In ovo *experiments*

We decided to compare the *in vitro* findings with an *in ovo* experiment that included vascular coupling. We studied acute temperature effects *in ovo* by videomicroscopy ($n = 19$ hearts). The experimental temperatures were chosen in the same range as the *in vitro* studies. We obtained heart rates 120 ± 11 beats min^{-1} in hypothermia, 160 ± 21 beats min^{-1} in normothermia and 197 ± 27 beats min^{-1} in hyperthermia. Increase in temperature from 34 to 37 °C leads to a 25% change of baseline heart rate and increase from 37 to 40 °C lead to 23% acceleration *in ovo* ($P < 0.001$). This dependence of heart rate on temperature was almost linear ($R^2 = 0.999$) and corresponded well with the *in vitro* findings.

We also observed rhythm disturbances, which developed in some embryos during hyperthermia. The most frequent were sinus pauses. On occasion, second-degree AV block developed (see Fig. 3). Third-degree AV block was not observed.

Electrical stimulation of the atrium and ventricle. We hypothesized that third-degree AV blocks found *in vitro* were caused by relative tissue hypoxia, which most profoundly affects conduction through the AV canal (Tran *et al.* 1996, Sedmera *et al.* 2002). To test this hypothesis, we measured the ability of the AV canal to propagate high frequencies induced by electrical stimulation from the atrium to the ventricle. The measurements of calcium transients *in vitro* (37 °C) showed that the APD_{90} under spontaneous rhythm was longest in the AV canal of whole ED4 hearts. The longer APD_{90} in the AV canal (330 ms) predisposes this cardiac segment to be a limiting factor in conduction of higher beat frequencies between the atrium and the ventricle. The APD_{90} in the ventricle

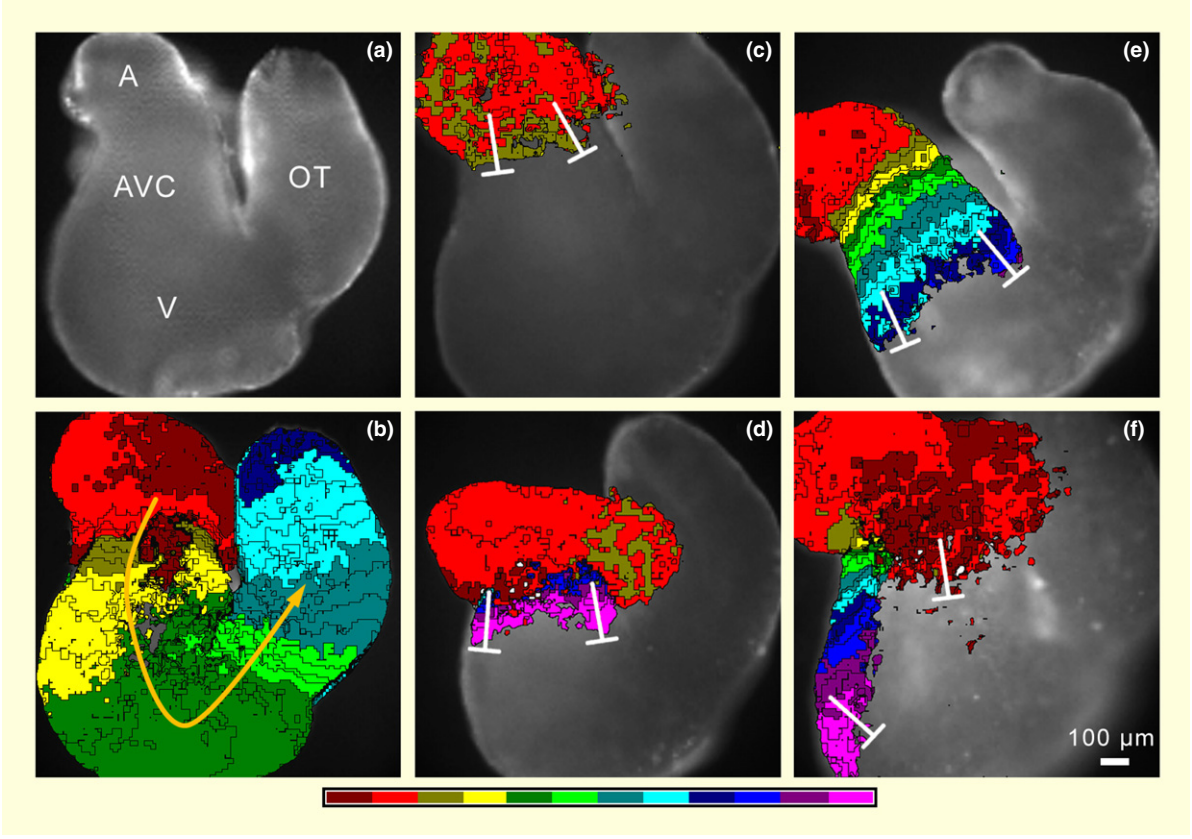

Figure 2 Comparison of third-degree atrioventricular (AV) block locations – different localization of conduction disturbances in the AV canal. (a) ED4 chick heart. (b) Standard conduction. (c) Proximal AV block. (d) Mid-AV block. (e) Distal AV block. (f) Distal AV block with preferential conduction along the outer curvature of the AV canal. Colour bands are in 32 ms (b) and 16 ms intervals (c–f), isochrones are in 8 ms intervals. A, atrium; AVC, AV canal; V, ventricle; OT, outflow tract.

(282 ms) was longer than in the atrium (223 ms, $P < 0.001$).

Electrical stimulation experiments *in ovo* showed that the AV canal of all experimental hearts ($n = 7$) was capable of propagating frequencies of up to 300 beats min^{-1}. AV canal conduction limit reached 360 beats min^{-1} during atrial stimulation in one case (Fig. 4a,b). During stimulation of atrium, an atrial conduction limit of 360 beats min^{-1} was found. This being said, second-degree AV block regularly occurred when pacing rates exceeded 300 beats min^{-1}. Hearts were capable of beating at high frequencies for only a few seconds without developing conduction block. Stimulation of the ventricle uncovered a maximal capture threshold at 600 beats min^{-1} (Fig. 4c). These results support our hypothesis that hypoxia could be one of several parameters that would explain our findings, as we never observed such high rates in sinus rhythm, even during the highest tachycardias in hyperthermia *in vitro* (270 beats min^{-1}) without AV block.

We performed electrical stimulation experiments on isolated ED4 hearts *in vitro* to uncover the conduction limits of isolated hearts without blood flow and vascular coupling ($n = 23$). The AV conduction limit (1 : 1 AV capture) was breached at 261 beats min^{-1} (see Fig. 4d). In the same heart, a maximum frequency of 353 beats min^{-1} was reached in the atrium, but second-degree AV block developed (see Fig. 4e). The next two highest heart rates successfully propagated through the AV canal in other hearts were 232 beats min^{-1} and 200 beats min^{-1}. The remaining hearts did not even reach 200 beats min^{-1} with normal AV conduction. A capture limit for the ventricle was reached at 476 beats min^{-1} (see Fig. 4f).

Discussion

Arrhythmias in the embryonic heart

High-speed imaging of calcium in the embryonic mouse heart (Valderrabano *et al.* 2006) results in increased sensitivity compared to imaging of voltage-sensitive dye. This modality also allows for signal detection in the AV canal, enabling the detection of various arrhythmias. Our experimental set-up (Vostarek *et al.* 2014) for imaging normal and stressed

  doi: 10.1111/apha.12691

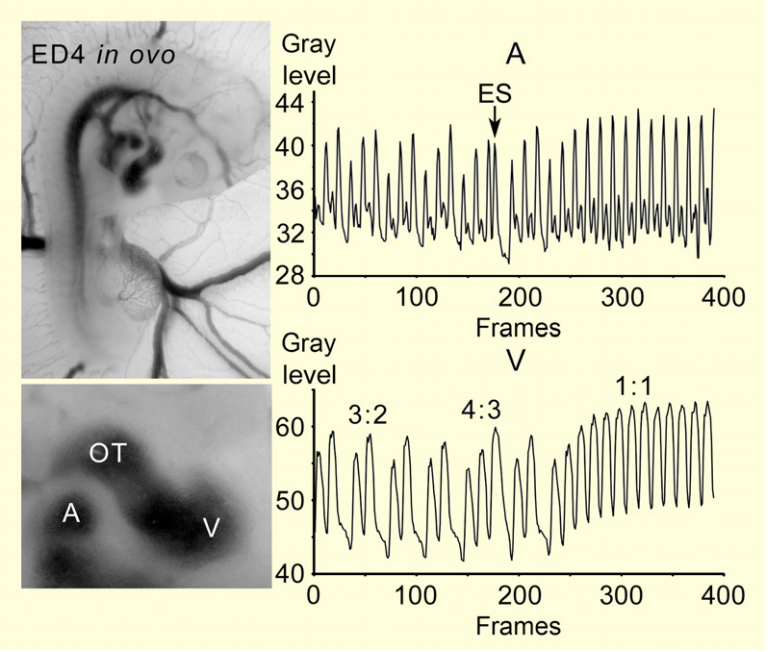

Figure 3 Second-degree atrioventricular (AV) block during hyperthermia *in ovo*. *In ovo* videomicroscopy recording of a transient second-degree AV block (Wenckebach phenomenon) during hyperthermia. Traces represent changes in grey level in time due to edge motion. Each peak represents one contraction. The *x*-axis is presented in frames (acquisition speed 30 fps). A, atrium; V, ventricle; OT, outflow tract; ES, atrial extrasystole.

embryonic hearts represents a significant technological improvement. Among other advances, it enables precise localization of sites of conduction block and the uncovering of ectopic pacemakers (Hoogaars *et al.* 2007, Leaf *et al.* 2008, Ammirabile *et al.* 2012, Benes *et al.* 2014) in the isolated embryonic heart model.

We measured correlation of PQ intervals in hypothermia, normothermia and hyperthermia, but no significant dependences were observed. PR interval was not significantly influenced by temperature or heart rate, similar to the results of Sarre *et al.* (2006). However, a modest trend towards the prolongation of PR interval was noted in their follow-up study, which included analysis of the bradycardic effects of ivabradine (Sarre *et al.* 2010). This probably reflects the limitation of ion pumps responsible for the restoration of membrane potential at higher heart rates during the pre-innervation stages of cardiogenesis. On the other hand, the mechanical PQ interval was described as negatively correlated with heart rate in human foetuses. It is notable that these more mature foetal hearts were measured under *in vivo* conditions and with full autonomic innervation (Tomek *et al.* 2011).

Temperature effects on heart rate and calcium transients

Results from calcium transient dynamics measurements *in vitro* showed that heart rate is linearly dependent on the temperature in the range from 34 to 40 °C. This corresponds well with a previous study using a ramp protocol (Sarre *et al.* 2006). Changes in heart rate were caused by direct influence on the pacemaker changing its kinetics. In the hypothermia group, we tried to change the temperature in both directions – cooling from 37 to 34 °C and warming from 34 to 37 °C. We did not observe any significant difference in heart rate change or arrhythmogenesis related to the direction of temperature change.

We expected changes in temperature to influence calcium transient amplitudes. During hyperthermia, we observed a significant decrease in amplitudes of calcium transients. We hypothesize that this is caused by higher heart rate with less time for calcium channels and pumps to establish calcium transients. We suggest that lowering of calcium transients could result in weaker contractility, which may lead over time to negative effects on pumping efficiency. These negative effects on cardiac output are equalized by higher heart rate, but limitations of energetic metabolism are crucial. On the other hand, we observed no significant changes during hypothermia. This is probably due to adaptation of chick embryos to hypothermia in natural conditions. Decreased activity of calcium transporters is balanced by a longer period available for establishing the equilibrium concentration. Cardiac output is maintained through Frank-Starling compensation by increased stroke volume (Benson *et al.* 1989).

Temperature and cardiac output

Experiments *in ovo*, including vascular coupling and blood flow, showed the same linear dependence of heart rate on temperature as *in vitro*. Chick ED4 hearts are not innervated, but β-adrenergic receptors are expressed at

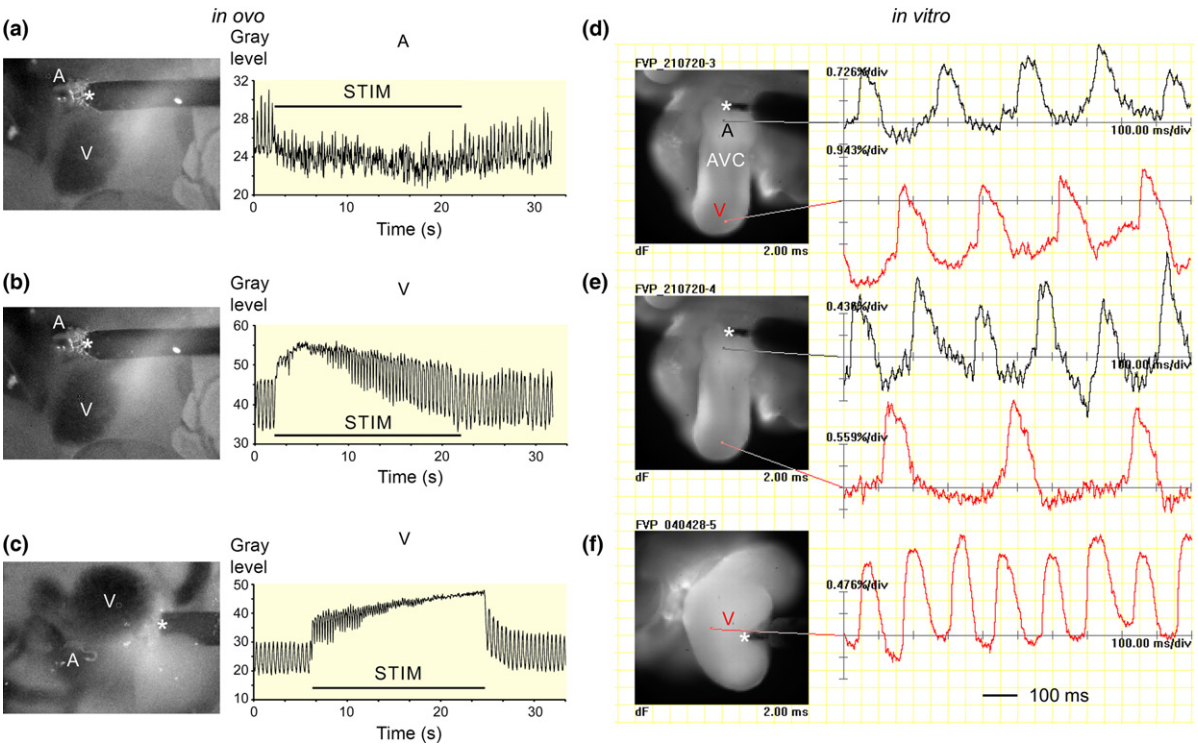

Figure 4 Artificial stimulation uncovers conduction limits. Left side shows recordings during electrical stimulation *in ovo* ($n = 7$). Atrioventricular (AV) canal conduction limit of chick ED4 heart *in ovo* reached 360 beats min^{-1} during electrical stimulation of the atrium. Atrium was stimulated gradually from 400 to 120 beats min^{-1}. (a) Motion signal from the atrium. (b) Edge movement signal from the ventricle. (c) Maximal measured conduction limit of ventricle *in ovo* reached 600 beats min^{-1}. Ventricle stimulated from 200 to 600 beats min^{-1}. Right side shows voltage imaging of electrical stimulation of ED4 chick hearts *in vitro* ($n = 23$). (d) Maximal measured AV canal conduction frequency of 261 beats min^{-1}. Atrium stimulated up to 300 beats min^{-1}. (e) Maximal measured conduction limit of atrium was 353 beats min^{-1}. Second-degree AV block (2 : 1) developed. Atrium stimulated up to 400 beats min^{-1}. (f) Maximal measured conduction limit of ventricle *in vitro* reached 476 beats min^{-1}. Ventricle stimulated up to 600 beats min^{-1}. A, atrium; AVC, AV canal; V, ventricle.

this stage. It was shown that ED4 chick heart responded to adrenaline stimulation by a significant increase in heart rate (up to 60%). Treatment by different β-blockers leads to a significant decrease of heart rate in ED4 chick hearts (Kockova *et al.* 2013). Heart function in ectothermic animals, such as fish or reptiles, is strongly affected and limited by hyperthermia, even when autonomic innervation is fully developed. The main regulating mechanisms are the same as in the embryonic heart of the chick, which physiologically develops at constant temperature maintained by the hen incubating the egg. The embryo is unable to generate its body heat by itself and therefore is well adapted to brief periods of hypothermia. A crucial limiting factor is oxidative phosphorylation in mitochondria and especially sufficient temperature-dependent ATP synthesis (Power *et al.* 2014).

Mechanisms of temperature-induced conduction defects

Increased temperature increases metabolic demands, and the availability of oxygen can become a limiting factor. This is especially the case *in vitro* where the thick AV region is probably not optimally oxygenated, as it physiologically receives nutrients and oxygen from the heart lumen. We thus focused on defects in impulse propagation in this cardiac segment, as almost 60% of all observed arrhythmias ($n = 106$) were caused by conduction block in the AV canal (Table 1). We analysed in detail various types of AV block (Fig. 2). Third-degree AV block developed in one case during hypothermia ($n = 45$ hearts), in 15% of cases in normothermia (stabilization, $n = 99$ hearts) and 39% of cases in hyperthermia ($n = 54$ hearts). This suggests that development of complete AV block is influenced by increased temperature or by another condition connected to hyperthermia. It probably corresponds with the increase of metabolic needs of hearts and concomitant decreases in oxygen concentration in the tissue bath with increasing temperature.

The slowing of conduction velocity in the AV canal is highly influenced by the presence of cardiac jelly and the endocardial cushions (Bressan *et al.* 2014). The

  doi: 10.1111/apha.12691

morphology of the AV canal is determined by large extracellular spaces, scarce membrane contacts and anionic extracellular matrix resulting in a low margin of conduction safety (Arguello *et al.* 1986). This principle is supported by new findings regarding ephaptic conduction of action potential between myocytes without recourse to gap junctions. This might happen via electric field mechanism or ion transients within the extracellular space between two tightly, <15 nm apposed myocytes, occurring, for example, in the perinexus – the cleft formed at the edge of gap junctions (Rhett & Gourdie 2012, Veeraraghavan *et al.* 2014).

The primitive cardiac tube is characterized by uniformly slow conduction velocity and expresses only one gap junction protein, Connexin45. The conduction in the AV canal is slow but robust, as noted already by Paff *et al.* (1964) and later by Sedmera *et al.* (2002), who noted that AV block could not be induced pharmacologically or by anoxia/reoxygenation prior to ED3. Chamber myocardium is characterized by Connexin40 expression, among other specific gene products, a gap junction protein essential for fast conduction. Transition between the slowly conducting AV canal and the ventricle might include heterotypic Cx45/Cx40 gap junctional coupling, which could represent a tissue sector with increased probability of functional block, similar to the substrate for sinoatrial blockade. In isolated cardiomyocytes, it was observed that cooling decreases the frequency of gap junction channel opening at all conductance levels (Chen & DeHaan 1993).

Action potentials with a low rate of rise and longer duration are typical for the AV canal (Sanders *et al.* 1984, de Jong *et al.* 1987, 1992). We measured APDs in the atrium, AV canal and ventricle in normothermia, to test the hypothesis that longer APDs predispose the AV canal to be the limiting segment of the heart. We obtained higher values than standard APDs measured by microelectrodes (Arguello *et al.* 1986), likely because of the prolongation of APD by blebbistatin – similar to the effects of cytochalasin D (Sedmera *et al.* 2006).

Our experiments showed that the pacemaker and AV canal were the most temperature-sensitive segments of the embryonic heart. The most common location of AV block was at the transition between the slowly conducting tissue of the AV canal and the fast conducting tissues of the ventricle. We suggest that the most critical region for the propagation of impulse is the connection site of trabecular network to the AV canal. It corresponds with similar finding of Coppen *et al.* in the embryonic and mature rodent heart. This observation uncovered the analogous sharp transitional interface between the Cx45-expressing component of the mouse AV node and Cx40-expressing His bundle (Coppen *et al.* 1999).

Hypoxia in the developing heart

During cardiac development, hypoxic regions are found in several locations of the myocardium (Nanka *et al.* 2006, 2008, Wikenheiser *et al.* 2006). These hypoxic regions correlate with areas of conduction system formation (Wikenheiser *et al.* 2006). Coincidentally, hypoxia is also detected in the thickest regions of the myocardium (AV canal, interventricular septum, outflow tract myocardium), and it is believed that hypoxia is a powerful stimulus for coronary vasculogenesis (Nanka *et al.* 2008). As the AV canal is one of the thickest areas of the embryonic myocardium, it lacks trabeculae and is separated from the oxygen-carrying blood in the lumen by the cardiac cushions, and it thus comes as no surprise that it is very sensitive to hypoxia. Because the normal routes of oxygenation in the chick embryonic heart prior to ED9 (establishment of coronary perfusion) is through the lumen, it is not surprising that hearts were more prone to develop AV block *in vitro*, where the direction of oxygen diffusion, as well as its concentration gradient, is perturbed.

We tested the ability of the AV canal to propagate high beat frequencies by electrical stimulation. The main point was to prove that AV blocks induced during comparatively mild tachycardia in hyperthermia were not due to the intrinsic absolute conduction limit of the AV conduction. Electrical stimulation experiments showed that the conduction limit of the AV canal was much higher *in ovo* (360 beats min^{-1}) than *in vitro* (261 beats min^{-1}). Also the conduction limits of the atrium and ventricle, respectively, were higher *in ovo* (atrium 360 beats min^{-1}, ventricle 600 beats min^{-1}) than *in vitro* (atrium 353 beats min^{-1}, ventricle 476 beats min^{-1}). This is probably caused by better oxygenation of the hearts from blood flow through the lumen. These results suggest that the observed AV blocks could be caused by relative tissue hypoxia and not by a low ability of the AV canal to propagate high frequencies.

In conclusion, this study provides a quantitative evaluation of temperature effects on conduction in the chick embryonic heart. Hypothermia is tolerated better than hyperthermia, the former of which embryos seem to be well adapted to. The most common arrhythmia observed under hyperthermia was AV block, which was observed typically at the transition between the AV canal and ventricle. Thus, morphological and molecular distinctions between different compartments of the developing heart have physiological consequences manifesting under increased metabolic demands.

Conflict of interest

None.

We would like to thank Dr. Zuzana Halasova for her assistance with the *in ovo* experiments, and Prof. Eric Raddatz and Prof. Robert Gourdie for critical reading of the manuscript. This work was supported by Ministry of Education PRVOUK P35/LF1/5, institutional RVO: 67985823 (DS), Grant Agency of the Czech Republic P302/11/1308, 13-12412S and 16-02972S to DS, and Grant Agency of the Charles University 716214 to FV.

References

Ammirabile, G., Tessari, A., Pignataro, V., Szumska, D., Sutera Sardo, F., Benes, J. Jr, Balistreri, M., Bhattacharya, S., Sedmera, D. & Campione, M. 2012. Pitx2 confers left morphological, molecular, and functional identity to the sinus venosus myocardium. *Cardiovasc Res* **93**, 291–301.

Arguello, C., Alanis, J., Pantoja, O. & Valenzuela, B. 1986. Electrophysiological and ultrastructural study of the atrioventricular canal during the development of the chick embryo. *J Mol Cell Cardiol* **18**, 499–510.

Benes, J. Jr, Ammirabile, G., Sankova, B., Campione, M., Krejci, E., Kvasilova, A. & Sedmera, D. 2014. The role of connexin40 in developing atrial conduction. *FEBS Lett* **588**, 1465–1469.

Benson, D.W. Jr, Hughes, S.F., Hu, N. & Clark, E.B. 1989. Effect of heart rate increase on dorsal aortic flow before and after volume loading in the stage 24 chick embryo. *Pediatr Res* **26**, 438–441.

Bers, D.M. 1991. Ca regulation in cardiac muscle. *Med Sci Sports Exerc* **23**, 1157–1162.

Bressan, M., Yang, P.B., Louie, J.D., Navetta, A.M., Garriock, R.J. & Mikawa, T. 2014. Reciprocal myocardial-endocardial interactions pattern the delay in atrioventricular junction conduction. *Development* **141**, 4149–4157.

Chen, Y.H. & DeHaan, R.L. 1993. Temperature dependence of embryonic cardiac gap junction conductance and channel kinetics. *J Membr Biol* **136**, 125–134.

Coppen, S.R., Severs, N.J. & Gourdie, R.G. 1999. Connexin45 (alpha 6) expression delineates an extended conduction system in the embryonic and mature rodent heart. *Dev Genet* **24**, 82–90.

DiFrancesco, D. 1993. Pacemaker mechanisms in cardiac tissue. *Annu Rev Physiol* **55**, 455–472.

Fedorov, V.V., Lozinsky, I.T., Sosunov, E.A., Anyukhovsky, E.P., Rosen, M.R., Balke, C.W. & Efimov, I.R. 2007. Application of blebbistatin as an excitation-contraction uncoupler for electrophysiologic study of rat and rabbit hearts. *Heart Rhythm* **4**, 619–626.

Haddock, P.S., Coetzee, W.A. & Artman, M. 1997. Na^+/Ca^{2+} exchange current and contractions measured under Cl(−)-free conditions in developing rabbit hearts. *Am J Physiol* **273**, H837–H846.

Hamburger, V. & Hamilton, H.L. 1951. A series of normal stages in the development of the chick embryo. *J Morphol* **88**, 49–92.

Hoogaars, W.M., Engel, A., Brons, J.F., Verkerk, A.O., de Lange, F.J., Wong, L.Y., Bakker, M.L., Clout, D.E., Wakker, V., Barnett, P., Ravesloot, J.H., Moorman, A.F., Verheijck, E.E. & Christoffels, V.M. 2007. Tbx3 controls the sinoatrial node gene program and imposes pacemaker function on the atria. *Genes Dev* **21**, 1098–1112.

de Jong, F., Geerts, W.J., Lamers, W.H., Los, J.A. & Moorman, A.F. 1987. Isomyosin expression patterns in tubular stages of chicken heart development: a 3-D immunohistochemical analysis. *Anat Embryol (Berl)* **177**, 81–90.

de Jong, F., Opthof, T., Wilde, A.A., Janse, M.J., Charles, R., Lamers, W.H. & Moorman, A.F. 1992. Persisting zones of slow impulse conduction in developing chicken hearts. *Circ Res* **71**, 240–250.

Kamino, K., Hirota, A. & Fujii, S. 1981. Localization of pacemaking activity in early embryonic heart monitored using voltage-sensitive dye. *Nature* **290**, 595–597.

Kockova, R., Svatunkova, J., Novotny, J., Hejnova, L., Ostadal, B. & Sedmera, D. 2013. Heart rate changes mediate the embryotoxic effect of antiarrhythmic drugs in the chick embryo. *Am J Physiol Heart Circ Physiol* **304**, H895–H902.

Leaf, D.E., Feig, J.E., Vasquez, C., Riva, P.L., Yu, C., Lader, J.M., Kontogeorgis, A., Baron, E.L., Peters, N.S., Fisher, E.A., Gutstein, D.E. & Morley, G.E. 2008. Connexin40 imparts conduction heterogeneity to atrial tissue. *Circ Res* **103**, 1001–1008.

Lee, S.J., Yeom, E., Ha, H. & Nam, K.H. 2011. Cardiac outflow and wall motion in hypothermic chick embryos. *Microvasc Res* **82**, 296–303.

Lin, E., Ribeiro, A., Ding, W., Hove-Madsen, L., Sarunic, M.V., Beg, M.F. & Tibbits, G.F. 2014. Optical mapping of the electrical activity of isolated adult zebrafish hearts: acute effects of temperature. *Am J Physiol Regul Integr Comp Physiol* **306**, R823–R836.

Moroni, A., Gorza, L., Beltrame, M., Gravante, B., Vaccari, T., Bianchi, M.E., Altomare, C., Longhi, R., Heurteaux, C., Vitadello, M., Malgaroli, A. & DiFrancesco, D. 2001. Hyperpolarization-activated cyclic nucleotide-gated channel 1 is a molecular determinant of the cardiac pacemaker current I(f). *J Biol Chem* **276**, 29233–29241.

Nakazawa, M., Clark, E.B., Hu, N. & Wispe, J. 1985. Effect of environmental hypothermia on vitelline artery blood pressure and vascular resistance in the stage 18, 21, and 24 chick embryo. *Pediatr Res* **19**, 651–654.

Nakazawa, M., Miyagawa, S., Takao, A., Clark, E.B. & Hu, N. 1986. Hemodynamic effects of environmental hyperthermia in stage 18, 21, and 24 chick embryos. *Pediatr Res* **20**, 1213–1215.

Nanka, O., Valasek, P., Dvorakova, M. & Grim, M. 2006. Experimental hypoxia and embryonic angiogenesis. *Dev Dyn* **235**, 723–733.

Nanka, O., Krizova, P., Fikrle, M., Tuma, M., Blaha, M., Grim, M. & Sedmera, D. 2008. Abnormal myocardial and coronary vasculature development in experimental hypoxia. *Anat Rec (Hoboken)* **291**, 1187–1199.

Paff, G.H., Boucek, R.J. & Klopfenstein, H.S. 1964. Experimental heart-block in the chick embryo. *Anat Rec* **149**, 217–223.

  doi: 10.1111/apha.12691

Peterka, M., Peterkova, R. & Likovsky, Z. 1996. Teratogenic and lethal effects of long-term hyperthermia and hypothermia in the chick embryo. *Reprod Toxicol* **10**, 327–332.

Power, A., Pearson, N., Pham, T., Cheung, C., Phillips, A. & Hickey, A. 2014. Uncoupling of oxidative phosphorylation and ATP synthase reversal within the hyperthermic heart. *Physiol Rep* **2**, e12138.

Rentschler, S., Vaidya, D.M., Tamaddon, H., Degenhardt, K., Sassoon, D., Morley, G.E., Jalife, J. & Fishman, G.I. 2001. Visualization and functional characterization of the developing murine cardiac conduction system. *Development* **128**, 1785–1792.

Rhett, J.M. & Gourdie, R.G. 2012. The perinexus: a new feature of Cx43 gap junction organization. *Heart Rhythm* **9**, 619–623.

Sanders, E., Moorman, A.F. & Los, J.A. 1984. The local expression of adult chicken heart myosins during development. I. The three days embryonic chicken heart. *Anat Embryol (Berl)* **169**, 185–191.

Sankova, B., Machalek, J. & Sedmera, D. 2010. Effects of mechanical loading on early conduction system differentiation in the chick. *Am J Physiol Heart Circ Physiol* **298**, H1571–H1576.

Sarre, A., Maury, P., Kucera, P., Kappenberger, L. & Raddatz, E. 2006. Arrhythmogenesis in the developing heart during anoxia-reoxygenation and hypothermia-rewarming: an in vitro model. *J Cardiovasc Electrophysiol* **17**, 1350–1359.

Sarre, A., Pedretti, S., Gardier, S. & Raddatz, E. 2010. Specific inhibition of HCN channels slows rhythm differently in atria, ventricle and outflow tract and stabilizes conduction in the anoxic-reoxygenated embryonic heart model. *Pharmacol Res* **61**, 85–91.

Sedmera, D., Grobety, M., Reymond, C., Baehler, P., Kucera, P. & Kappenberger, L. 1999. Pacing-induced ventricular remodeling in the chick embryonic heart. *Pediatr Res* **45**, 845–852.

Sedmera, D., Kucera, P. & Raddatz, E. 2002. Developmental changes in cardiac recovery from anoxia-reoxygenation. *Am J Physiol Regul Integr Comp Physiol* **283**, R379–R388.

Sedmera, D., Reckova, M., deAlmeida, A., Sedmerova, M., Biermann, M., Volejnik, J., Sarre, A., Raddatz, E., McCarthy, R.A., Gourdie, R.G. & Thompson, R.P. 2003. Functional and morphological evidence for a ventricular conduction system in zebrafish and *Xenopus* hearts. *Am J Physiol Heart Circ Physiol* **284**, H1152–H1160.

Sedmera, D., Wessels, A., Trusk, T.C., Thompson, R.P., Hewett, K.W. & Gourdie, R.G. 2006. Changes in activation sequence of embryonic chick atria correlate with developing myocardial architecture. *Am J Physiol Heart Circ Physiol* **291**, H1646–H1652.

Sperelakis, N. & Lehmkuhl, D. 1967. Effects of temperature and metabolic poisons on membrane potentials of cultured heart cells. *Am J Physiol* **213**, 719–724.

Tamaddon, H.S., Vaidya, D., Simon, A.M., Paul, D.L., Jalife, J. & Morley, G.E. 2000. High-resolution optical mapping of the right bundle branch in connexin40 knockout mice reveals slow conduction in the specialized conduction system. *Circ Res* **87**, 929–936.

Tomek, V., Janousek, J., Reich, O., Gilik, J., Gebauer, R.A. & Skovranek, J. 2011. Atrioventricular conduction time in fetuses assessed by Doppler echocardiography. *Physiol Res* **60**, 611–616.

Tran, L., Kucera, P., de Ribaupierre, Y., Rochat, A.C. & Raddatz, E. 1996. Glucose is arrhythmogenic in the anoxic-reoxygenated embryonic chick heart. *Pediatr Res* **39**, 766–773.

Valderrabano, M., Chen, F., Dave, A.S., Lamp, S.T., Klitzner, T.S. & Weiss, J.N. 2006. Atrioventricular ring reentry in embryonic mouse hearts. *Circulation* **114**, 543–549.

Veeraraghavan, R., Gourdie, R.G. & Poelzing, S. 2014. Mechanisms of cardiac conduction: a history of revisions. *Am J Physiol Heart Circ Physiol* **306**, H619–H627.

Vostarek, F., Sankova, B. & Sedmera, D. 2014. Studying dynamic events in the developing myocardium. *Prog Biophys Mol Biol* **115**, 261–269.

Warbanow, W. 1970. [Morphologic and functional studies of the hypothermia-induced hypertrophy of the embryonic chick heart]. *Acta Biol Med Ger* **25**, 281–293.

Warbanow, W. 1971. Contractility of the embryonic chick heart in hypothermia-induced cardiac hyperplasia and hypertrophy. *Acta Biol Med Ger* **26**, 859–861.

Wikenheiser, J., Doughman, Y.Q., Fisher, S.A. & Watanabe, M. 2006. Differential levels of tissue hypoxia in the developing chicken heart. *Dev Dyn* **235**, 115–123.

Supporting Information

Additional Supporting Information may be found online in the supporting information tab for this article:

Video S1. Examples of arrhythmias observed in the embryonic chick heart using calcium imaging.